

AD 1040628

NOSC / TR 113

NOSC

12

NOSC / TR 113

Technical Report 113

SPATIAL DIVERSITY CHARACTERISTICS OF EQUATORIAL SCINTILLATION

UHF and L-Band SATCOM Tests at Guam,
July — December 1976

MR Paulson and RUF Hopkins

2 May 1977

D D C
RECEIVED
JUN 16 1977
NOSC

Prepared for
NAVAL ELECTRONIC SYSTEMS COMMAND
PME 106
Washington DC 20360

Final Report for Period
January 1975 — March 1977

Approved for public release; distribution is unlimited

NAVAL OCEAN SYSTEMS CENTER
SAN DIEGO, CALIFORNIA 92152

DDC FILE COPY



NAVAL OCEAN SYSTEMS CENTER, SAN DIEGO, CA 92152

AN ACTIVITY OF THE NAVAL MATERIAL COMMAND

RR GAVAZZI, CAPT, USN

HOWARD L BLOOD, PhD

Commander

Technical Director

ADMINISTRATIVE INFORMATION

Work was performed under Elex Element 33109N, Project X0731, Task X0731 (NELC J200) by members of the LOS and Satellite Communications Division. This report covers work from January 1975 to March 1977 and was approved for publication 2 May 1977.

The authors would like to express their appreciation to a number of people who contributed to the success of this field test program, notably

The NOSC Test Team

Code 7242 CG Norgard
PW Bauer

Code 7245 JE Britt

NAVSEEACTION, Guam

J Servino
N Kong

NAVCAMS, WestPac

CWO D Thomas
C DeNight

and numerous personnel at the UHF SATCOM Facility.

Released by
FM Tirpak, Head
LOS and Satellite Communications
Division

Under authority of
PC Fletcher, Head
Electromagnetic Systems
Department

UNCLASSIFIED

SECURITY CLASSIFICATION OF THIS PAGE (When Data Entered)

REPORT DOCUMENTATION PAGE		READ INSTRUCTIONS BEFORE COMPLETING FORM
1. REPORT NUMBER NOSC Technical Report 113 (TR 113)	2. GOVT ACCESSION NO.	3. RECIPIENT'S CATALOG NUMBER
4. TITLE (and Subtitle) SPATIAL DIVERSITY CHARACTERISTICS OF EQUATORIAL SCINTILLATION UHF and L-Band SATCOM Tests at Guam, July-December 1976	5. TYPE OF REPORT & PERIOD COVERED Final January 1975-March 1977	
	6. PERFORMING ORG. REPORT NUMBER	
7. AUTHOR(s) MR Paulson, RUF/Hopkins	8. CONTRACT OR GRANT NUMBER(s) <i>(14) NOSC/TR-113</i>	
9. PERFORMING ORGANIZATION NAME AND ADDRESS Naval Ocean Systems Center San Diego, CA 92152	10. PROGRAM ELEMENT, PROJECT, TASK AREA & WORK UNIT NUMBERS 33109N, X0731, X0731, NELC J200	
11. CONTROLLING OFFICE NAME AND ADDRESS NAVELEX PME 106	12. REPORT DATE 2 May 1977	13. NUMBER OF PAGES 64
14. MONITORING AGENCY NAME & ADDRESS (if different from Controlling Office) <i>1 The ...</i>	15. SECURITY CLASS. (of this report)	
15a. DECLASSIFICATION/DOWNGRADING SCHEDULE		
16. DISTRIBUTION STATEMENT (of this Report) Approved for public release; distribution is unlimited. <i>M. R. ...</i>		
17. DISTRIBUTION STATEMENT (of the abstract entered in Block 20, if different from Report)		
18. SUPPLEMENTARY NOTES		
19. KEY WORDS (Continue on reverse side if necessary and identify by block number) Scintillation - equatorial zone Diversity reception Ionosphere - scintillation Ultrahigh frequencies Spacecraft communication - Fleet SATCOM Frequencies - L-band Spacecraft communication - Global Positioning System		
20. ABSTRACT (Continue on reverse side if necessary and identify by block number) This report describes the results of space diversity tests conducted at Guam in the summer and fall of 1976 to evaluate the utility of this technique for mitigating the corrupting effects of equatorial scintillation on SATCOM links. Two wavelengths were employed for different systems evaluation: one at UHF for Fleet SATCOM and one at L-Band for the Global Positioning System (GPS). Down-link results at UHF showed that error rates approaching 50 percent can be completely eliminated by use of space diversity. Various statistical representations of data obtained using three diversity spacings enabled thorough analysis required to investigate optimization of the diversity configuration. L-Band scintillation, though		

DDC
FORM 1
JUN 16 1977
RECEIVED
C

DD FORM 1 JAN 73 1473

EDITION OF 1 NOV 68 IS OBSOLETE
S/N 0102-LF-014-8601

UNCLASSIFIED

SECURITY CLASSIFICATION OF THIS PAGE (When Data Entered)

393159

UNCLASSIFIED

SECURITY CLASSIFICATION OF THIS PAGE(When Data Entered)

less intense than at UHF, did occur at levels that may affect the performance of the GPS. Estimates of reduced system margins at both the L1 and L2 frequencies used in the GPS are presented. Phase measurements at UHF are shown and a discussion relative to its effects on both systems is presented. Considered in the discussion is low-angle fading which is predicted to be of concern relative to the Indian Ocean GAPFILLER.

ADDITIONAL INFORMATION

When Available
Diff Section

Availability Class
and/or Sr. Class

A

UNCLASSIFIED

SECURITY CLASSIFICATION OF THIS PAGE(When Data Entered)

OBJECTIVE

Evaluate the use of a space diversity system for mitigating the effects of ionospheric scintillation on UHF SATCOM at NAVCAMS, WestPac, Guam. Conduct space diversity measurements necessary to optimize performance of the system. Conduct parallel measurements at L-Band to determine the magnitude of scintillation fading and its spatial diversity characteristics.

RESULTS

1. Space diversity completely eliminated high digital error rates caused by equatorial scintillation.
2. The optimum baseline dimension of the three baselines tested was 700 meters.
3. The AN/SSR-1 Fleet Broadcast receiver using predetection diversity combining is ideally implemented for space diversity applications.
4. Three-level diversity is somewhat better than two-level diversity and permits use of three baseline dimensions, which can compensate for long term (years) and short term changes in the fading statistics.
5. Scintillation activity is dependent on solar activity as quantified by sun-spot numbers and therefore is predicted to increase substantially as the solar activity increases from the 1976 minimum.
6. L-Band scintillation intensity is considerably less than at UHF and the optimum baseline dimension for space diversity is about one-half that for UHF. Though L-Band scintillation intensity was small, it was large enough to adversely affect the small link margins associated with the Global Positioning System.

RECOMMENDATIONS

1. Implement reception space diversity in the Fleet Broadcast service at equatorially located NAVCAMS.
2. Plan for implementation of reception diversity in multiple channel Fleet SATCOM at equatorial NAVCAMS.
3. Conduct further investigation of diversity techniques for UHF uplinks. Consider future use (FleetSatcom II) of SHF uplinks from NAVCAMS for all channels.
4. Analyze in detail the data at the Guam Global Positioning System monitoring station with respect to the effects of ionospheric scintillation.
5. Install permanent satellite signal strength recording equipment at Guam as an aid in isolation of system problems from propagation effects.

CONTENTS

INTRODUCTION . . .	page 1
TEST OBJECTIVES . . .	1
UHF diversity . . .	1
L-band diversity . . .	2
TEST CONFIGURATIONS . . .	2
DATA PRESENTATION . . .	7
Scintillation activity . . .	7
UHF down-link diversity results . . .	7
Space diversity characteristics . . .	13
UHF up-link diversity results . . .	34
L-band diversity results . . .	34
Related data . . .	48
A note concerning low-angle fading . . .	48
CONCLUSIONS . . .	57
RECOMMENDATIONS . . .	57
REFERENCES . . .	58

ILLUSTRATIONS

1	Link configuration used in the Guam diversity tests . . .	3
2	Simplified instrumentation configuration at Guam . . .	4
3	UHF and L-band diversity arrangement at Guam . . .	5
4	Block diagram of L-band receiver . . .	6
5	Periods of scintillation occurrences greater than 6 dB below the undisturbed signal at Guam . . .	8
6	Dependence of scintillation occurrence on solar activity . . .	9
7	Down-link error rates recorded at Guam: A. No diversity. B. Using diversity . . .	10
8	Data error rates during scintillation without the use of diversity . . .	11
9	Reception diversity test results . . .	12
10	Spatial cross-correlation functions for 3 antenna separations . . .	14
11	Cross-correlation curves for five-minute samples starting with curve 1 at 1115-1120 GMT. Spacing was east-west at 300 meters . . .	15
12	Correlation between fading signals received with 3 different antenna spacings in the east-west direction as a function of time lag between the recordings . . .	16
13	Temporal variation of 3 values taken from the correlation functions . . .	17
14	Temporal variation of 3 values taken from the correlation functions . . .	18
15	Temporal variation of 3 values taken from the correlation functions . . .	19
16	Temporal variation of 3 values taken from the correlation functions . . .	20
17	Temporal variation of 3 values taken from the correlation functions . . .	21
18	Temporal variation of 3 values taken from the correlation functions . . .	22
19	Temporal variation of 3 values taken from the correlation functions . . .	23
20	Temporal variation of 3 values taken from the correlation functions . . .	24

Illustrations (Continued)

- 21 Temporal variation of 3 values taken from the correlation functions . . . 25
- 22 Temporal variation of 3 values taken from the correlation functions . . . 26
- 23 Temporal variation of 3 values taken from the correlation functions . . . 27
- 24 Temporal variation of 3 values taken from the correlation functions . . . 28
- 25 Maximum fades observed for five-minute samples as a function of time for different signal combinations . . . 29
- 26 Maximum fades observed for five-minute samples as a function of time for different signal combinations . . . 30
- 27 Maximum fades observed for five-minute samples as a function of time for different signal combinations . . . 31
- 28 Maximum fades observed for five-minute samples as a function of time for different signal combinations . . . 32
- 29 Maximum fades observed for five-minute samples as a function of time for different signal combinations . . . 33
- 30 Cumulative probability distributions for different diversity combinations compared to the case of no diversity . . . 35
- 31 Cumulative probability distributions for different diversity combinations compared to the case of no diversity . . . 36
- 32 Comparison of up-link error rates with and without the use of diversity . . . 37
- 33 Chart record reproductions comparing L-band and UHF scintillation fading . . . 39
- 34 Temporal variation of UHF and L-band standard deviations about the mean signal level . . . 40
- 35 Comparison of UHF and L-band cumulative probability distributions . . . 41
- 36 Comparative cumulative distribution function (CDF) values for UHF and L-band amplitude scintillation . . . 42
- 37 Spatial cross correlation functions for two wavelengths on 1000 meter baseline . . . 44
- 38 Spatial cross correlation functions for two wavelengths on 1000 meter baseline . . . 45
- 39 Spatial cross correlation functions for two wavelengths on 1000 meter baseline . . . 46
- 40 Comparison of scintillation intensities between L-band and UHF . . . 47
- 41 The east-west component of the apparent drift velocity, uncorrected for time decorrelation effects, is shown as a function of time and compared to the scintillation activity where the standard deviation divided by the mean is used as an indication of scintillation intensity . . . 49
- 42 The east-west component of the apparent drift velocity, uncorrected for time decorrelation effects, is shown as a function of time and compared to the scintillation activity where the standard deviation divided by the mean is used as an indication of scintillation intensity . . . 50
- 43 The east-west component of the apparent drift velocity, uncorrected for time decorrelation effects, is shown as a function of time and compared to the scintillation activity where the standard deviation divided by the mean is used as an indication of scintillation intensity . . . 51
- 44 Temporal variation of UHF phase difference with the 1000 meter antenna spacing . . . 52
- 45 Fade duration distribution observed at Guam in 1976 . . . 53

Illustrations (Continued)

- 46 Fade duration distribution observed near Guam in 1971 . . . 54
- 47 Fade duration distribution observed at Guam in 1976 . . . 55
- 48 Fade duration distribution observed near Guam in 1971 . . . 56

TABLES

- 1 Unjammed link margins (dB) . . . 38
- 2 Jammed link margins (dB) . . . 43

INTRODUCTION

The highly disruptive effects of equatorial scintillation to UHF Satellite Communications has been recognized since operations at equatorial sites began with TACSAT-I. Scintillation fading is caused by the drift motion of ionospheric irregularities of electron density at F-layer heights and above. Many of the characteristics of equatorial scintillation were observed during field tests conducted by Naval Electronics Laboratory Center (NELC) workers in the early 1970's. The results of these tests were summarized in reference (1) which has provided a unique data base concerning scintillation effects.

One aspect of the early NELC tests was the measurement of the apparent speed and direction of the drift motion of the fading pattern on the ground using a triangle of spaced receivers oriented in the east-west and north-south directions. UHF signals from TACSAT-I were used in this test. An important conclusion resulting from the measurements made was that highly decorrelated fading occurred between the two receivers spaced 1100 meters in the east-west direction. This, of course, provided the necessary condition for application of diversity techniques to minimize the effects of scintillation. Concurrently, the Navy was developing a receiver for Satellite Fleet Broadcast use that employed up to 4 channels of pre-detection diversity combining. Thus, the critical instrumentation was available to test the diversity concept. This report describes the results of diversity tests conducted at Guam from 1 July 1976 to 4 December 1976 using the Pacific Gapfiller Satellite.

In addition to the UHF tests a parallel test at L-Band (1541.5 MHz) was included using the MARISAT beacon on the Pacific Gapfiller Satellite. This was implemented to obtain data for performance evaluation for the Global Positioning System (GPS).

Significant levels of scintillation amplitude at L-Band were observed during the tests. This implies that large phase scintillation also occurred (though not measured) that could have considerable effect on the GPS spread spectrum signals. Data being obtained by other activities confirms that large phase scintillation amplitudes do occur.

The results of both the UHF and L-Band tests are presented in this report since several cross-frequency relationships are significant products of the combined testing.

TEST OBJECTIVES

Primarily, the objectives of the tests reported herein were to evaluate the effectiveness of space diversity for mitigating the effects of scintillation fading on UHF SATCOM circuits and determining what the optimum spatial parameters are. Both up-link and down-link techniques were to be evaluated. Specifically, the following tests were implemented:

UHF Diversity

Measurement of down-link error rates with and without diversity.

Measurement of down-link signal fading amplitudes at individual channels and combined channels for statistical analysis.

Measurement of 3 different diversity baseline distances to determine optimum spatial parameters.

Up-link switching diversity error rate measurements.

L-Band Diversity

Measurement of separate spaced receiver fading amplitudes.

In addition to the above measurements another objective was to derive certain morphological information regarding equatorial scintillation, which will also be included.

TEST CONFIGURATIONS

The overall UHF diversity test configuration is shown in figure 1. The use of the Army "Narrow Band Alpha" (NB/A) 25 kHz channel on Gapfiller was requested (and granted) so that special test signals could be transmitted in either direction between San Diego and Guam without mutual interference with other signals. The level of Fleet Broadcast signals on narrow band bravo (NB/B) were recorded 24 hours a day at Guam except during the periods that the use of NB/A was authorized and access originated at NELC. Access from NELC consisted of either CW carrier or 2400 B.P.S. PN sequences for error rate measurements at Guam. Modulation was differentially encoded PSK employing OM-43 Modems. Alternately, the up-link diversity measurements originated at Guam and error rates were measured at NELC.

A more detailed diagram of the configuration at Guam is shown in figure 2. This illustrates the method of deriving the signal level records for individual and combined channels as well as the technique employed for developing up-link diversity. When using up-link diversity the NB/B fleet broadcast signal was used for channel status sensing. The up-link test procedure was to operate alternate ten minute periods with and without diversity. A comparison of error rates measured at NELC was made to evaluate the effectiveness of the technique.

In addition to the configuration in figure 2 a third receiver was used one-third the distance between the receivers on the 1000 meter base line. Its output was recorded individually also, as well as being the third contribution to the diversity combiner as shown in figure 1. Data derived from the individual recordings was digitized and computer processed to obtain statistics necessary to determine optimum parameters for the diversity system.

The overall configuration of the UHF and L-Band receivers at Guam is shown in figure 3. All data were recorded at a central location on two 4 channel analog magnetic tape recorders. A time code was recorded along with the data for later use in the digital processing. The UHF receivers were the engineering development models of the AN/SSR-1 SATCOM Fleet-Broadcast receiver. The L-Band receivers were built at NELC using in-house funding. A block diagram of the L-Band receiver is shown in figure 4. These receivers yielded about 17 dB signal-to-noise ratio on the MARISAT CW beacon using 2.4 kHz bandwidth. The UHF receivers operating on the 16 element phased array antennas developed about 30 dB signal-to-noise ratio.

The remote antennas for the diversity system were connected to the central processing and recording area using combinations of 3 inch and 7/8 inch Heliac coaxial lines. The necessary D.C., R.F. and I.F. signals were multiplexed on a single line. At the central processing area the AN/SSR-1 front ends and processing components were connected in their normal ways. The same arrangement is envisioned for a future operational system.

Two NELC Bit-Error-Rate (BER) monitors were used at Guam to simultaneously measure this factor for both diversity and non-diversity configurations. This enabled comparison of performance for the same sample interval. The main Bit-Error-Rate measurements were performed using 2400 B.P.S. data rate which required up-conversion of the AN/SSR-1 I.F. signals to 70 MHz to interface with the OM-43 modems.

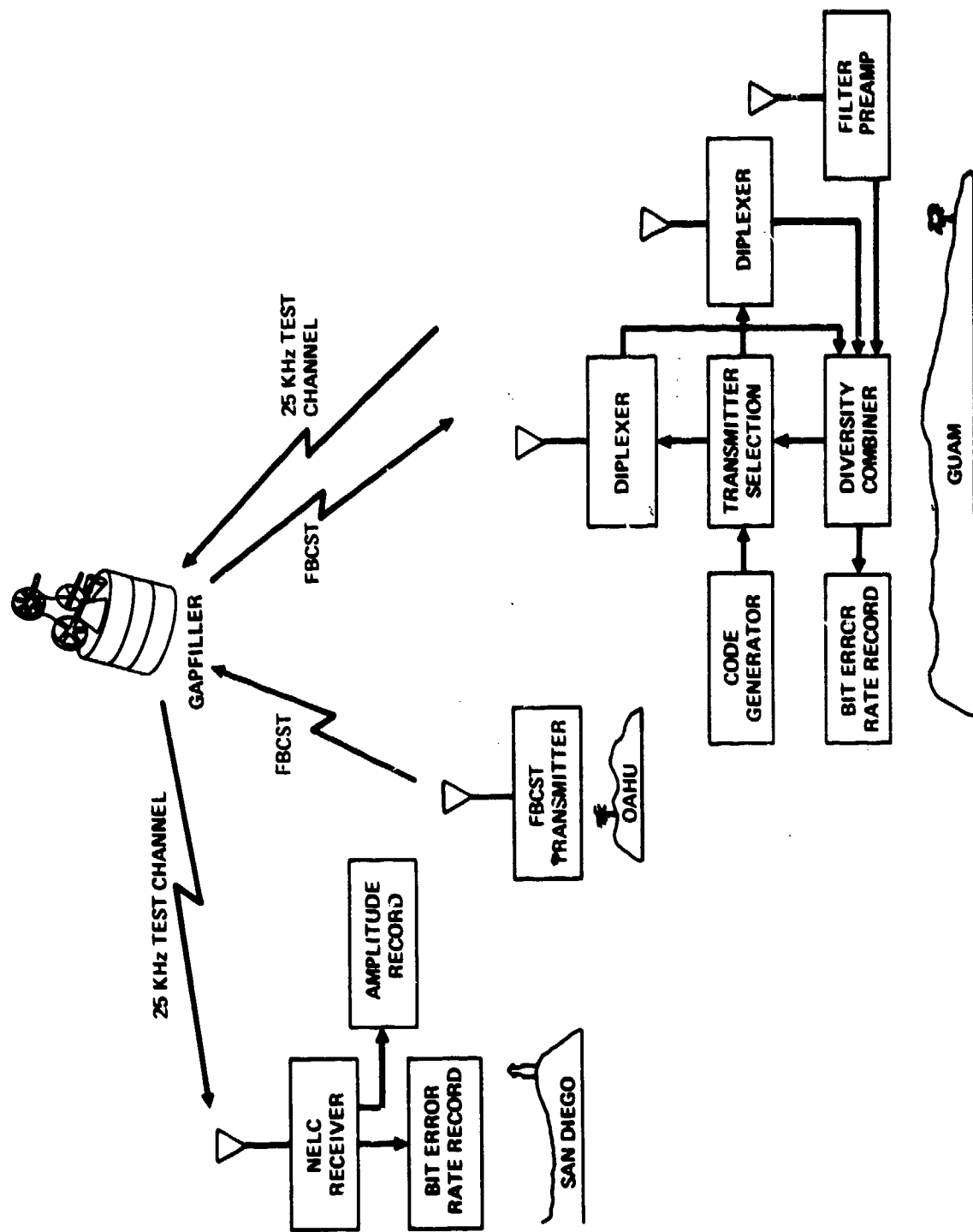


Figure 1. Link configuration used in the Guam diversity tests.

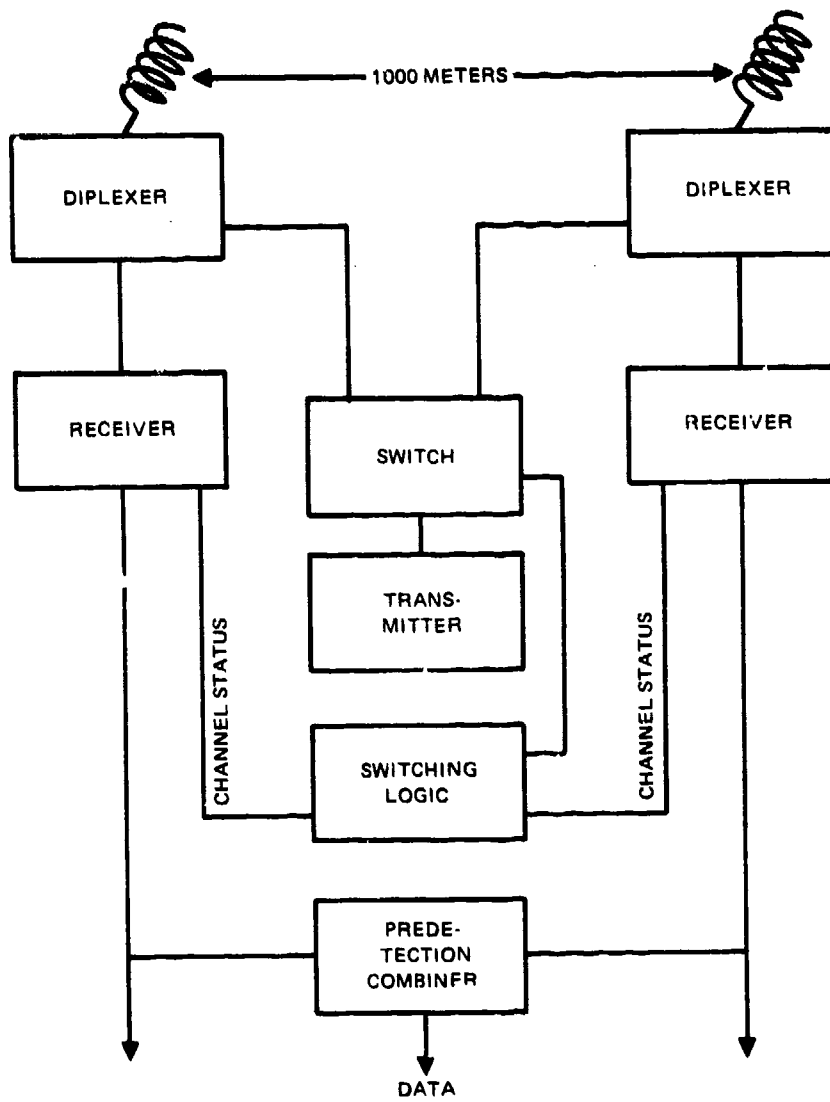


Figure 2. Simplified instrumentation configuration at Guam.

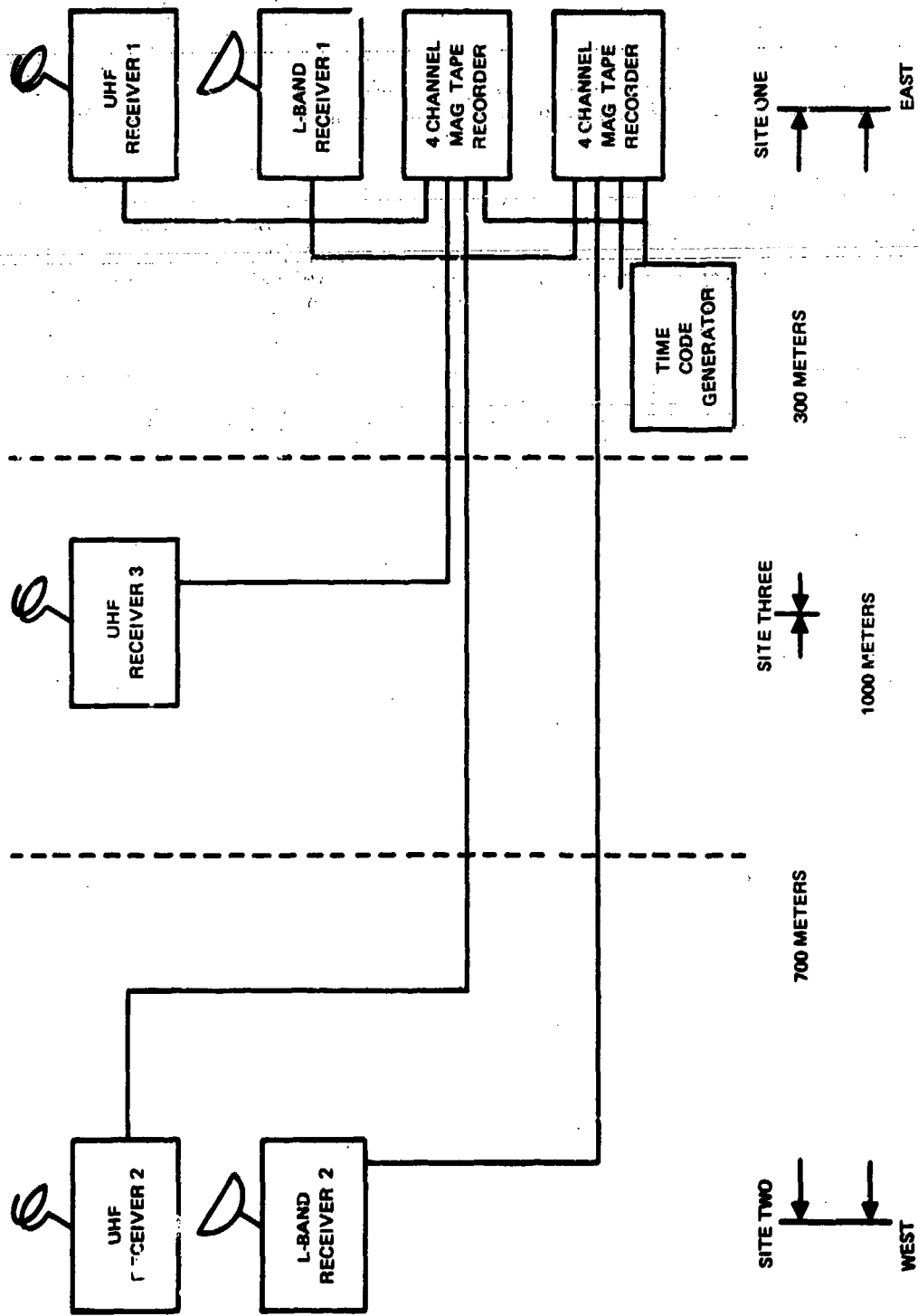


Figure 3. UHF and L-band diversity arrangement at Guam.

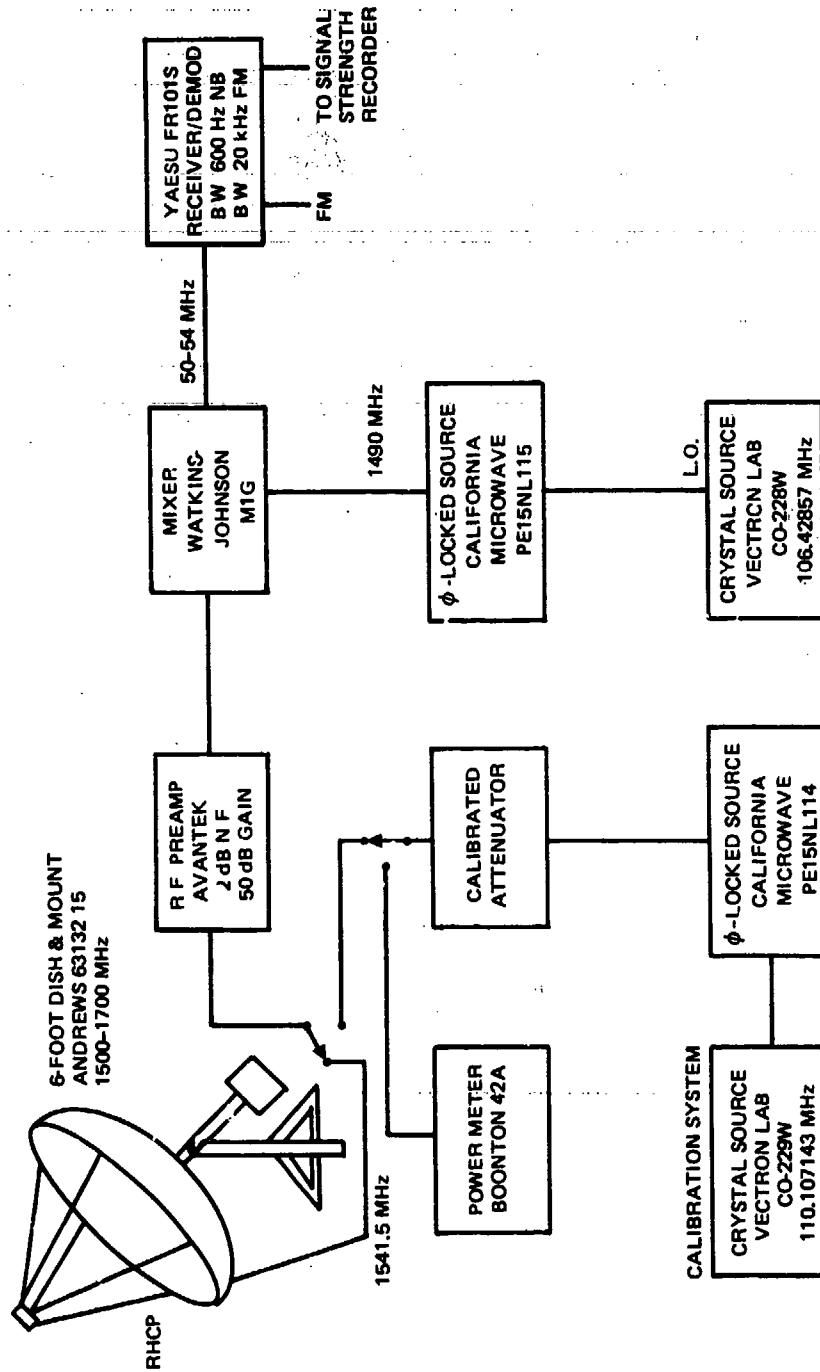


Figure 4. Block diagram of L-band receiver.

DATA PRESENTATION

Scintillation Activity

Periods of scintillation activity at Guam between 1 July and 1 November 1976 are shown in figure 5. The activity during this period was the least observed over four different years of declining sun-spot numbers. In order to quantify this effect the percent of scintillation occurrence over a common eleven-day period for the four years was plotted against the average sun-spot number as shown in figure 6. A direct dependence is evident. The significance of this is that estimates of activity in the near future years can be made. According to an analysis of the solar cycle conducted at NELC, cycle 21 would commence by December 1976 and reach a peak sun-spot number of about 200 around 1981. Cycle 21 began as predicted. Time will reveal if the extent of solar activity several years from now is according to this prediction. The above mentioned analysis is described in reference 2 along with a companion article that compares it with several other predictions for solar cycle 21. If the extrapolation shown in figure 6 is valid, at least six hours of intense scintillation every night might well be expected two to three years from now.

Scintillation activity during the on-site test periods was limited to the extent that some of the system parameter variations could not be accomplished; however, the basic effectiveness of diversity for mitigating the damage caused by scintillation was measured and will be presented in the following paragraphs.

UHF Down-link Diversity Results

Down-link Bit-Error-Rate (BER) measurements were conducted at Guam using 2400 bit-per-second data rate signals transmitted from NELC via the narrow-band alpha channel of the Pacific GAFILLER Satellite. Simultaneous recordings of BER were taken for the diversity system and the system not employing diversity. Figure 7 shows typical results obtained for a one-hour period during strong scintillation. This is the most graphic evidence of the improvement obtained through the use of space diversity with errors as high as 4300 in 10 000 bits recorded using the 18 dB gain OE-82, 16 element array. Curve "B" in the figure indicates that no errors were received by the diversity system for the entire hour of high error rates on the receiver not employing diversity. The diversity system used employed two OE-82, 16 element arrays at the extremes of the 1000 meter baseline and a bifilar helical antenna about 1/3 the total distance from the receiving end. The helical gain was about 4 dB less than the arrays. In order to quantify the above results further, a distribution of error rates observed for the non-diversity case was prepared to show the serious degradation that occurred due to scintillation. The result is shown in figure 8. This shows that 45% of the hour error rates were greater than 10^{-4} and 27% of the time the rate was greater than 10^{-2} . During the same hour 8.64×10^6 bits were received error free using the diversity configuration. In figure 9 a shorter segment of the same period as figure 7 is shown to resolve individual samples and give an indication of how errors are distributed. The following paragraphs address the statistical characteristics of space diversity and considerations relative to configuration optimization.

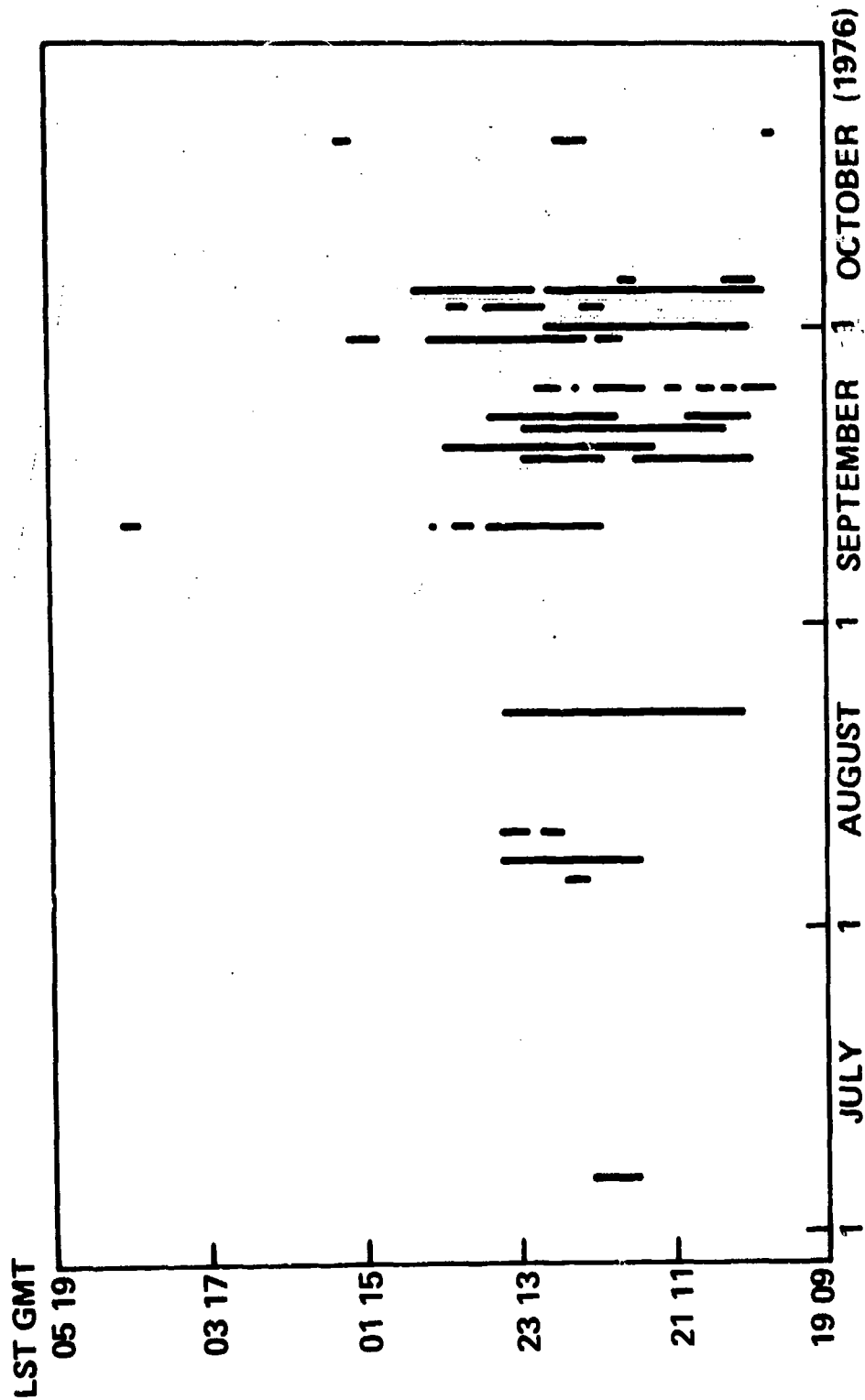


Figure 5. Periods of scintillation occurrences greater than 6 dB below the undisturbed signal at Guam.

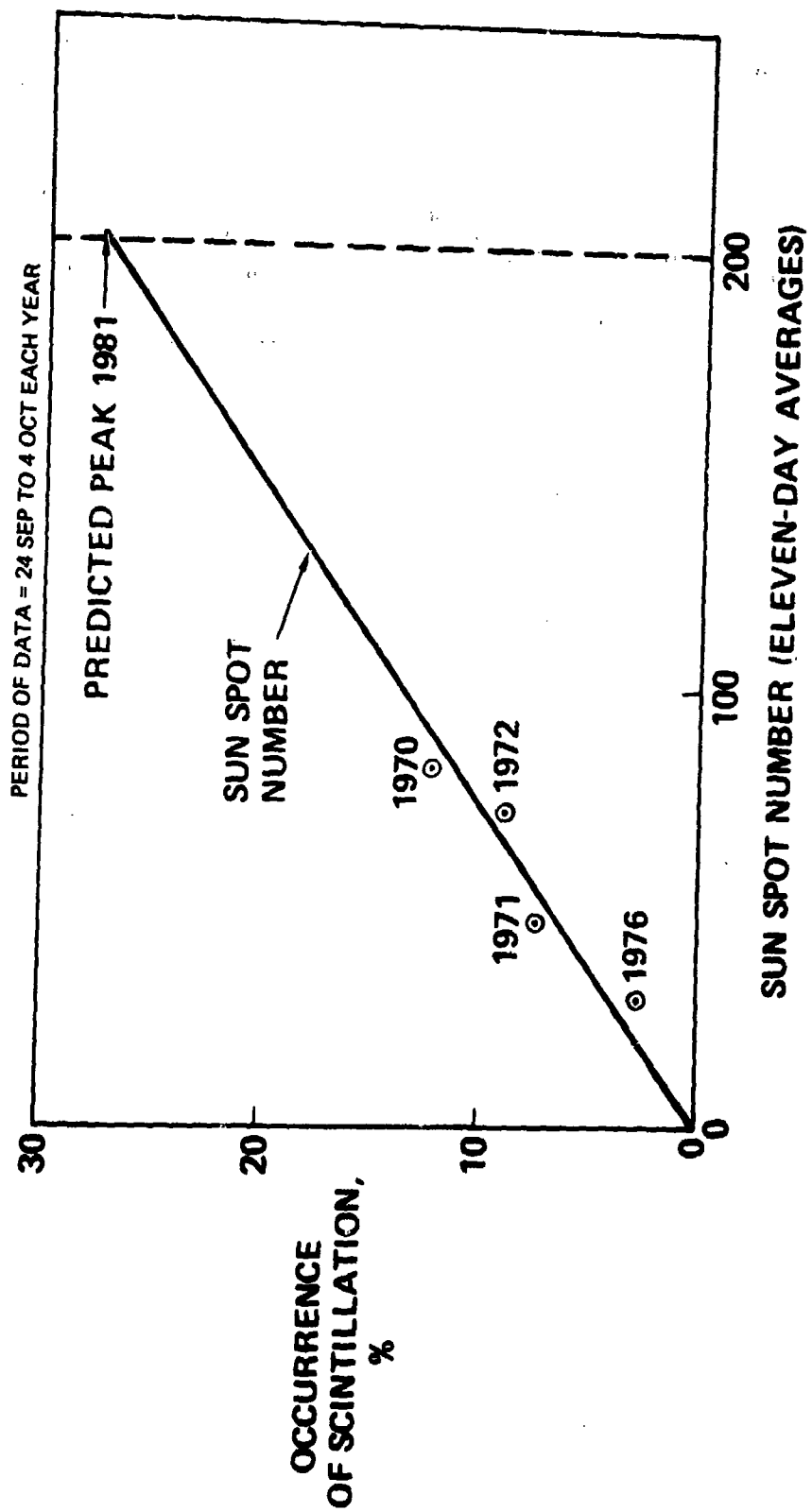


Figure 6. Dependence of scintillation occurrences on solar activity.

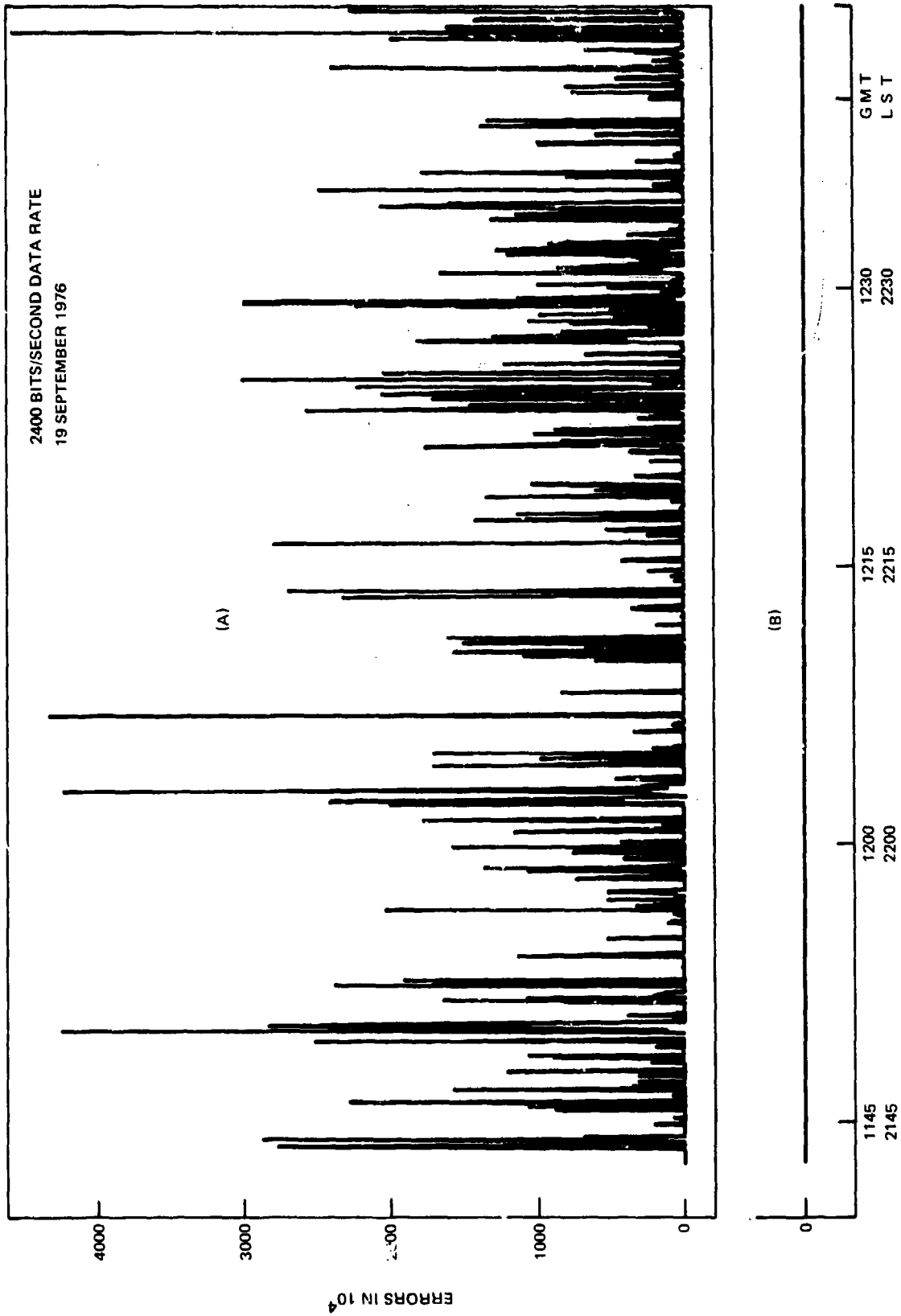


Figure 7. Down-link error rates recorded at Guam: A. No diversity. B. Using diversity.

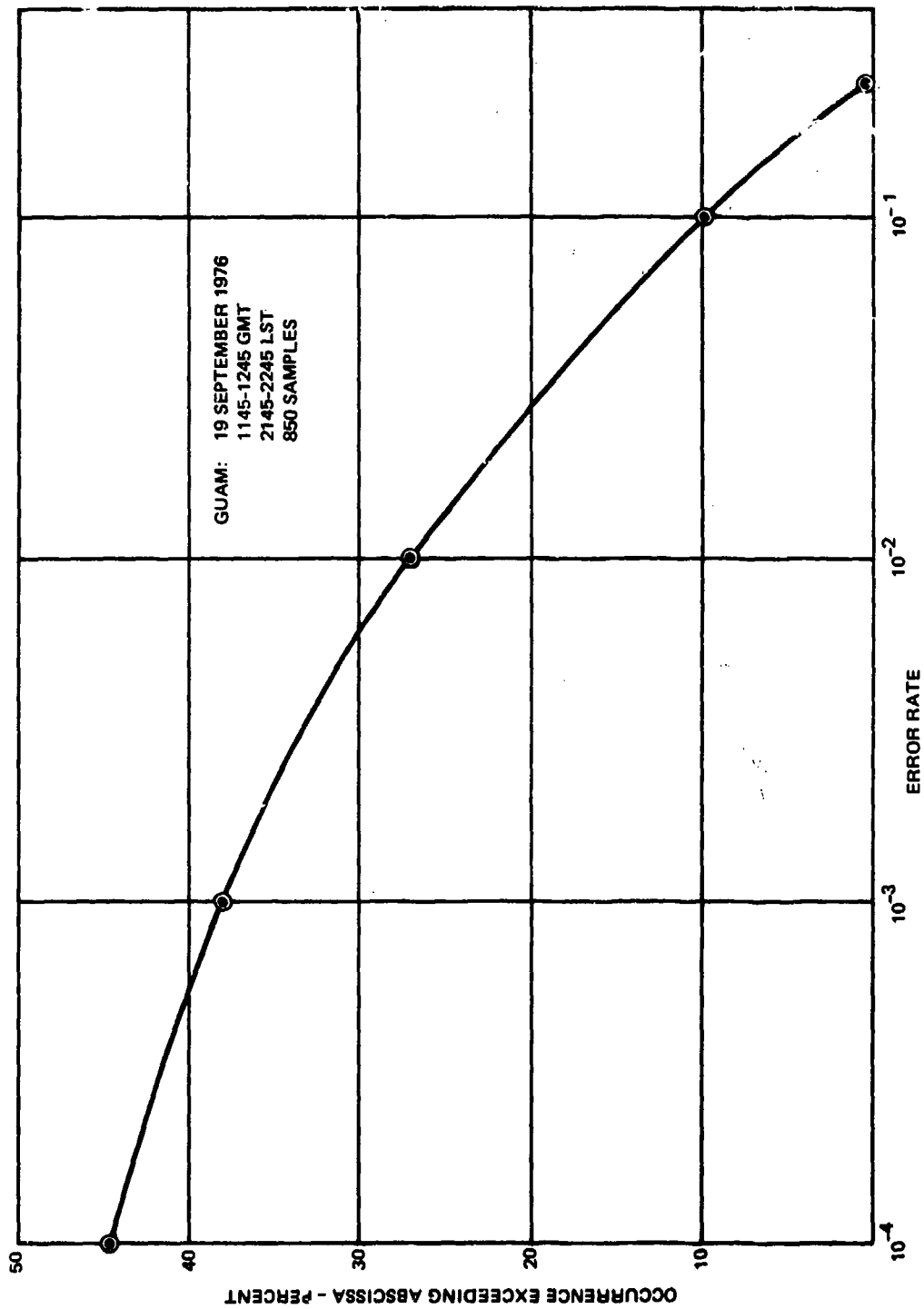


Figure 8. Data error rates during scintillation without the use of diversity.

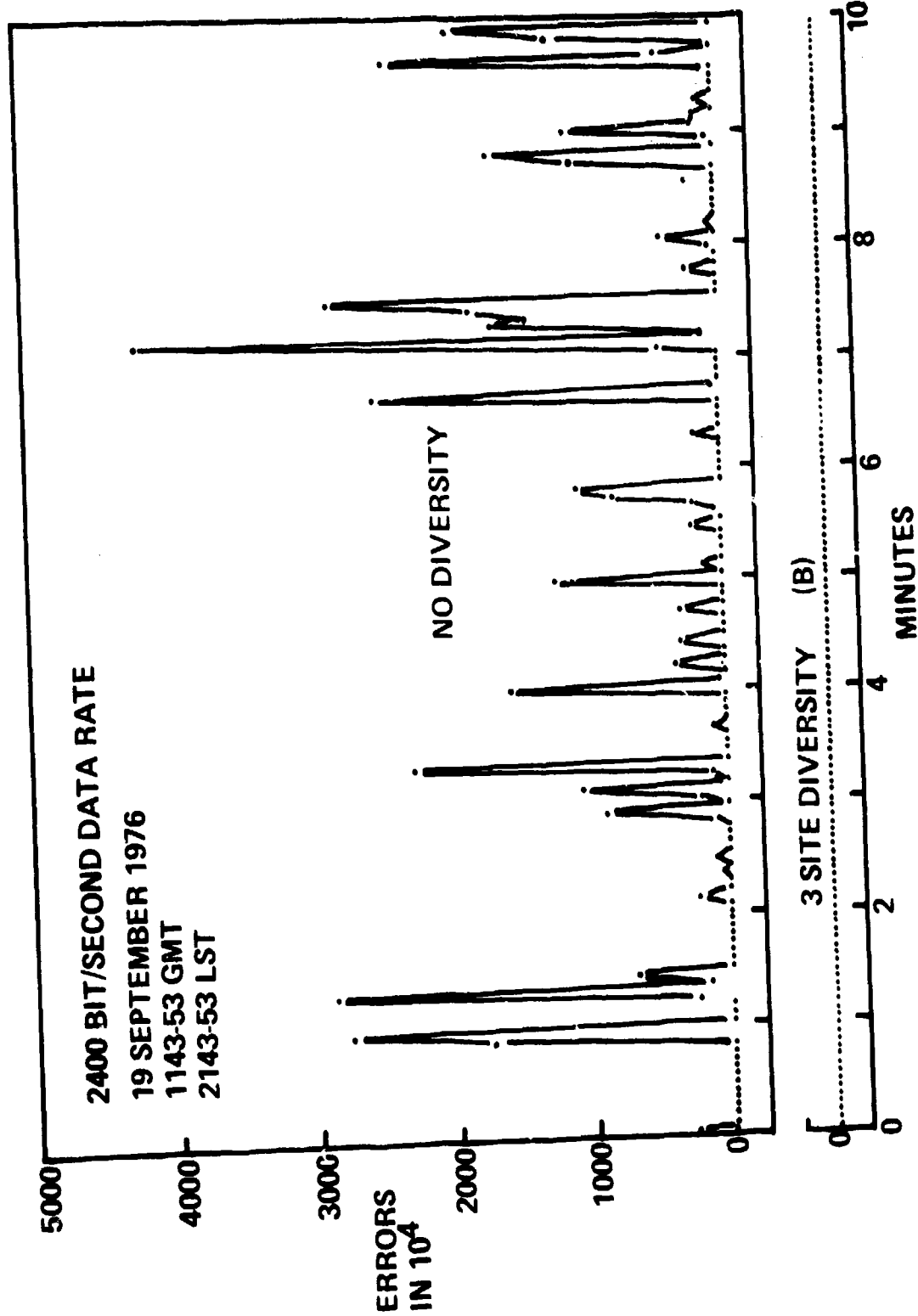


Figure 9. Reception diversity test results.

Space Diversity Characteristics

Effective use of any diversity technique depends upon appropriate processing of two or more signals whose fluctuations are decorrelated. For useful diversity improvement correlation of the fading between channels used should not exceed 0.6. Diversity implementation techniques include ratio squared combining as employed in the AN/SSR-1 employed in the Guam testing. This is an optimal technique which results in 1.5 dB improvement over switching diversity assuming Rayleigh fading. Thus, the up-link switching diversity used in the Guam tests was expected to be only slightly less effective than that used for down-link diversity, however other factors modified this picture somewhat as will be discussed later.

Separate channels of the receiving diversity system were all recorded separately so that computer analyses could be performed on the data to derive complete statistical characteristics of the signals and their inter-relationships. A particularly useful result of this analysis is the spatial correlation function. This is obtained by computing the correlation coefficients for the fading of a given pair of receivers (300, 700 or 1000 meters spacing) as a function of the delay between records. The correlation coefficient at zero delay is the value involved in real-time diversity; however, values at other delays enable determination of performance if a different spacing were used. Figure 10 is an example of the correlation functions for the three spacings during the error distributions shown in figures 7 and 9. In this case the correlation coefficients are all negative at zero delay (delay can be plus or minus) indicating that any of the baselines chosen would provide useful diversity. The diminishing correlation peak as the baseline lengthens is evidence that the scattering irregularities in the ionosphere responsible for the scintillation are changing structure as they drift to the East. Obviously the shortest baseline exhibiting adequate decorrelation of fading would be used in a diversity application. Figure 11 shows how the correlation functions vary with time. From curve 1 to 5 the correlation peak essentially disappears then reappears during sample 6. The delay of the correlation peak provides a means to determine the effective drift velocity and therefore, the spatial distance between points on the correlation function. For instance, the minimum correlation for curve 1 occurs at about plus twelve seconds for the 300 meter baseline. Since the drift time over the 300 meter baseline is about 10 seconds according to the delay of the correlation peak, an additional spacing of 360 meters ($12/10 \times 300$) or a total of 660 meters would have placed the minimum correlation at zero time delay and provided the optimum diversity spacing. However, it is evident this is a function of time and some average value must be chosen. More on this point will be considered below. Figure 12 is a set of correlation functions obtained for the same sample interval in July 1976. In this set the position of the 3 correlation minima are clearly shown with the 700 meter baseline being nearest optimum for diversity purposes.

In order to examine the variation of the correlation functions with time 3 values of the function were plotted as a function of time: The Correlation Maxima, the Minima and the Value at Zero Delay. The results are shown in figures 13-24. There are 3 figures for each day, one for each of the baselines used. Determination of the optimum diversity spacing over the long time periods shown is of particular interest. This is the condition met when the zero delay line most nearly matches the minimum correlation line. It is readily apparent on scanning the various days and baseline configurations that the 700 meter baseline was the optimum spacing of the three for these days. The correlation coefficients for all baselines were always low enough to provide effective diversity improvement, however, thereby providing some latitude in choice of the baseline dimension. Another way to present the test data to examine time dependency is shown in figures 25-29. These are

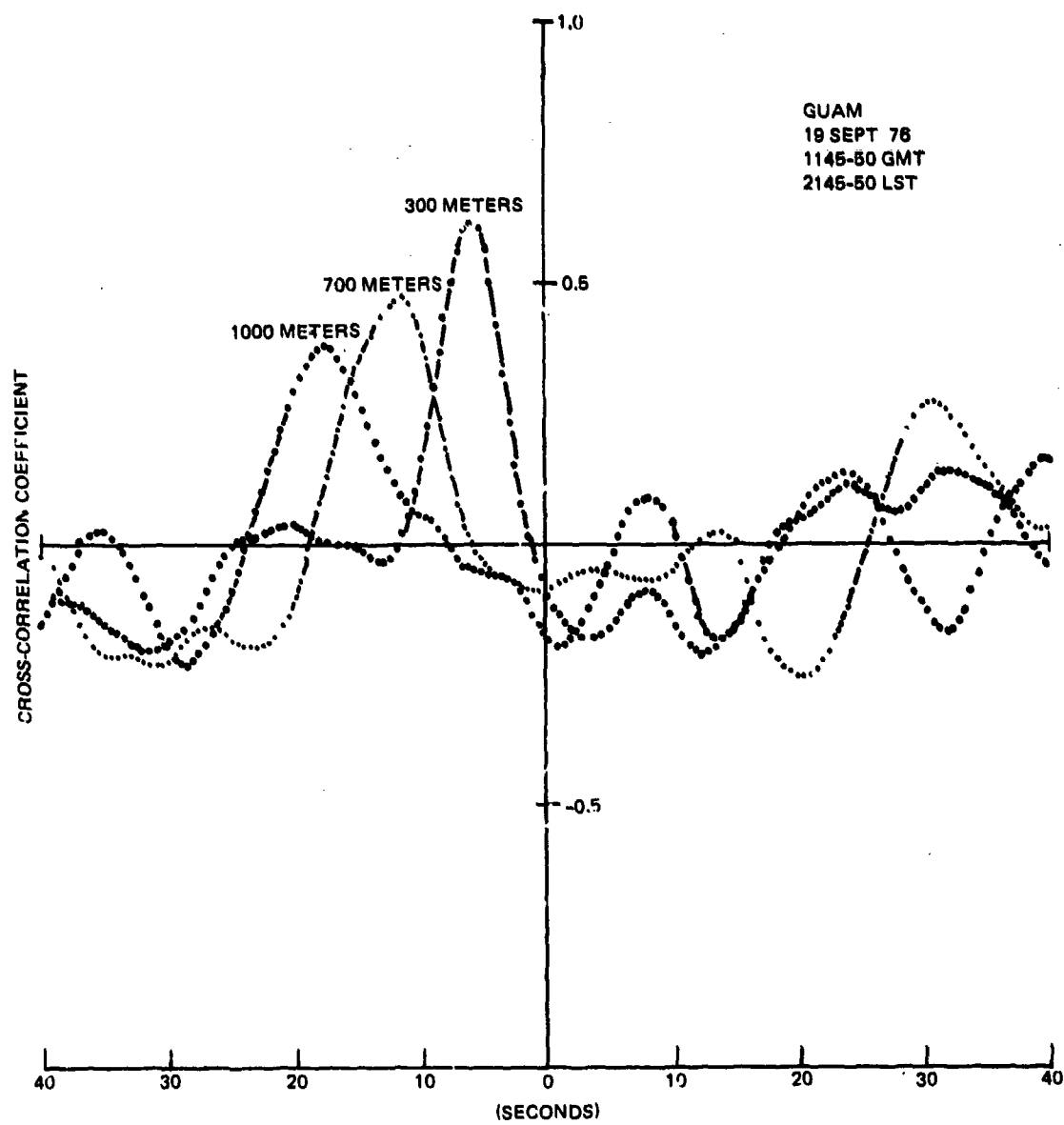


Figure 10. Spatial cross-correlation functions for 3 antenna separations.

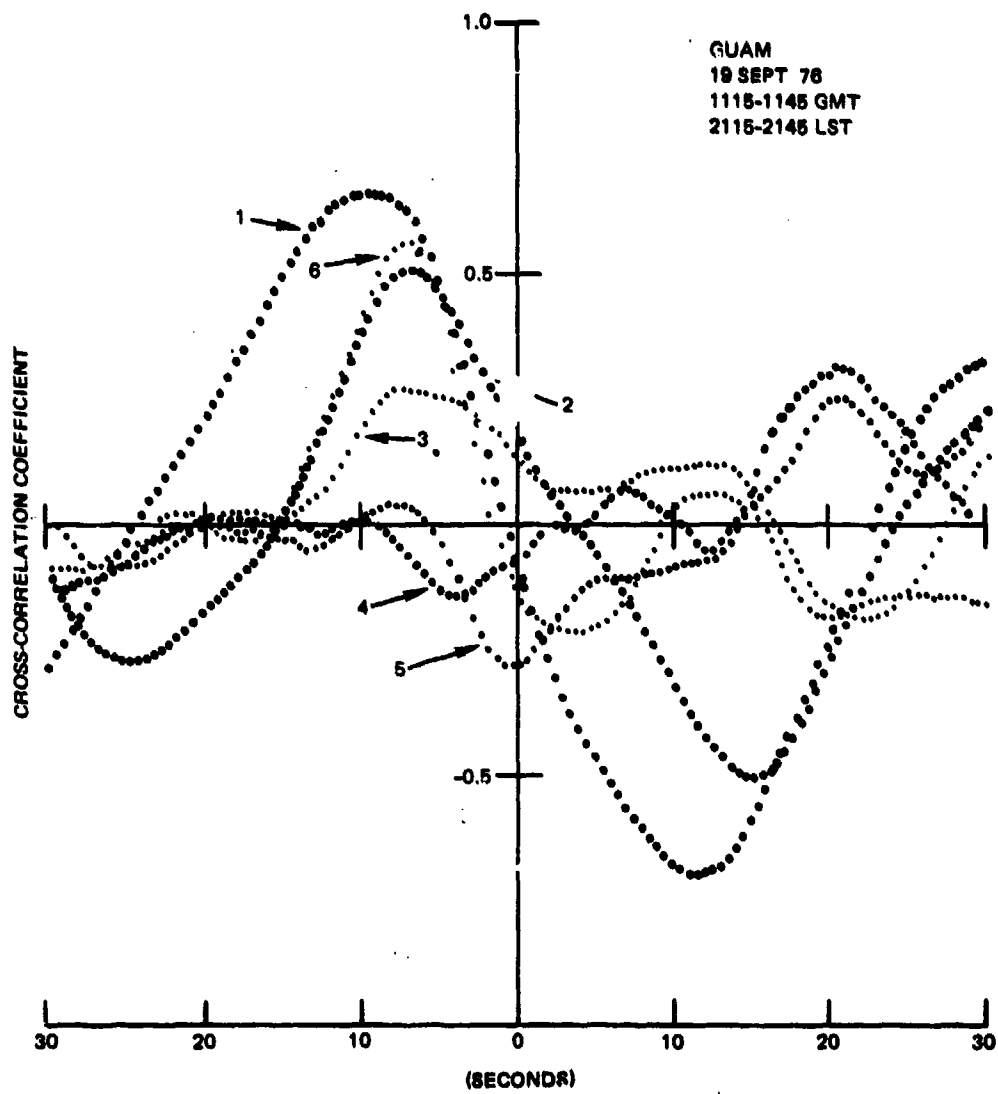


Figure 11. Cross-correlation curves for five-minute samples starting with curve 1 at 1115-1120 GMT. Spacing was east-west at 300 meters.

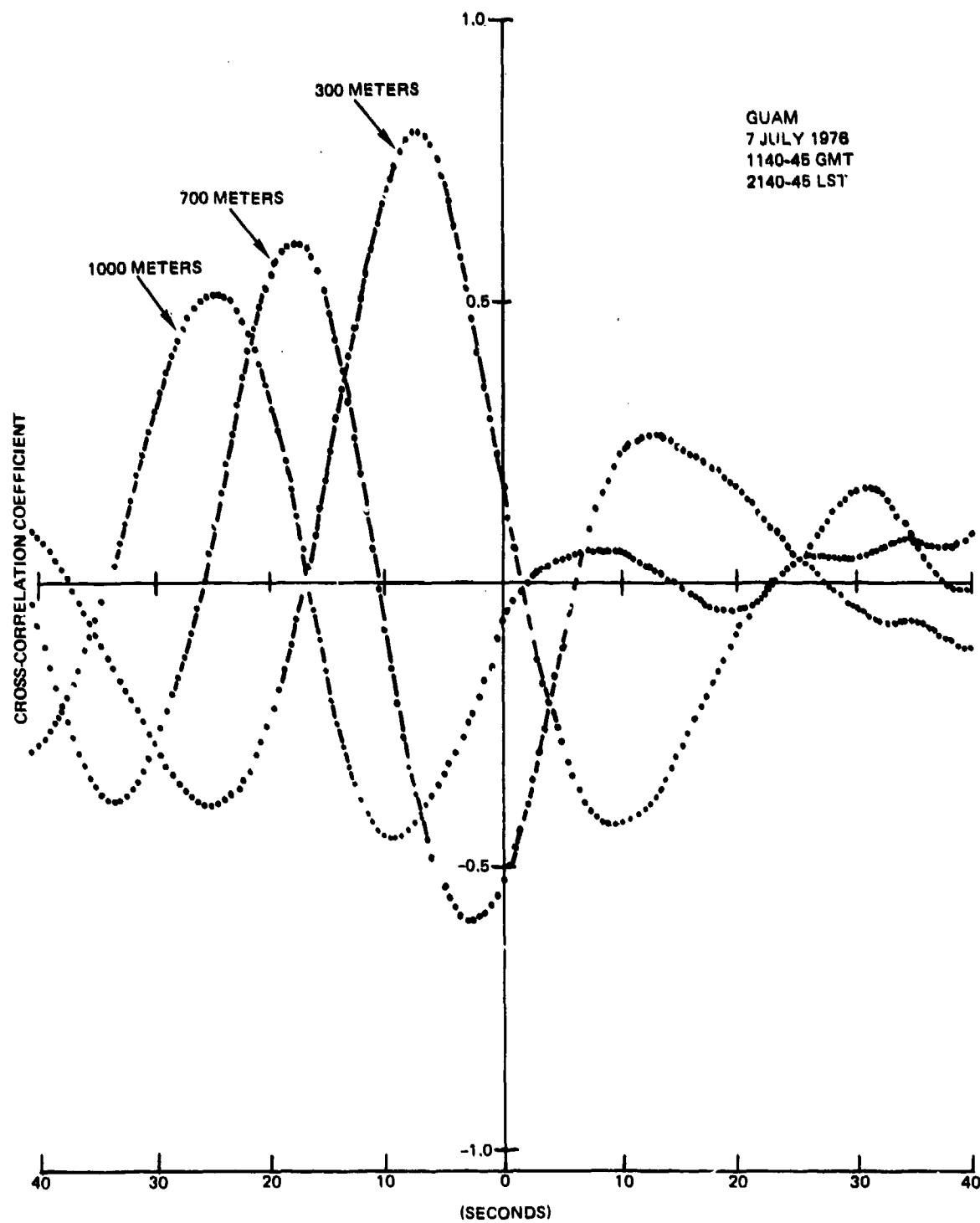


Figure 12. Correlation between fading signals received with 3 different antenna spacings in the east-west direction as a function of time lag between the recordings.

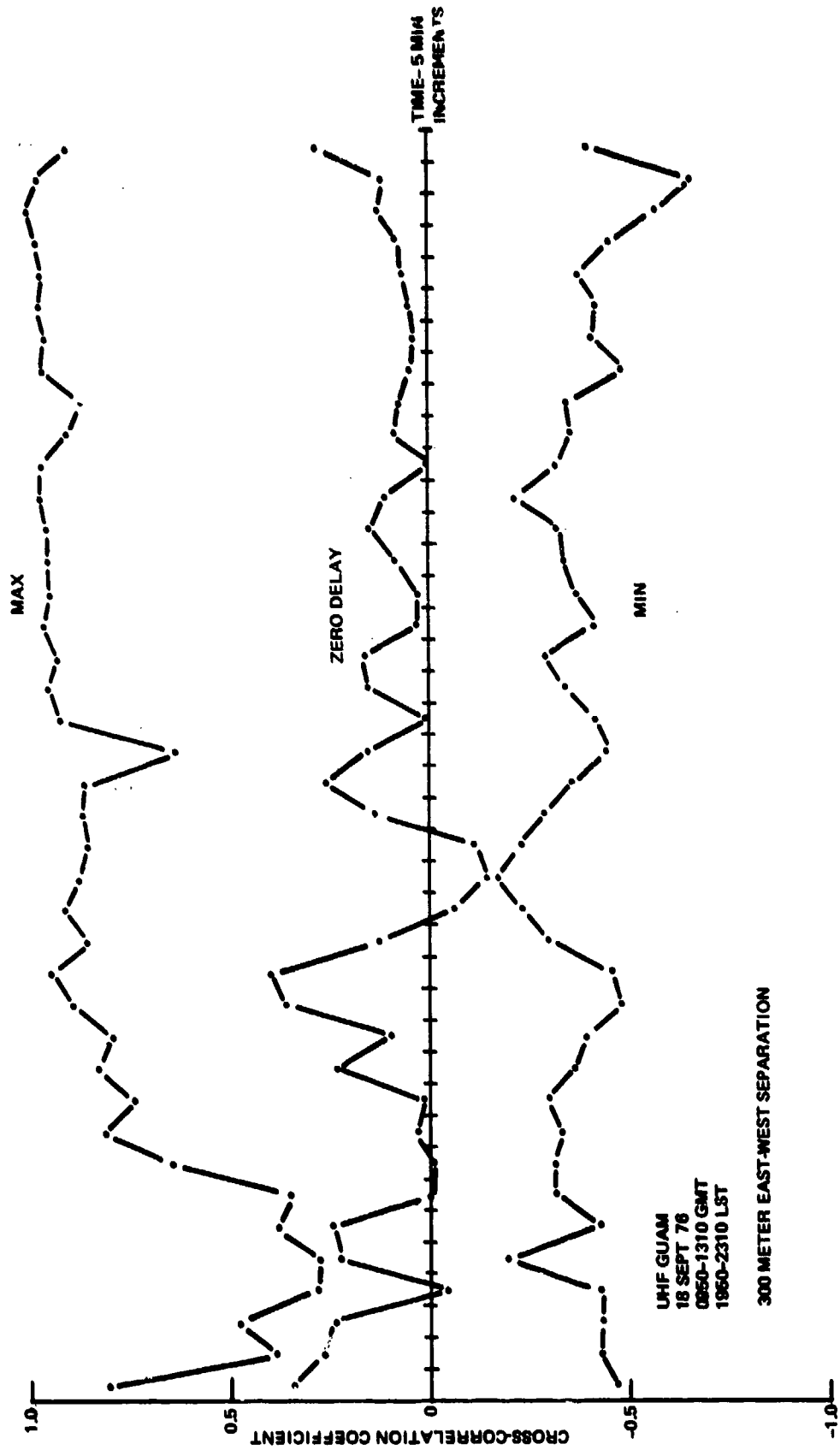


Figure 13. Temporal variation of ρ values taken from the correlation functions.

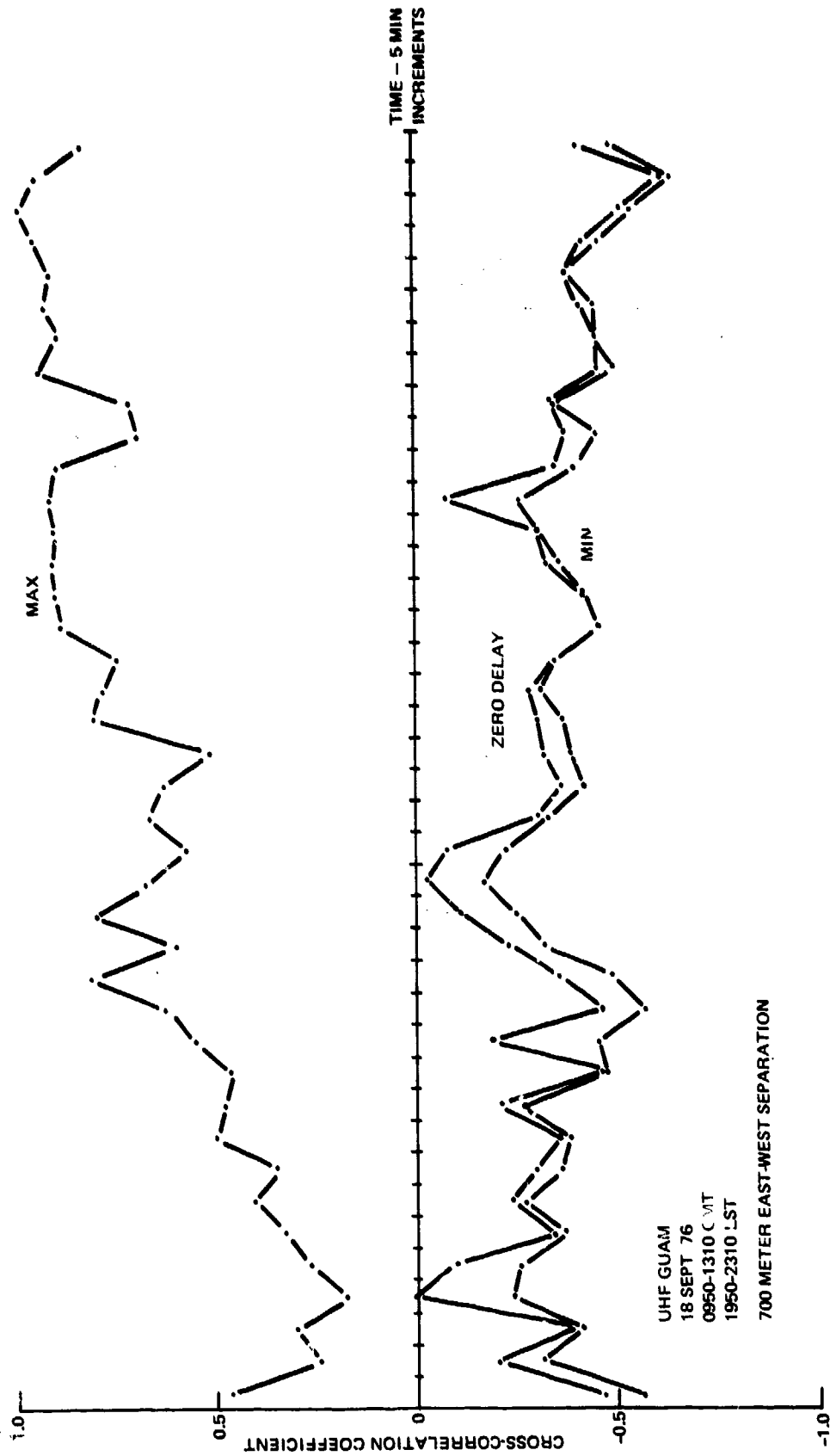


Figure 14. Temporal variation of 3 values taken from the correlation functions.

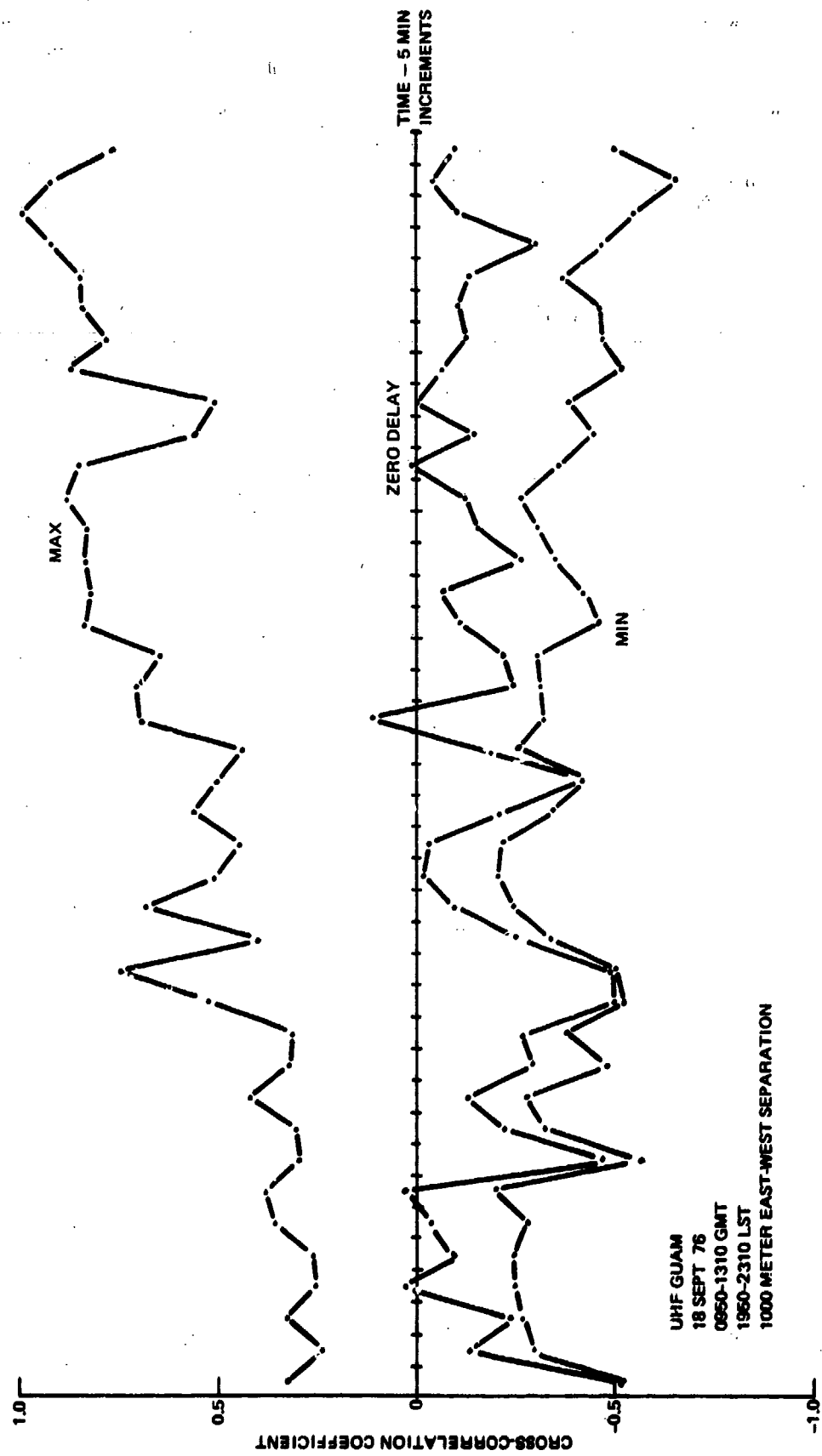


Figure 15. Temporal variation of 3 values taken from the correlation functions.

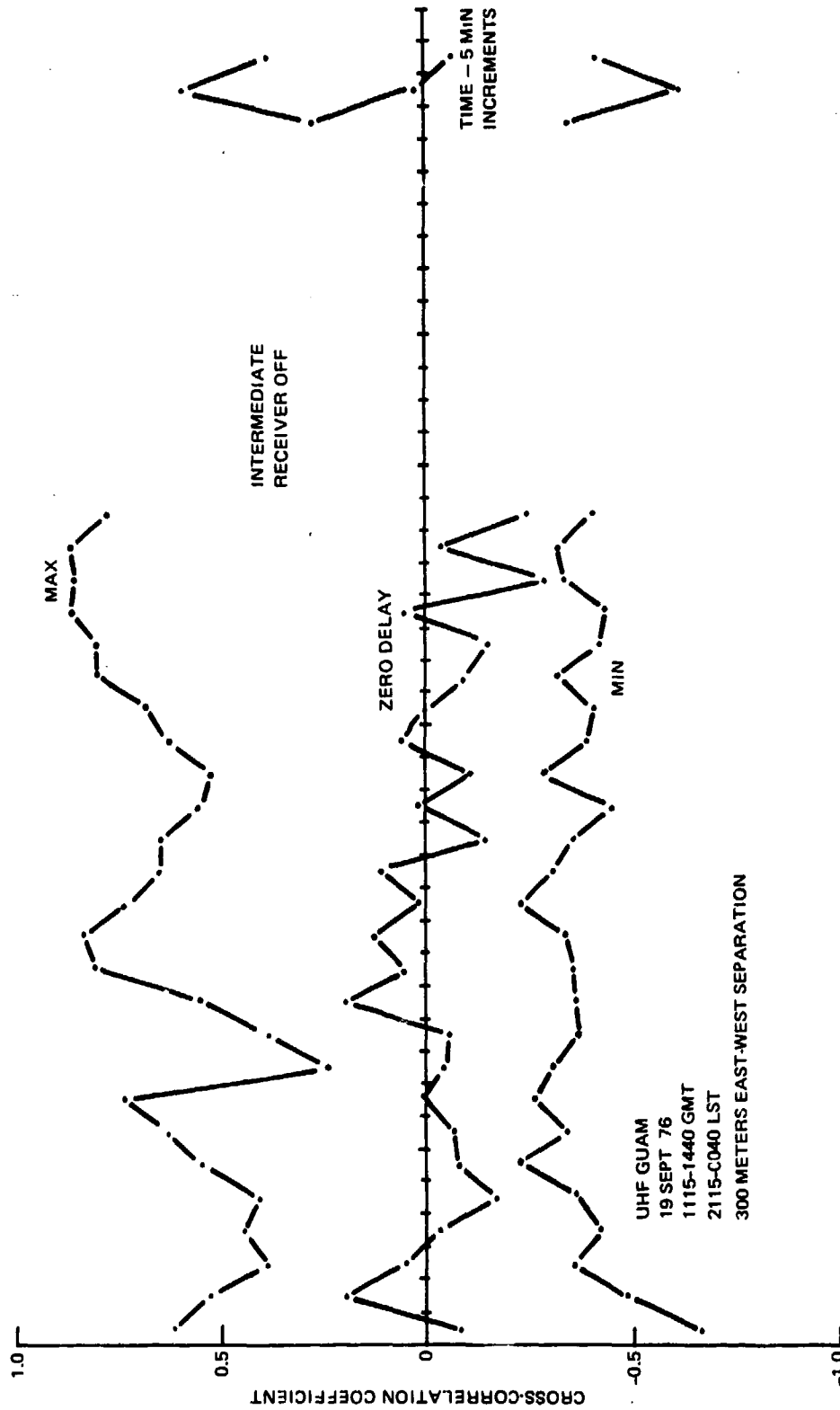


Figure 16. Temporal variation of 3 values taken from the correlation functions.

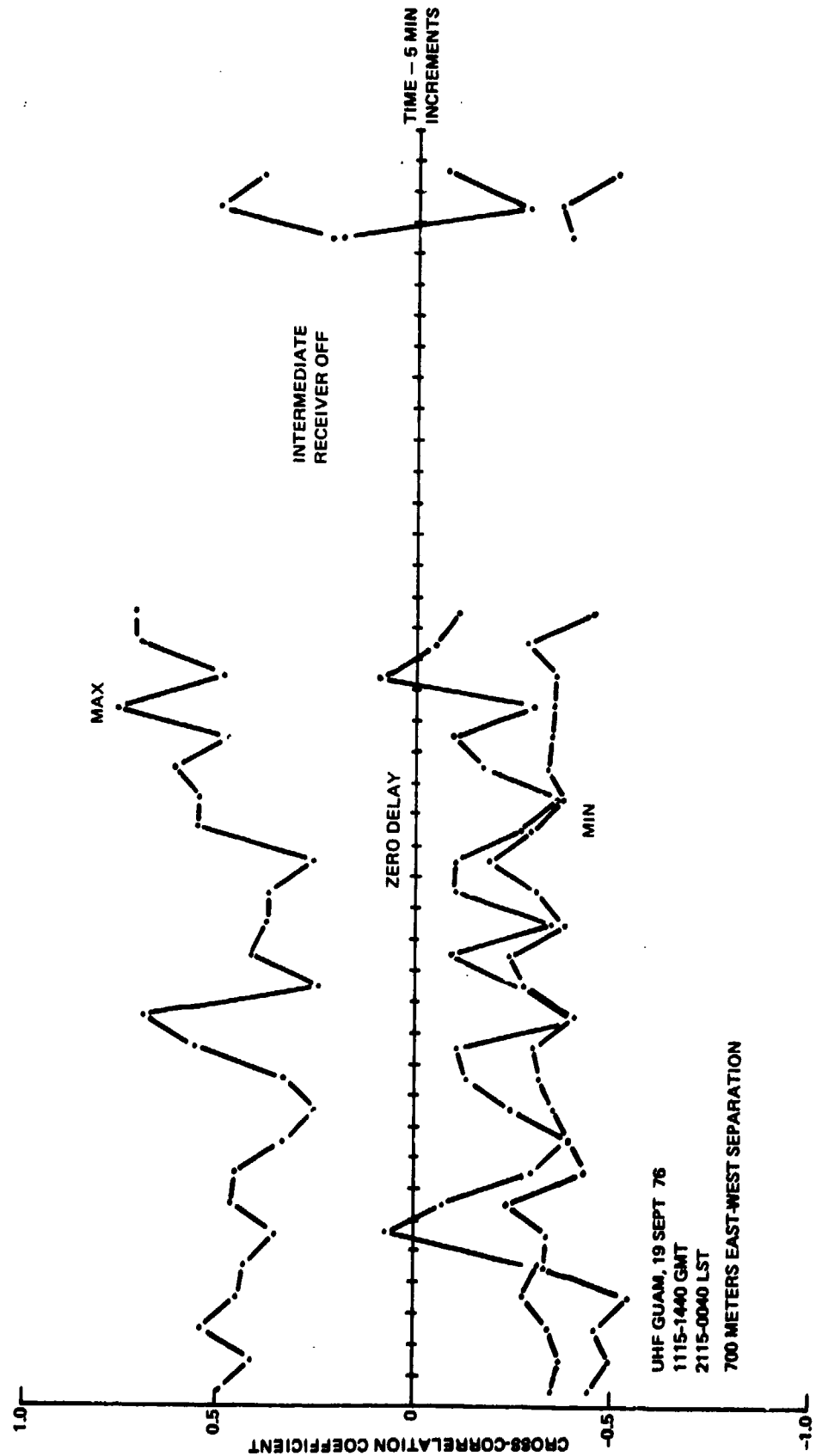


Figure 17. Temporal variation of 3 values taken from the correlation functions.

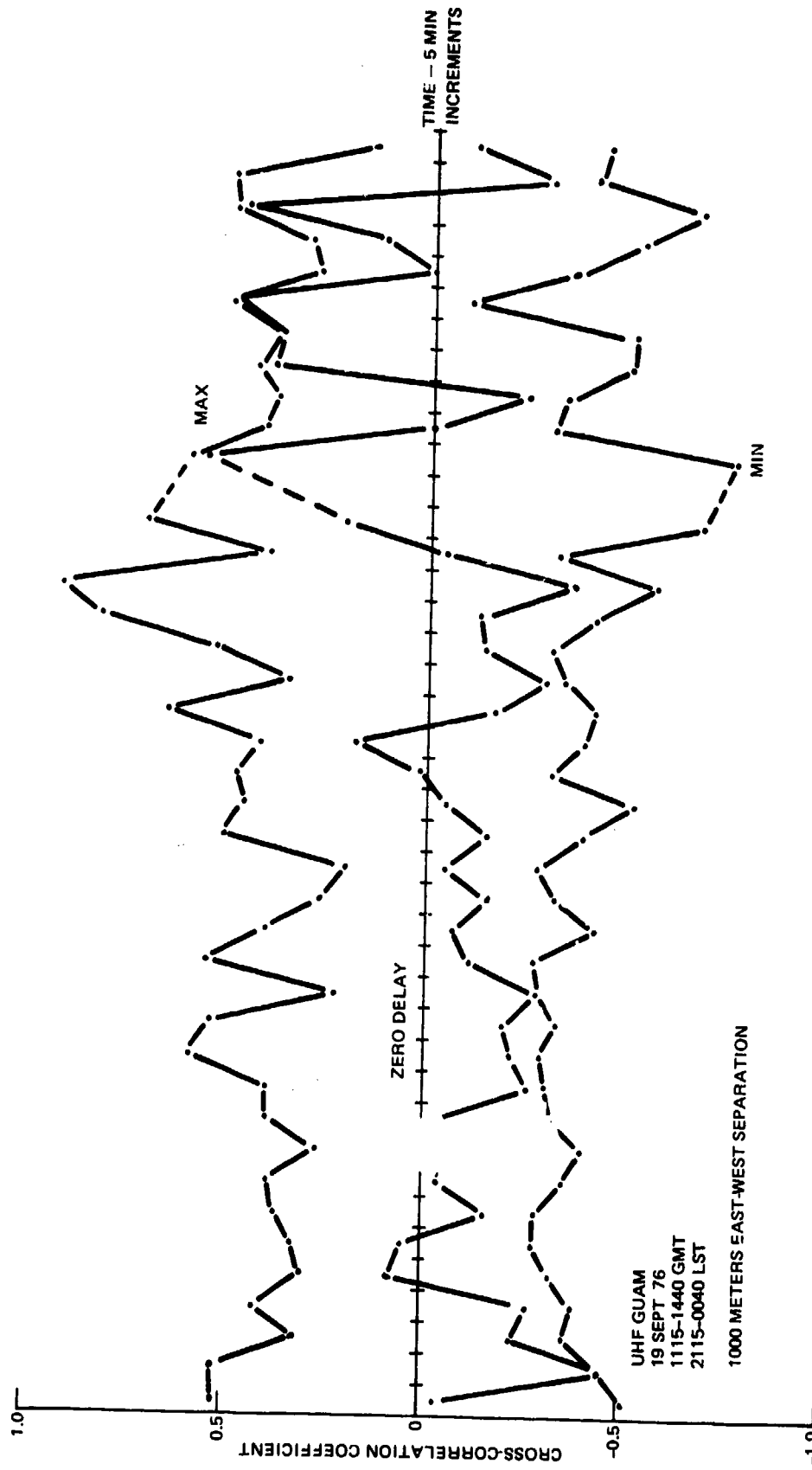


Figure 18. Temporal variation of 3 values taken from the correlation functions.



Figure 19. Temporal variation of 3 values taken from the correlation functions.

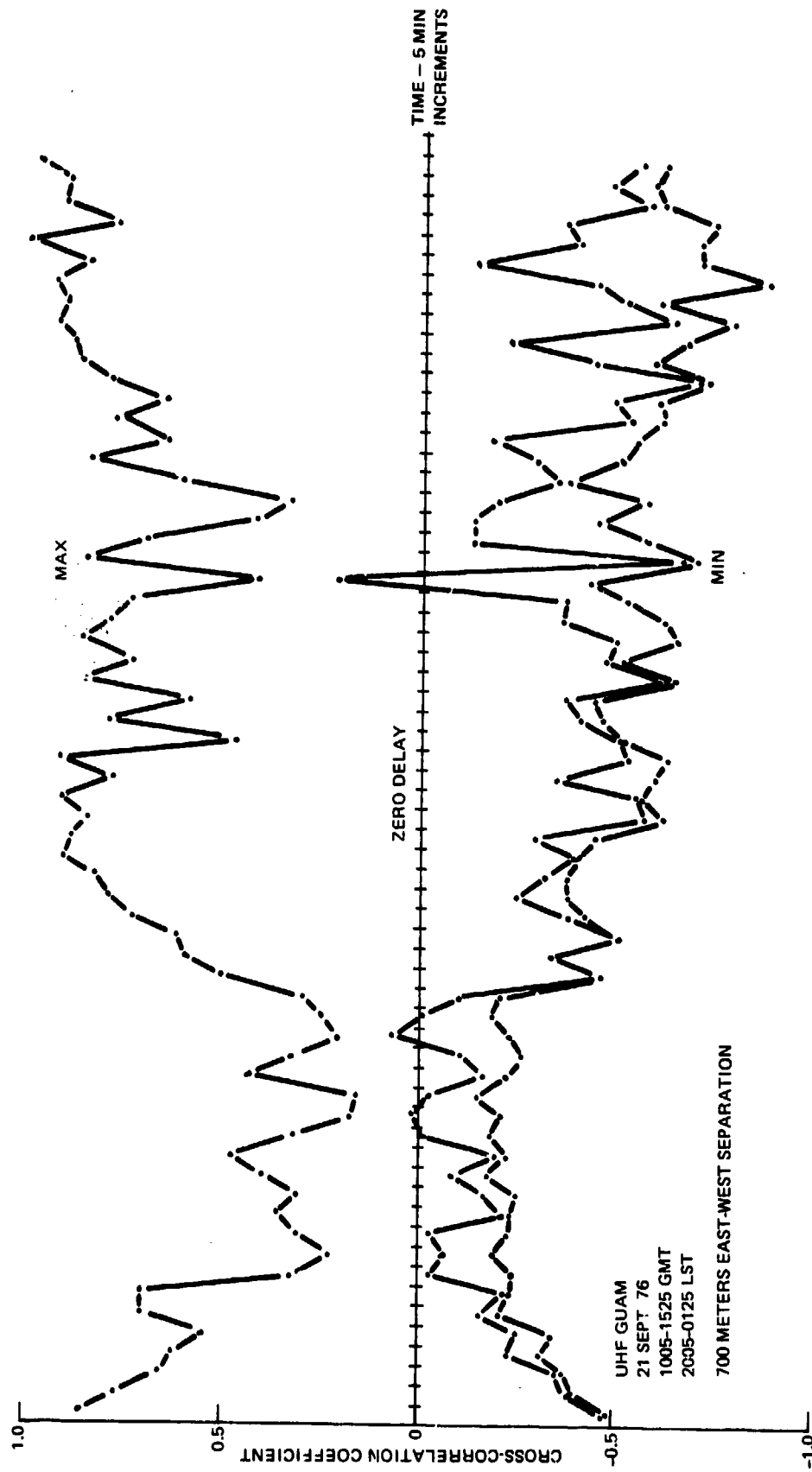


Figure 20. Temporal variation of 3 values taken from the correlation functions.

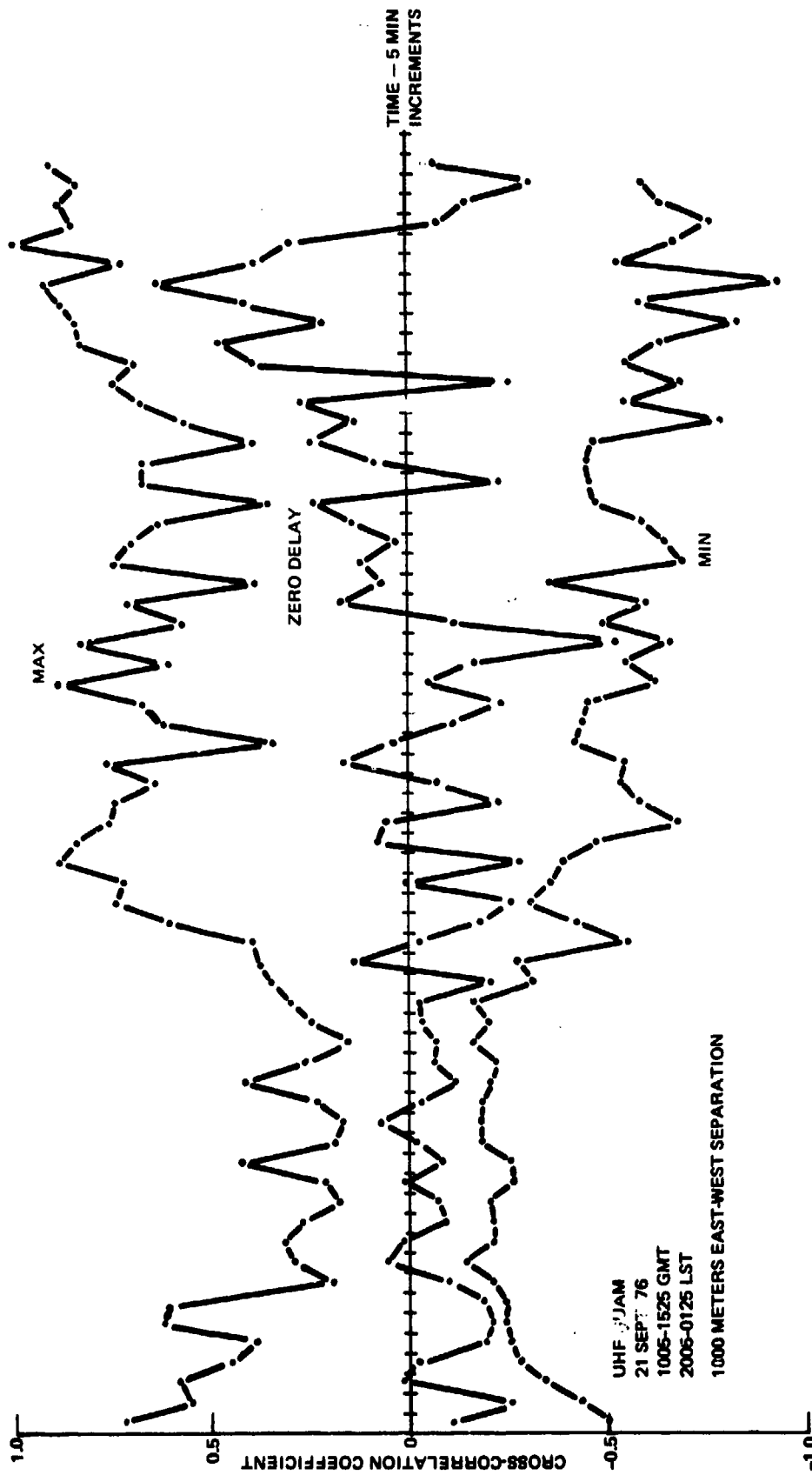


Figure 21. Temporal variation of 3 values taken from the correlation functions.

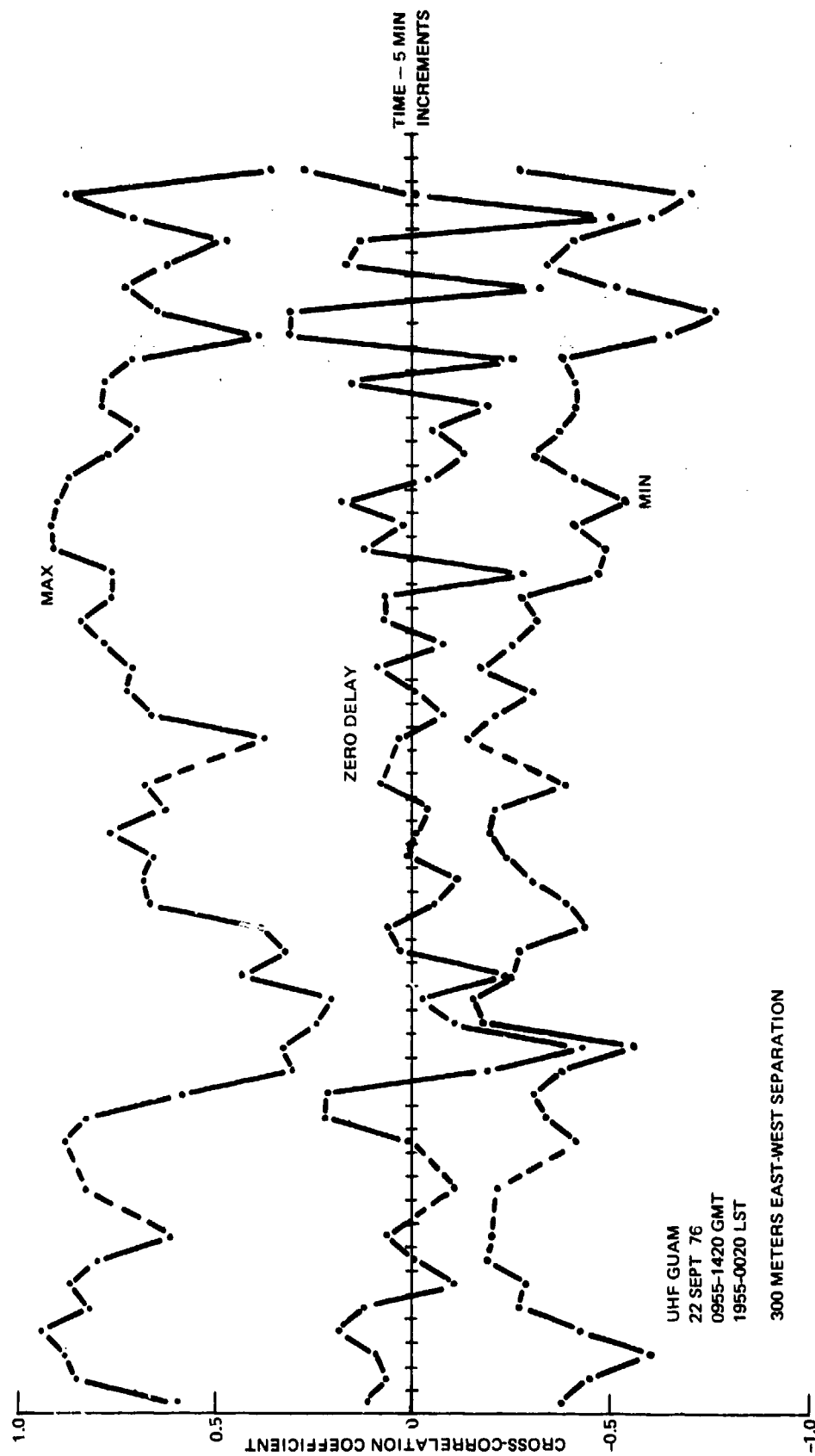


Figure 22. Temporal variation of 3 values taken from the correlation functions.

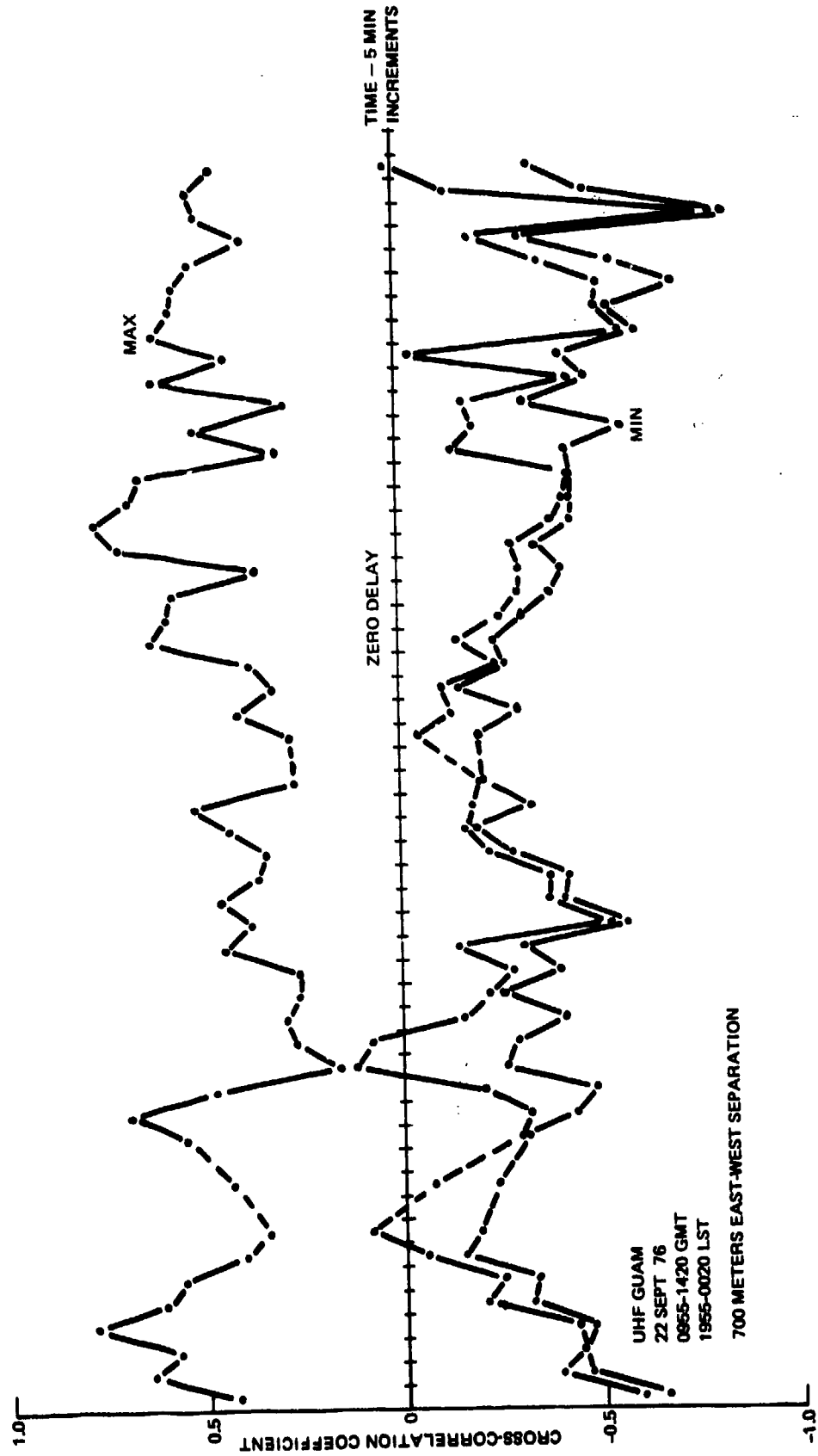


Figure 23. Temporal variation of 3 values taken from the correlation functions.

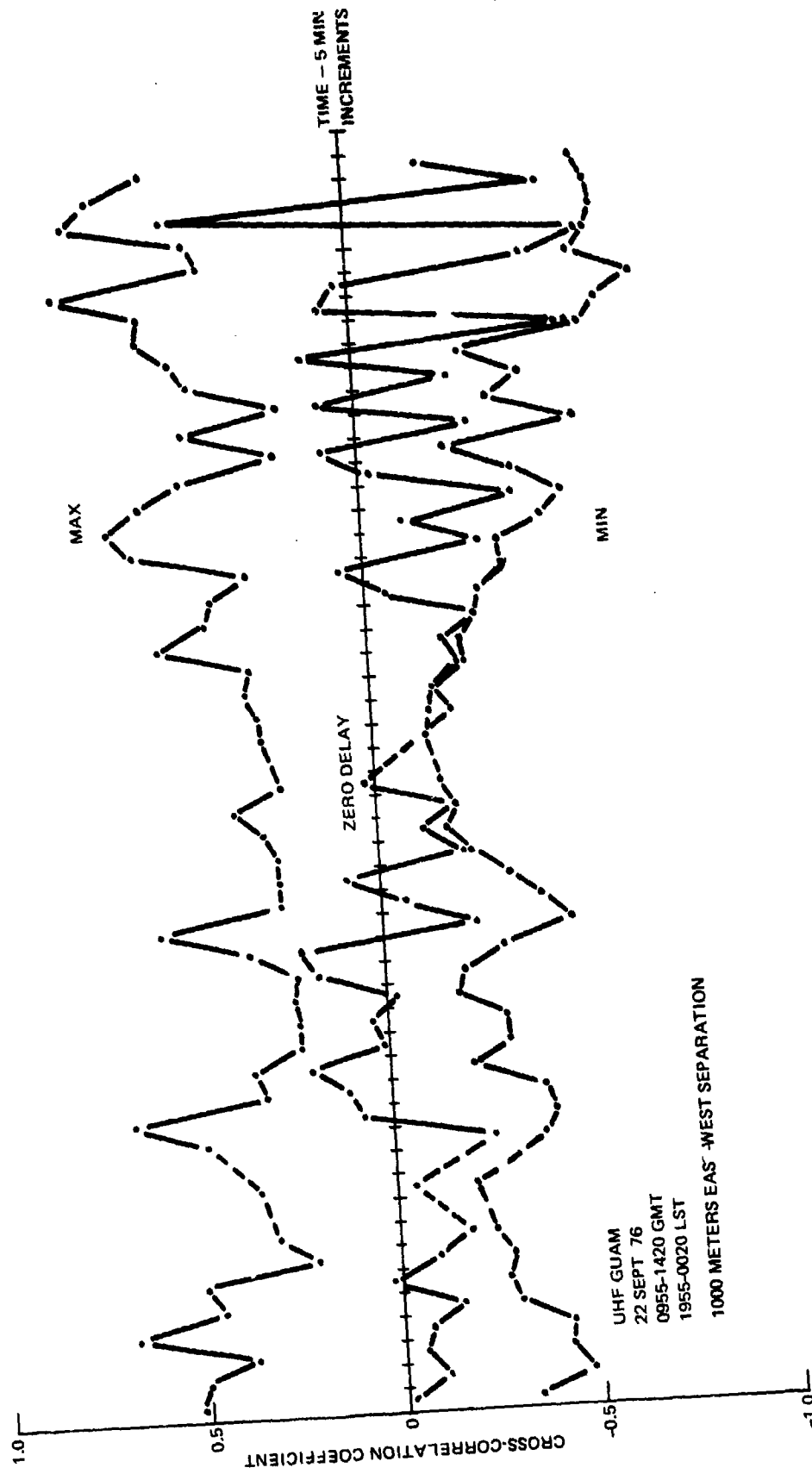


Figure 24. Temporal variation of 3 values taken from the correlation functions.

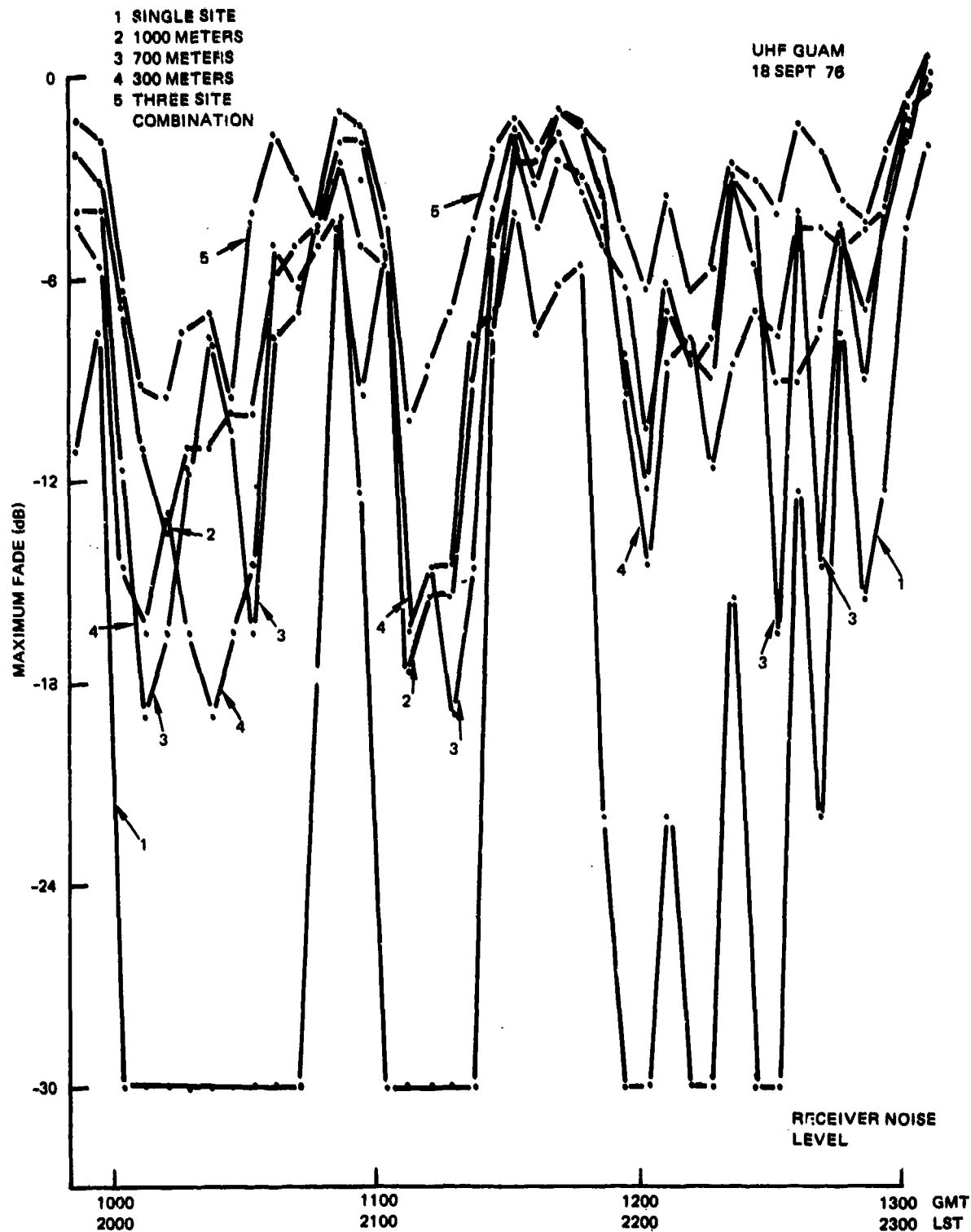


Figure 25. Maximum fades observed for five-minute samples as a function of time for different signal combinations.

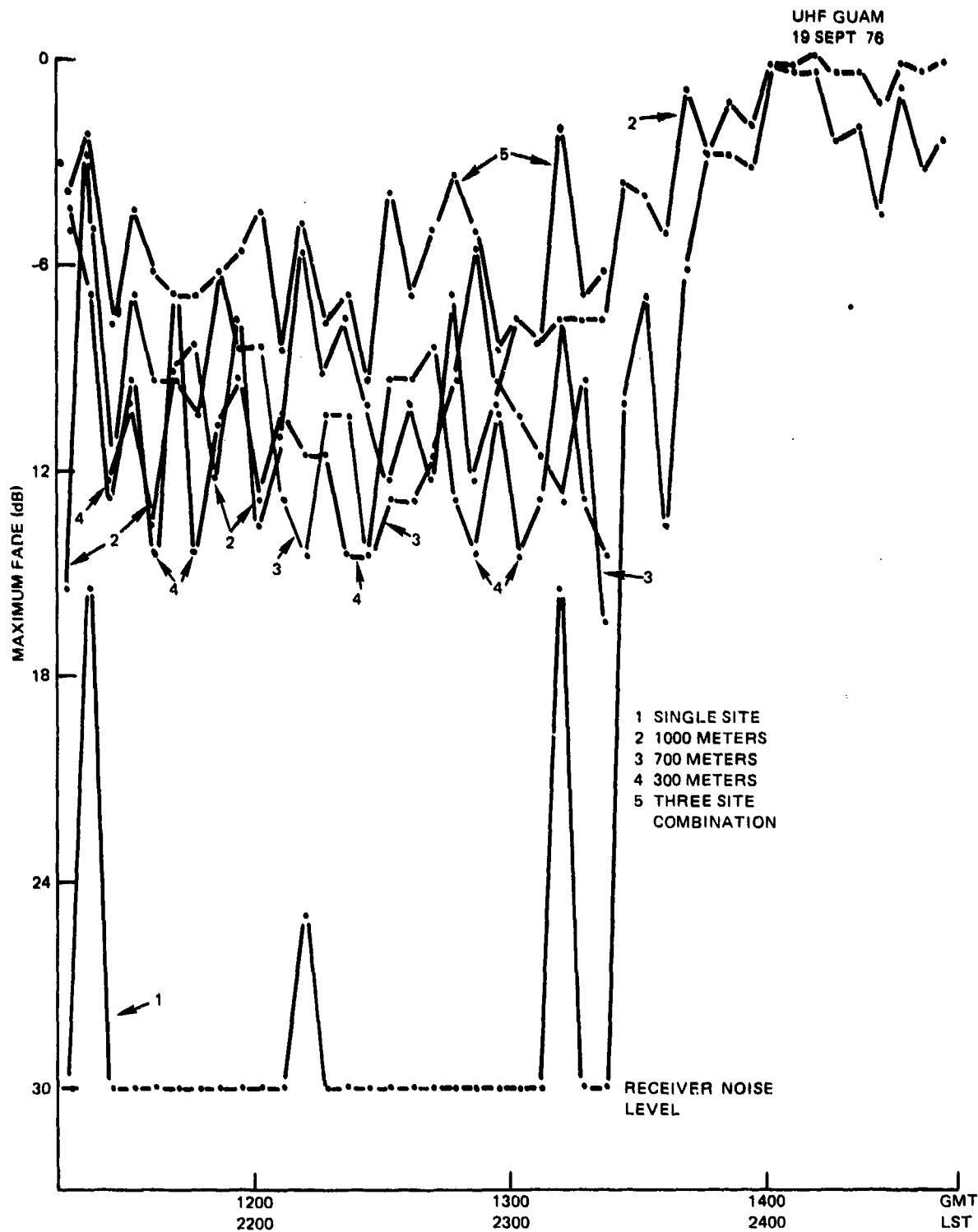


Figure 26. Maximum fades observed for five-minute samples as a function of time for different signal combinations.

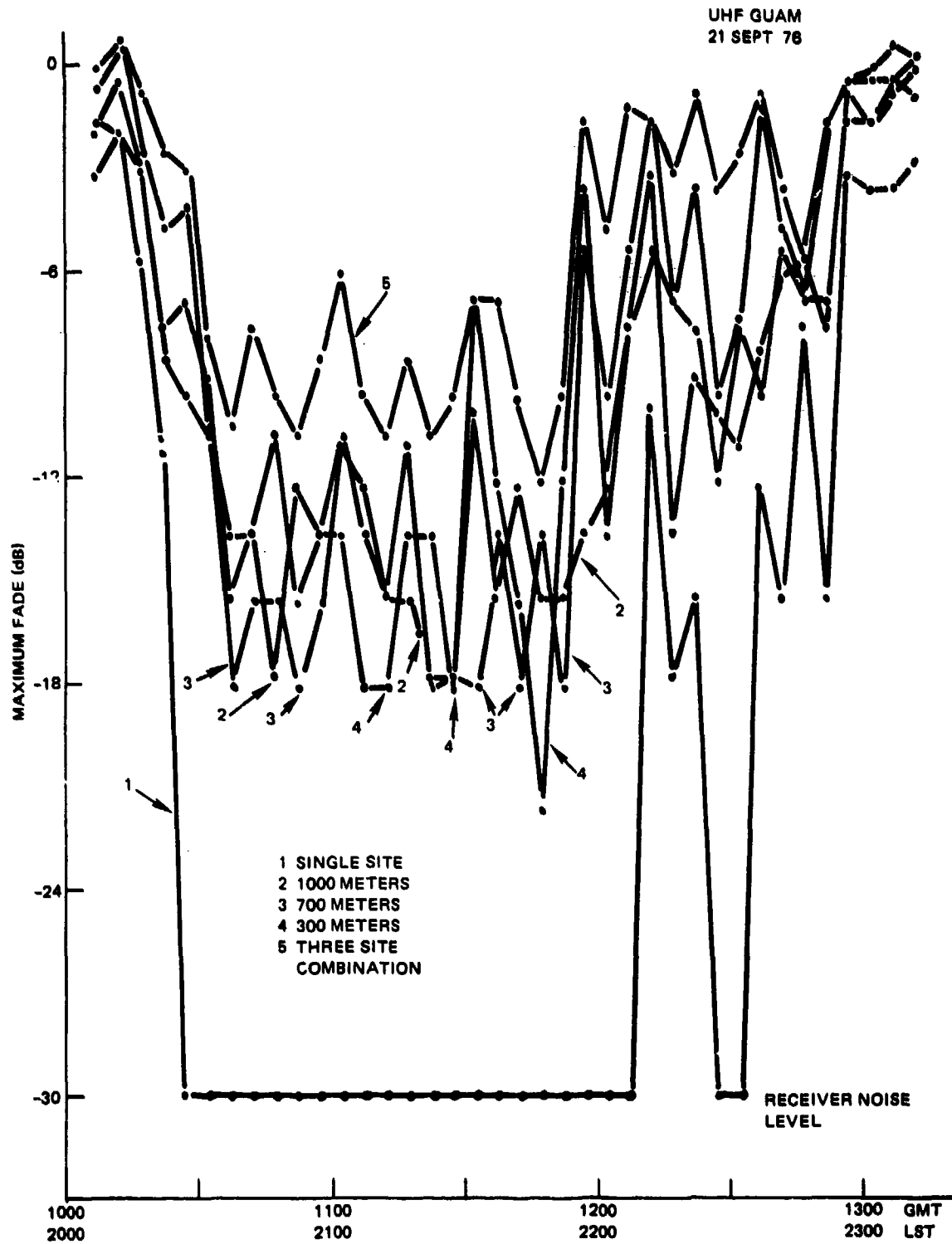


Figure 27. Maximum fades observed for five-minute samples as a function of time for different signal combinations.

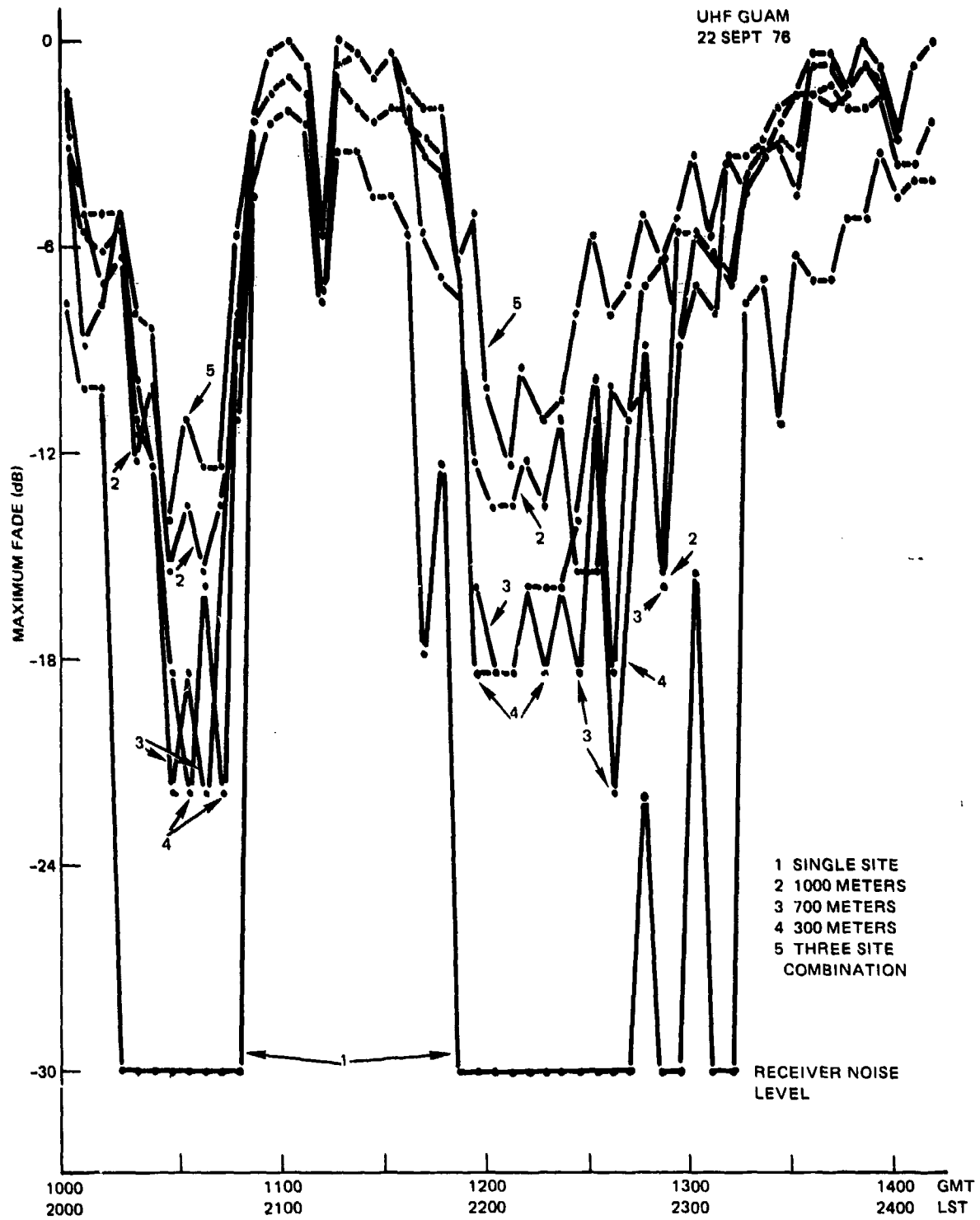


Figure 28. Maximum fades observed for five-minute samples as a function of time for different signal combinations.

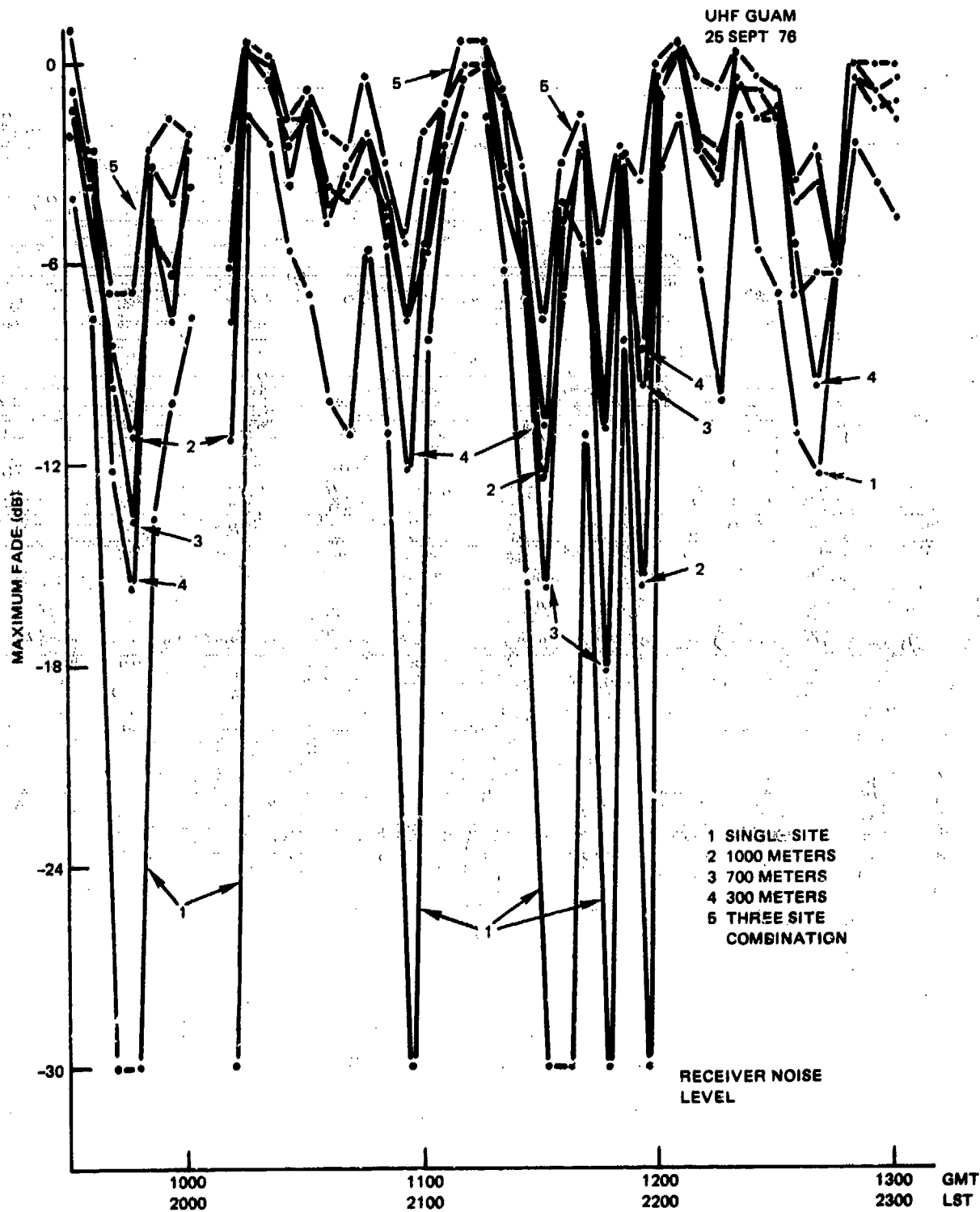


Figure 29. Maximum fades observed for five-minute samples as a function of time for different signal combinations.

plots of maximum fades observed during 5 minute sample periods for various diversity combinations. Observation of the 19 September plots shows that during intense scintillation when the single channel receiver was fading greater than 30 dB, the two channel diversity combinations reached fades of 15 dB at most and the 3 channel combination stayed above the 10 dB fade level. The period from 1145 to 1245 GMT was the period of the error rate comparison shown in figure 7. Similar results prevailed during other periods of intense scintillation.

Cumulative probability distributions (CDFs) provide a statistical representation of the signal fading and demonstrate quantitatively the diversity gain of the various combinations tested. CDFs for the 1145-50 GMT period on 19 September are shown in figure 30 with the lower decile reproduced in figure 31 for better resolution. Here, again, the 300 meter baseline dual diversity exhibits deeper fading than the longer baselines and the combination of three is most improved over the single channel. An important point to note is that all of the CDFs show signal enhancements of 10 dB above the mean or undisturbed signal. Extreme amplitude variations are evident without the use of diversity which would have the effect of completely disrupting power balance of up-links in multiple carrier per channel (GAPFILLER wideband) systems. As higher order diversity is used the power swings are minimized.

UHF Up-link Diversity Results

Up-link diversity measurements were conducted by transmitting alternate ten-minute periods with and without diversity from Guam. 2400 bits per second data containing PN sequence structure enabled measurement of error rates at the receiving location in San Diego for each alternate mode. The 1000 meter baseline system was used for this test. Results of a two-hour run during intense scintillation (see figure 27) are shown in figure 32. These results are not as impressive as the down-link results since the improvement only resulted in a reduction of errors by a factor of 2. These data were obtained under conditions that proved to be sub-optimum. Reference to figure 21 indicates that correlation coefficients for the 1000 meter baseline, though low, were somewhat above the minimum values that occurred. This coupled with possible decorrelation between the down-link sensing frequency and the up-link frequency may explain the less than satisfactory up-link diversity results. Parametric variations in up-link power were planned, but could not be performed because of the limited scintillation activity.

It must be concluded that the optimum up-link diversity configuration remains uncertain and further tests will be required to determine its ultimate value. One positive result of the up-link diversity tests was the excellent performance of the switching technique developed for this purpose. A 3-level diversity switch logic has been considered which could be readily implemented to add another dimension to an up-link diversity system.

L-Band Diversity Results

Equatorial scintillation data at L-Band was obtained simultaneously with the UHF data with receivers spaced on the 1000 meter baseline. The L-Band results will be used to estimate the effects on performance of the Global Positioning System (GPS) at both the L1 and L2 frequencies (1575 MHz and 1227 MHz). Substantial scintillation in amplitude at

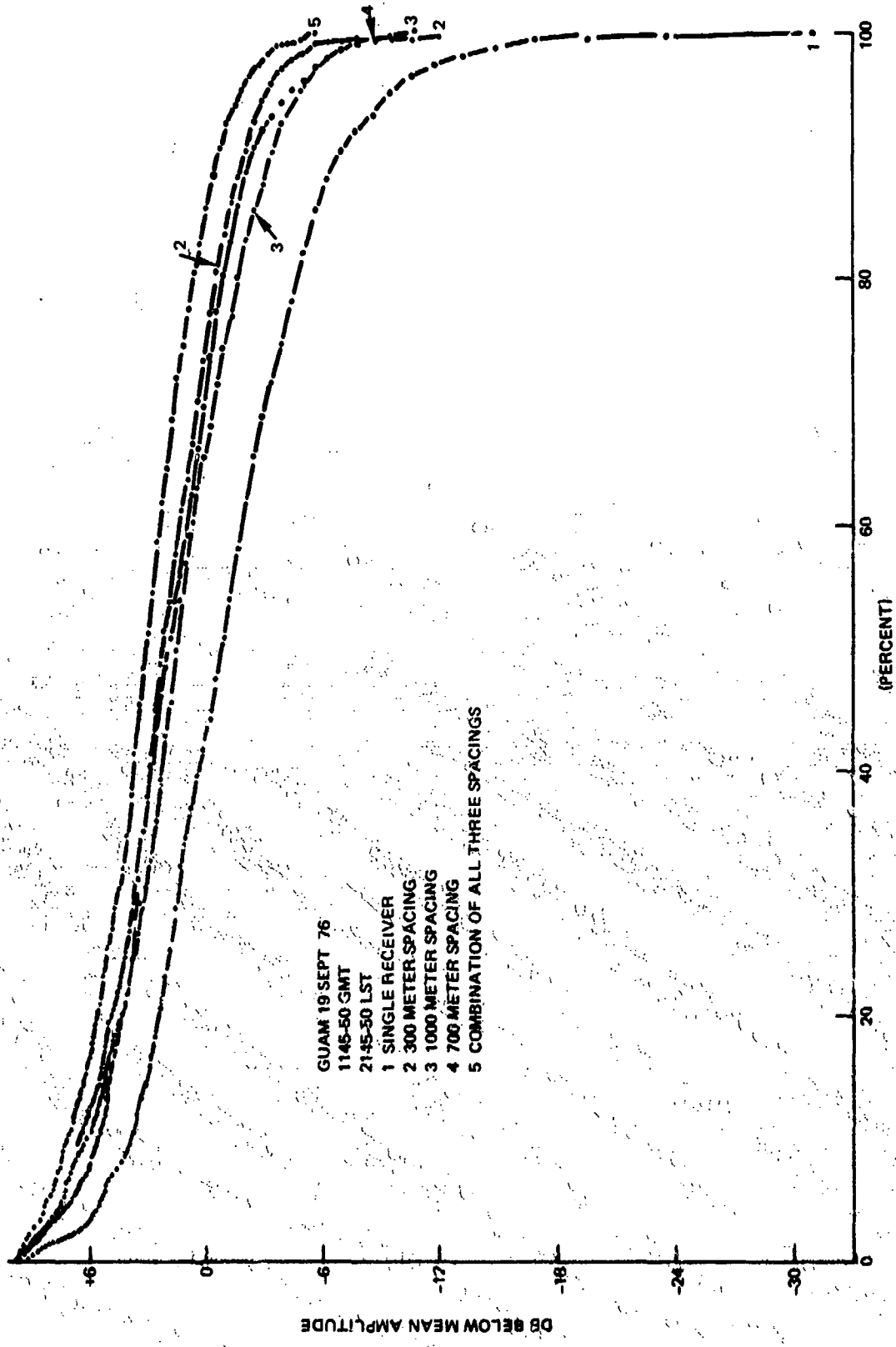


Figure 30. Cumulative probability distributions for different diversity combinations compared to the case of no diversity.

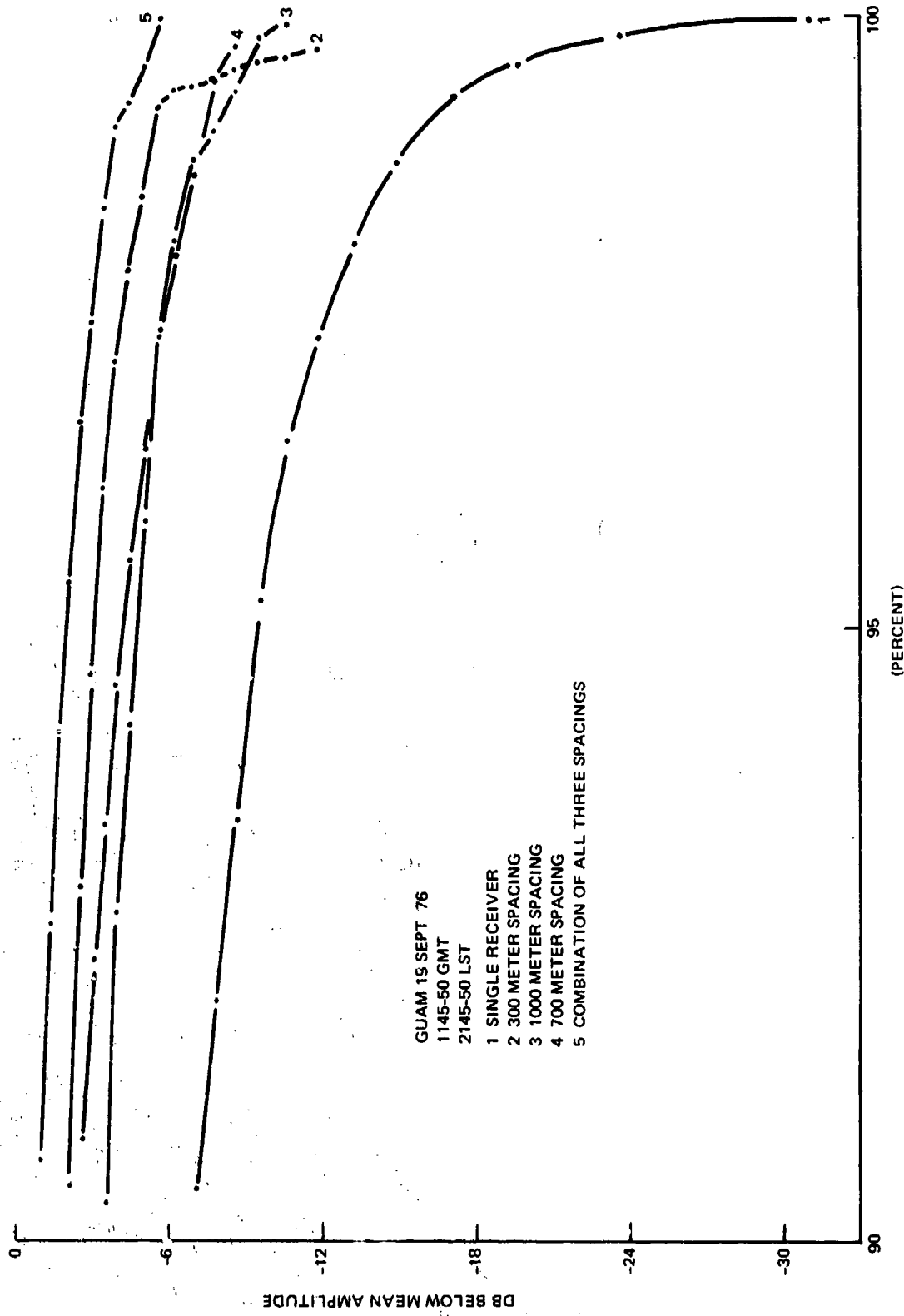


Figure 31. Cumulative probability distributions for different diversity combinations compared to the case of no diversity.

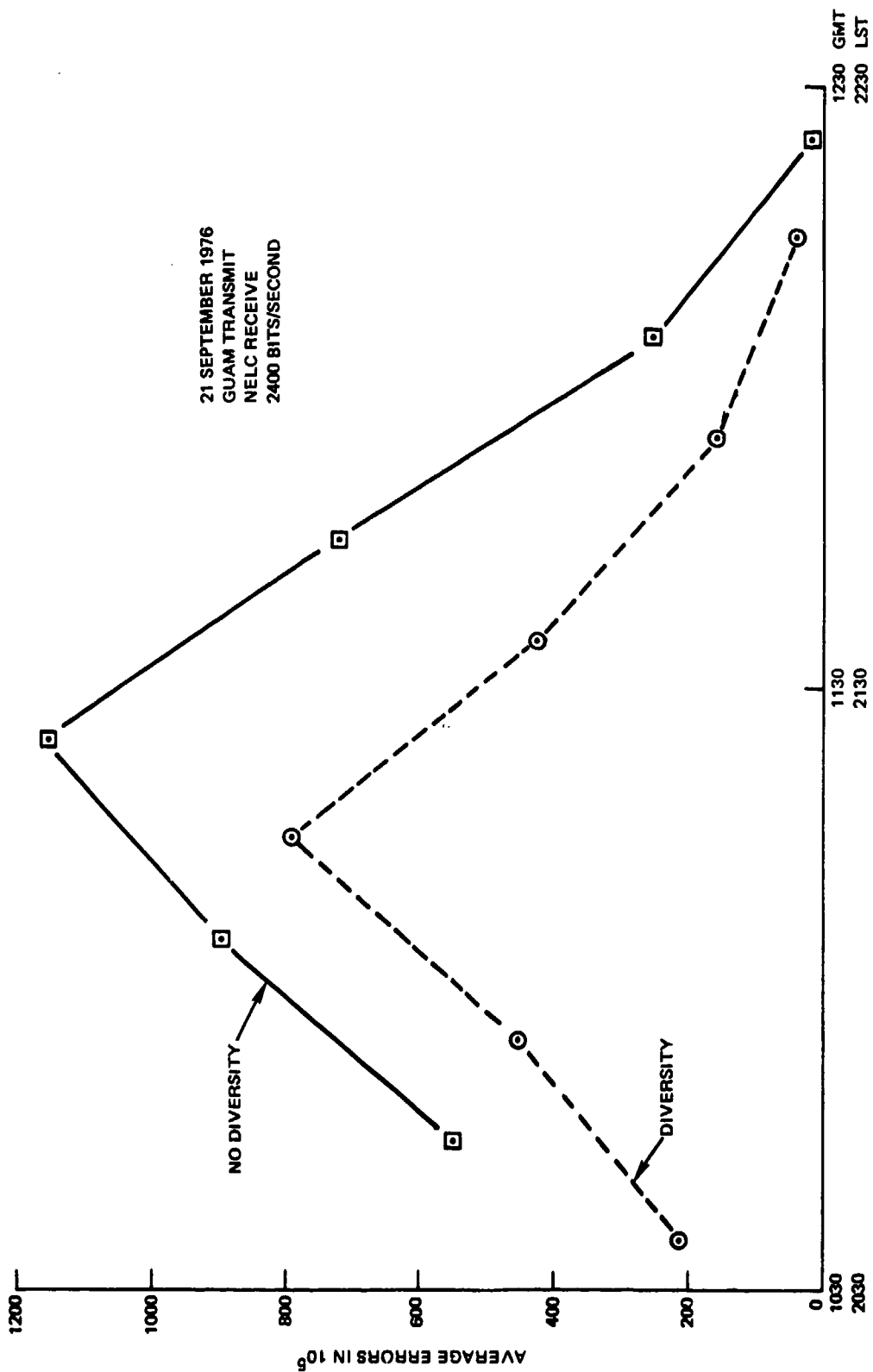


Figure 32. Comparison of up-link error rates with and without the use of diversity.

L-Band was observed during the periods of intense UHF scintillation. The results will be reported in this section, but it should be noted that no phase information was obtained in these tests and data being obtained currently in another experiment (the DNA/SRI wide-band satellite) indicates that large scintillation in phase may occur at L-Band with little or no amplitude scintillation. This may have considerable effect on the GPS system which is dependent on linear phase across the channel transfer function. The coherence bandwidth of these phase scintillations at L-Band will remain unknown until specific investigations of it are conducted.

Chart records showing scintillation fading at L-Band compared to UHF for 21 September 1976 are reproduced in figure 33. This was the most intense L-Band scintillation observed during the tests; however, it is likely that as the solar activity increases the effect will become not only more prevalent but also more intense. Statistics presented below are based on this data.

Data analysis included computation of probability density functions and the standard deviation about the mean for 5-minute sample periods. A time sequence of these values for the night of 21 September 1976 comparing the standard deviation for L-Band with UHF is shown in figure 34. It is evident that a relationship exists between the two wavelengths in that higher L-Band fading range corresponds to higher UHF fading and a threshold UHF level exists below which L-Band amplitude fading is not observable. The latter point as mentioned earlier does not mean that no phase scintillation exists.

Another statistical representation of this data is the cumulative distribution function. A comparison of the L-Band CDF with the UHF CDF for a 15-minute sample period of 21 September is shown in figure 35. From this data values are obtained in two ways to derive a measure of frequency dependence between UHF and L-Band. The spread of the CDF between the 1% and 99% levels is used in one case and between the mean and 99% level in the other case. The latter is useful in predicting the depths of fading to be expected below the mean or undisturbed signal level. Following this procedure the results are shown in figure 36. Using linear interpolation it is next possible to estimate the fading to be expected at frequencies between the data points. The predicted values for the L2 frequency of the GPS system are indicated on figure 36. Thus, for this sample interval, fading below the undisturbed signal level would occur 1% of the time below 4.5 dB at L2 and 2.5 dB at L1.

The effects of a 4.5 dB fade at L2 and 2.5 dB at L1 are to reduce the GPS system margins. Data on the GPS system margins obtained from reference 3 were used to generate the following tables of system margins under observed scintillation fading:

TABLE I. UNJAMMED LINK MARGINS (dB)

	L1 (P)	L1 (C/A)	L2
Acquisition	NA/NA*	+5.1/2.6*	NA/NA*
Precision track	+6.9/4.4	+9.1/6.6	+4.9/0.4
Data	+10.9/8.4	+13.1/10.6	NA/NA
Hold-on	+12.9/10.4	+15.1/12.6	+10.9/6.4

* 1st number is from reference 3/second number is first number less scintillation fading.

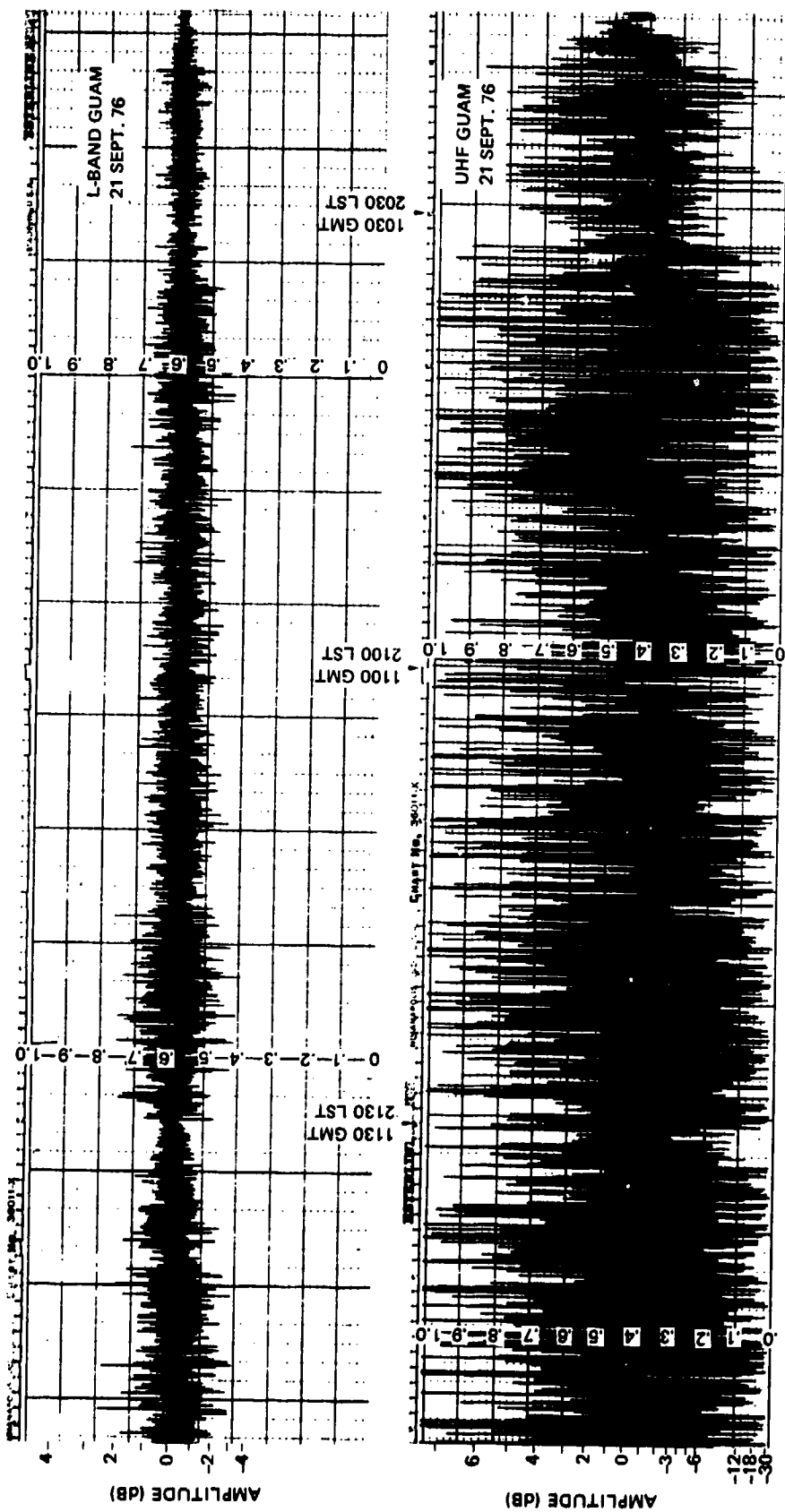


Figure 33. Chart record reproductions comparing L-band and UHF scintillation fading.

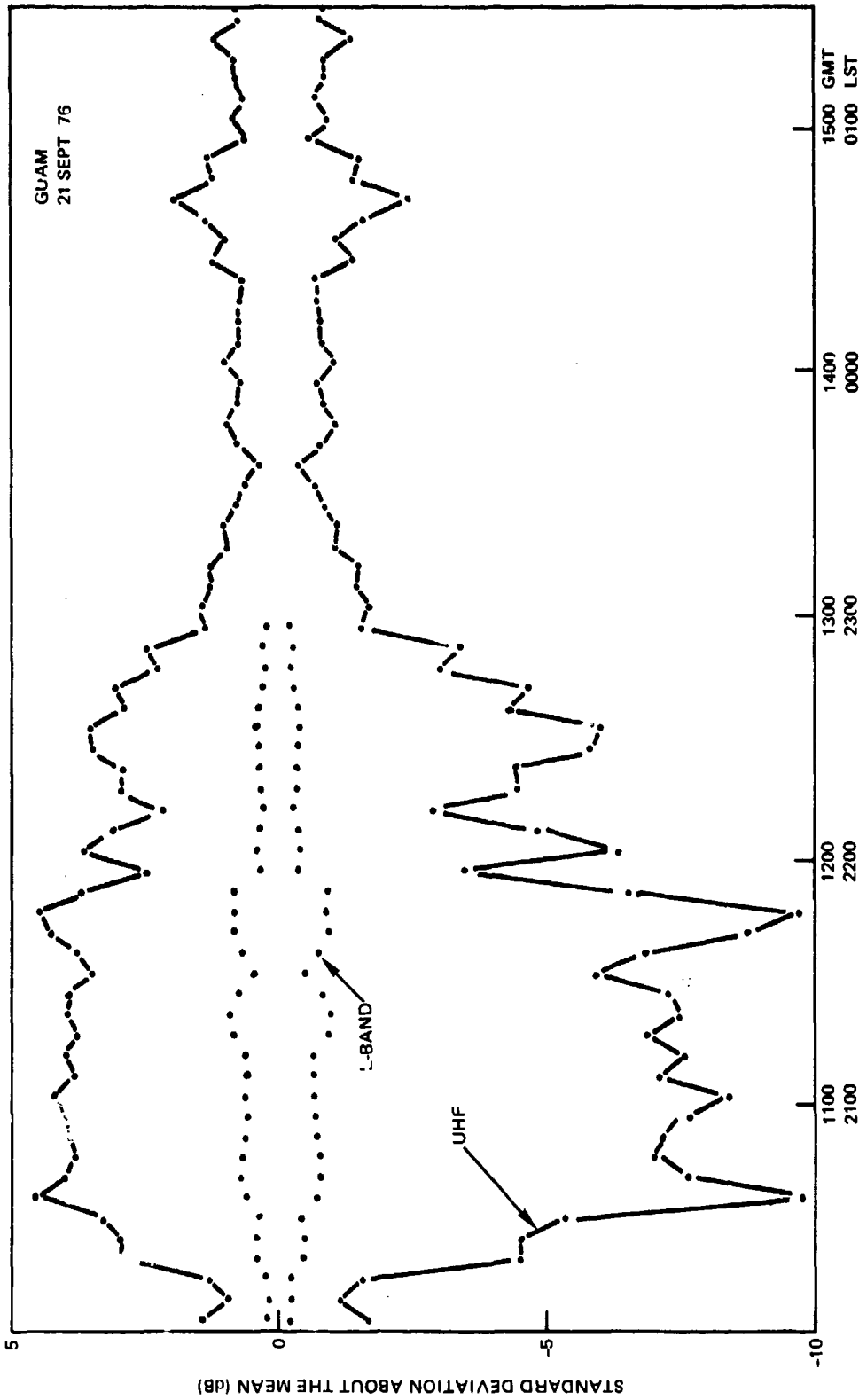


Figure 34. Temporal variation of UHF and L-band standard deviations about the mean signal level.

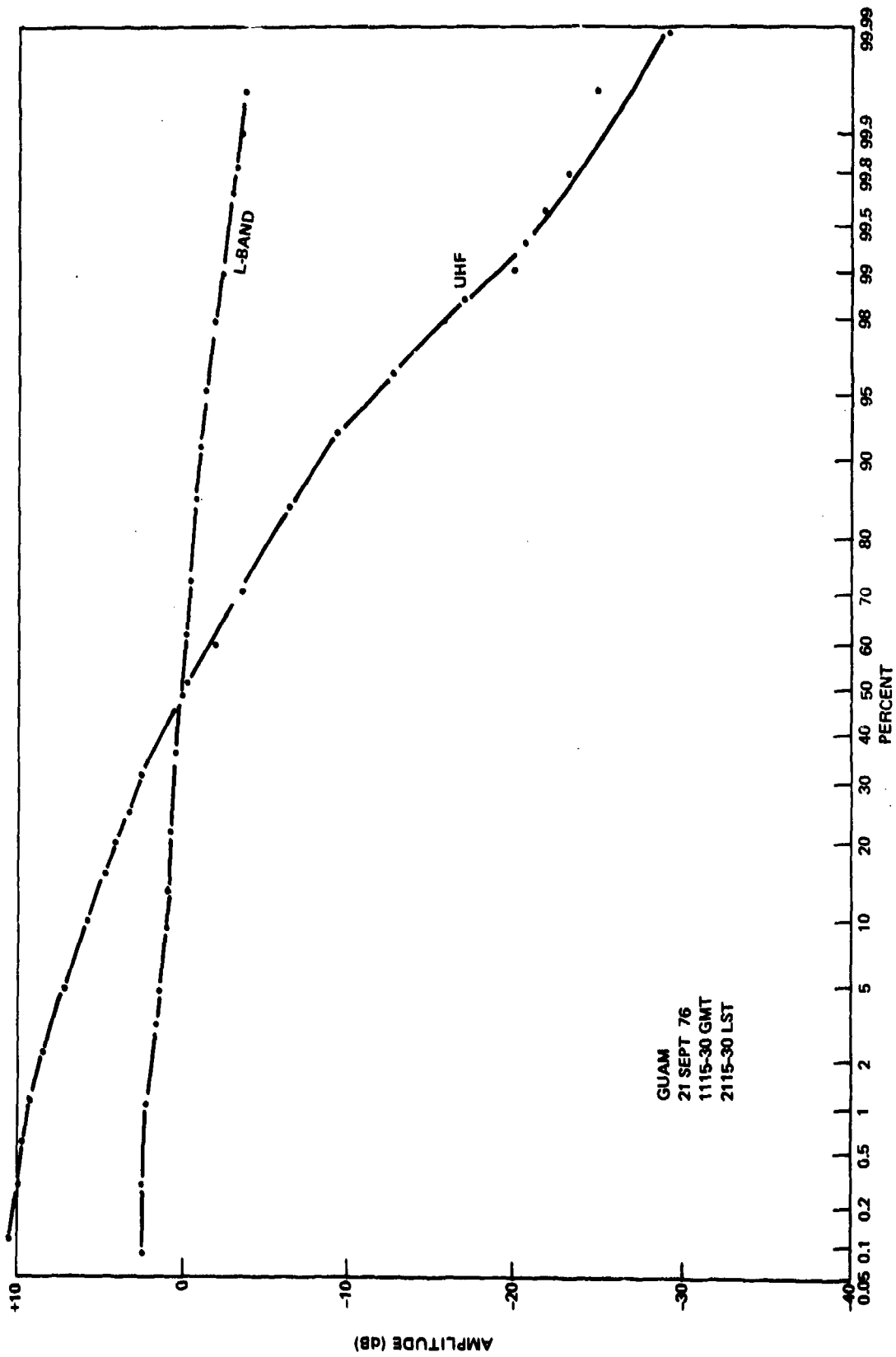


Figure 35. Comparison of UHF and L-band cumulative probability distributions.

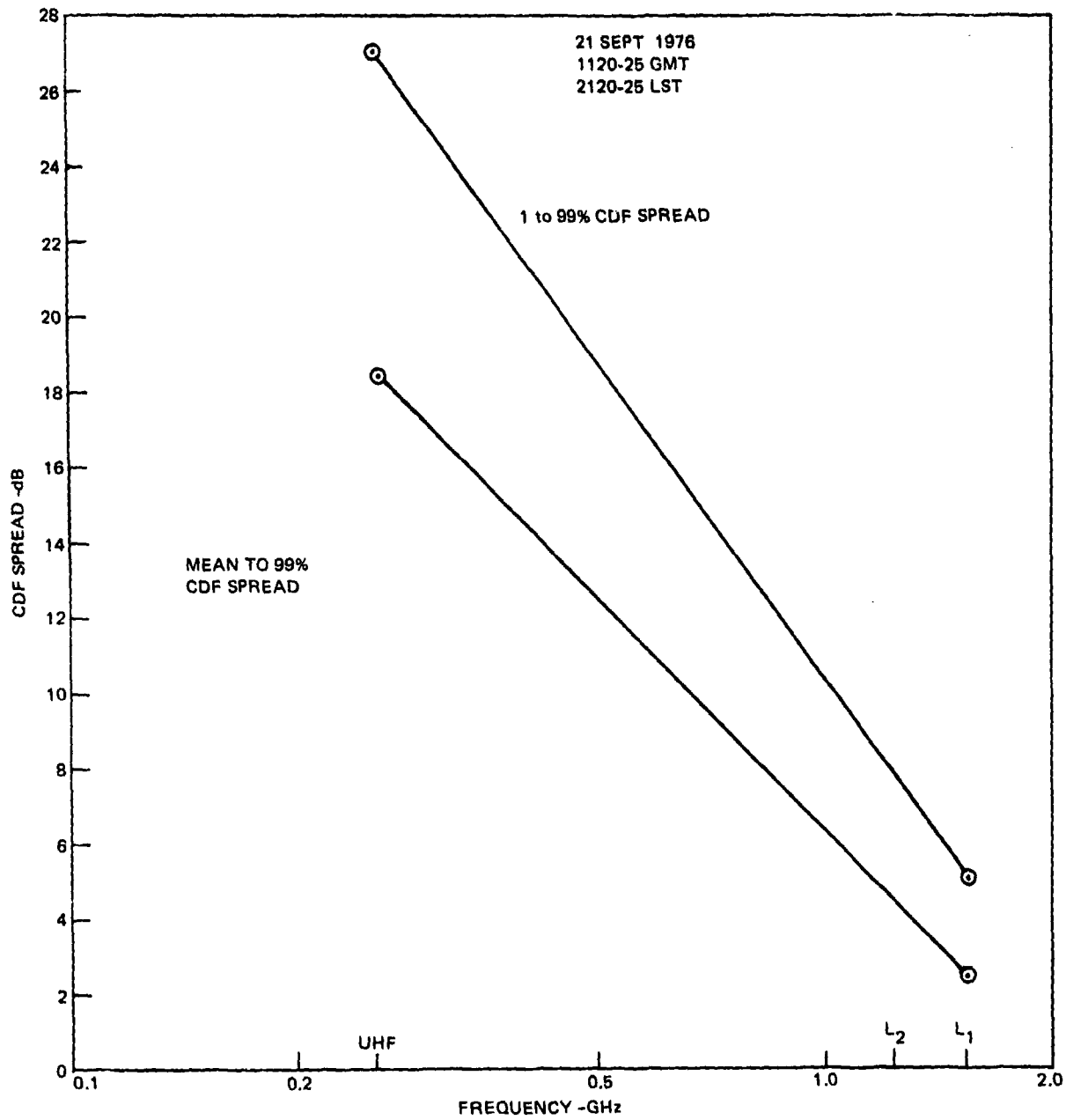


Figure 36. Comparative cumulative distribution function (CDF) values for UHF and L-band amplitude scintillation.

TABLE II. JAMMED LINK MARGINS (dB)

	L1 (P)	L1 (C/A)	L2
Acquisition	NA/NA*	NA/NA*	NA/NA
Precision Track	0/-2.5	NA/NA	-2/-6.5
Data	+4/+1.5	NA/NA	NA/NA
Hold-on	+6/+3.5	NA/NA	+4/-0.5

* 1st number is from reference 3/second number is first number less scintillation fading.

It is understood that the above figures pertain to performance of the X set and also that margins for the Y and Z sets are 3 dB less. This would bring the acquisition level 0.4 dB below the required acquisition margin in the scintillation environment. Precision track becomes impossible also with the X set under these conditions in a jamming scenario. The L-Band scintillation amplitudes observed at Guam must be considered quite moderate since information has been supplied by Stanford Research Institute* that the DNA "wideband" satellite tests have revealed much greater scintillation intensity at 1239 MHz in the South American Sector. Some values observed during one pass over ANCON, Peru, were as follows:

Maximum peak-to-peak fading	23 dB
Deepest fade below undisturbed level	19 dB
98% level of CDF	15.4 dB

Such levels of scintillation, if widespread and frequent, would be quite serious. Several samples of correlation functions obtained using the spaced L-Band receivers are shown in figures 37-39 compared to the corresponding UHF functions. The results in figure 37 were obtained from the period in which the cumulative distributions of figure 35 were obtained. In this sample no well developed correlation peak is evident for the UHF curve although one does exist for L-Band. In figures 38 and 39 both UHF and L-Band curves exhibit definite correlation peaks which occur at the same time delay indicating that there is a common drift mechanism in the ionosphere for both wavelengths. The minima of the correlation functions however, occur closer to the maxima at the L-Band than at UHF; therefore shorter diversity spacings are possible at L-Band than UHF. Using the time delay between the maxima and minima it is possible to derive the optimum diversity spacing since the velocity can be determined from the delay of the correlation peak and the diversity dimension. The optimum diversity spacing at L-Band for the functions shown in figures 37-39 varies from 300 to 360 meters. This is about one-half of the necessary spacing at UHF. The minor correlation peak at zero delay is due to amplitude variation on the satellite EIRP. Figure 40 compares the scintillation intensities observed on UHF and L-Band for 21 September 1976. The standard deviation of the signal fluctuations divided by the mean signal level is plotted for the two wavelengths. The significance of this plot is that while the UHF scintillation intensity has reached saturation the L-Band scintillation is still about 17 dB below this level. Thus, under more disturbed ionospheric conditions L-Band scintillation can increase substantially while UHF cannot.

*EJ Fremouw, private communication from Stanford Research Institute

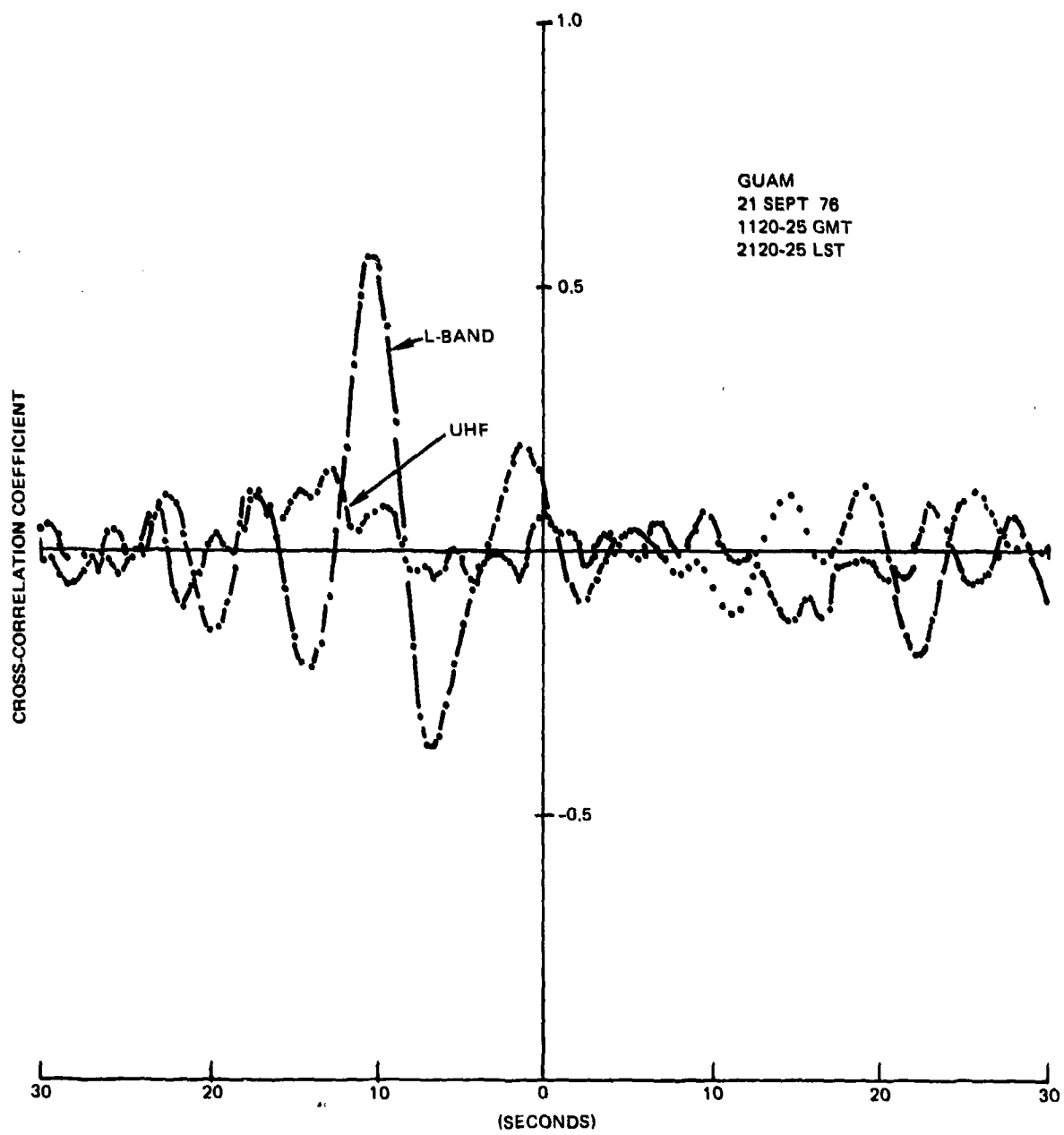


Figure 37. Spatial cross correlation functions for two wavelengths on 1000 meter baseline.

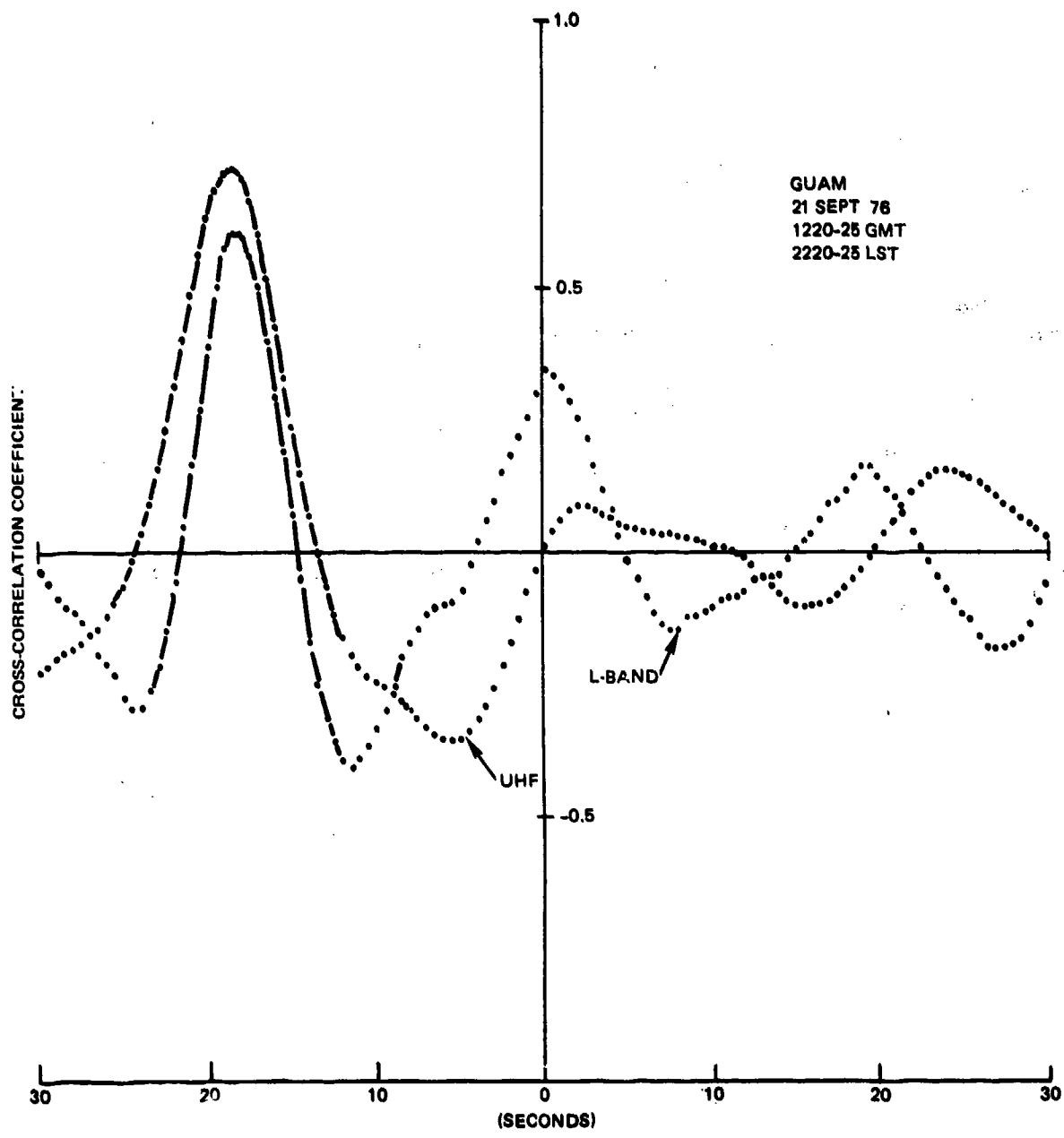


Figure 38. Spatial cross correlation functions for two wavelengths on 1000 meter baseline.

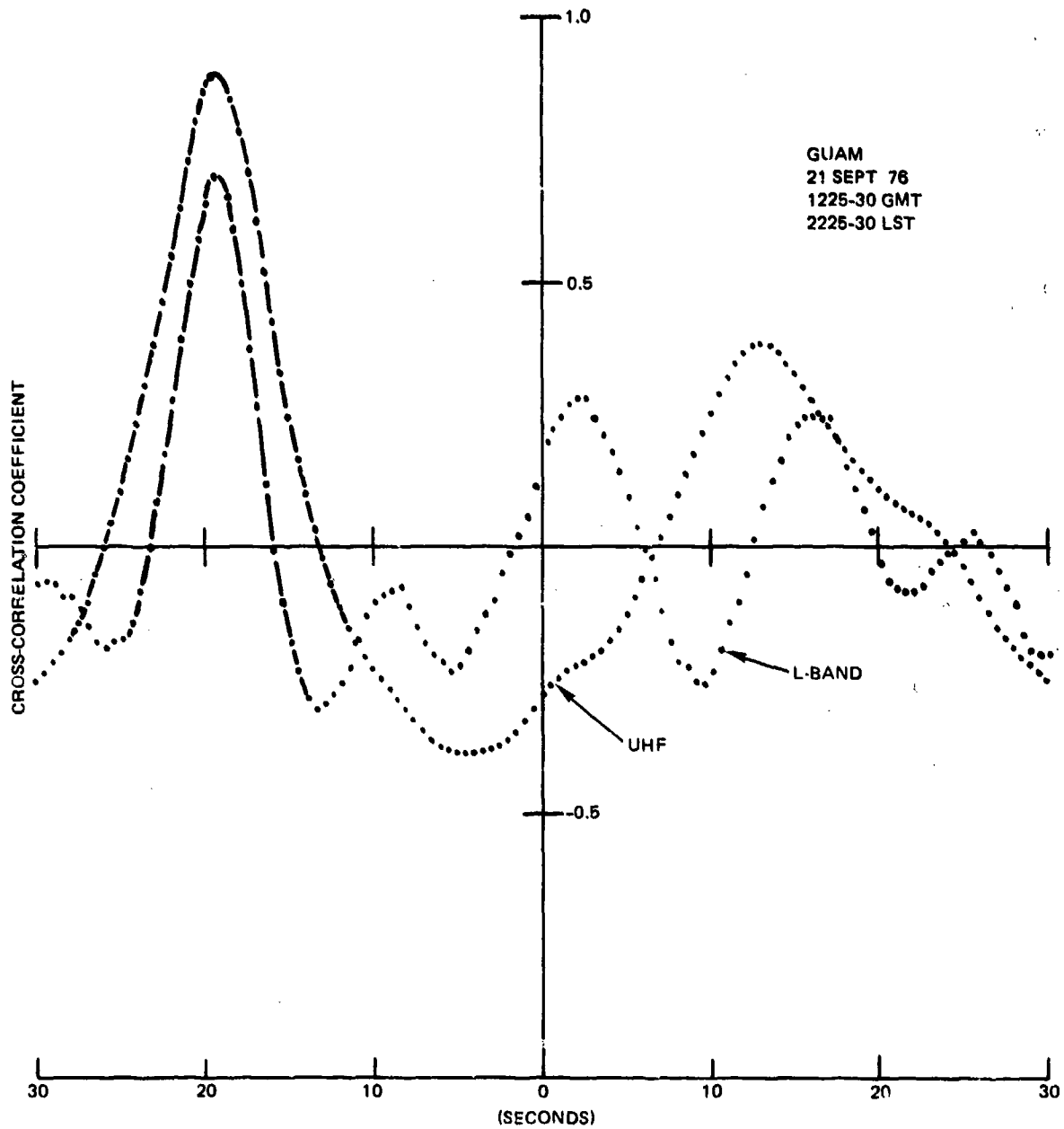


Figure 39. Spatial cross correlation functions for two wavelengths on 1000 meter baseline.

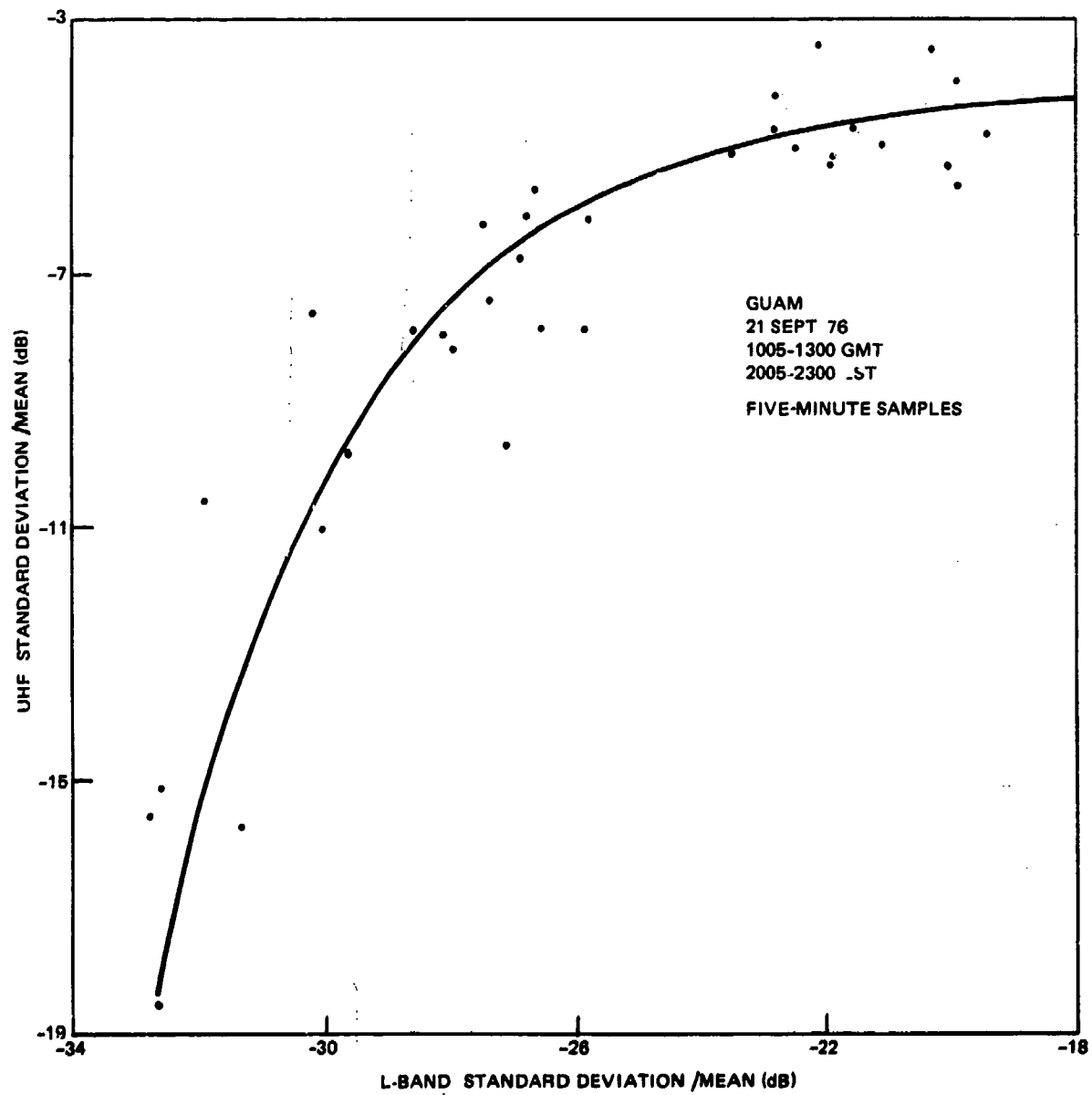


Figure 40. Comparison of scintillation intensities between L-band and UHF.

Related Data

A correlation between scintillation intensity and the drift velocity of the fading pattern had been suspected from the original diversity data obtained by NELC in 1971 so several time plots of these quantities were made to see if this were true. The results for 3 days are shown in figures 41-43. On 21 September when the scintillation built up rapidly to high intensity the correlation with velocity was exceedingly good (figure 41). The other two days also exhibited fair correlation in spite of greater variation of scintillation activity. Since the higher velocities permit shorter diversity base lines, assuming the scattering structure is finer, designing the system with this in mind will optimize the system for the condition when it is needed most - for stronger scintillation. It is also of interest to conjecture that as the ionospheric winds increase in velocity more turbulence and mixing is produced to create the irregularities that cause the scintillation.

A few brief measurements were made of the differential phase received on the 1000 meter UHF baseline. One five-minute sample is shown in figure 44. Between minutes 58 and 59 a total phase variation of 1500 degrees or over 8π radians occurred. This means a peak-to-peak tilt of the arriving wave front of 0.37 degree. The average phase rate between the signals from the spaced antennas for the 1500 degree variation was 25 degrees per second; however, the minor fluctuations resulted in phase rates as high as 75 degrees per second. These values present no problems relative to the diversity combiner efficiency as used in the AN/SSR-1 but could if phase lock loops of very narrow bandwidth were employed (less than .5 Hz). The above numbers are considered useful for system design applications.

A final result of the data analysis was the statistics of fade durations 6 dB and 12 dB below the mean signal levels (undisturbed level). Since data taken in 1971 near Guam were similarly analyzed a comparison between the different years was possible and of interest because of the noticeably slower fading rates in 1976. Figures 45 and 46 compare the fade duration distributions below the -6 dB level for 1976 and 1971 and figures 47 and 48 compare the two years for the -12 dB level. The curves have not been scaled for direct comparison but it is obvious on inspection that the drop-off of long duration fades was much more rapid in 1971 than 1976. For instance at the -12 dB level the one-second fade dropped to 19% of the peak in 1971 and only 46% of the peak in 1976. Similarly the values for 2-second fades were 5.9% in 1971 and 21.7% in 1976.

A Note Concerning Low-Angle Fading

This report has addressed equatorial scintillation effects relative to a high (50.3 degree) elevation look angle satellite. It has been observed that at low look angles (below 20° elevation) intense fading of UHF satellite signals occurs even at mid-latitudes. It has been speculated that this fading is caused by sporadic E activity since seasonal and diurnal correlation exists with it. A summary of TACSAT-1 beacon recordings from 1969 to 1972 taken at Camp Parks Radiometric Test Site was presented in reference 5 along with similar recordings obtained at NELC in 1972. The data presented clearly established the 20° critical elevation angle and correlations between the Camp Parks and NELC data recorded in San Diego.

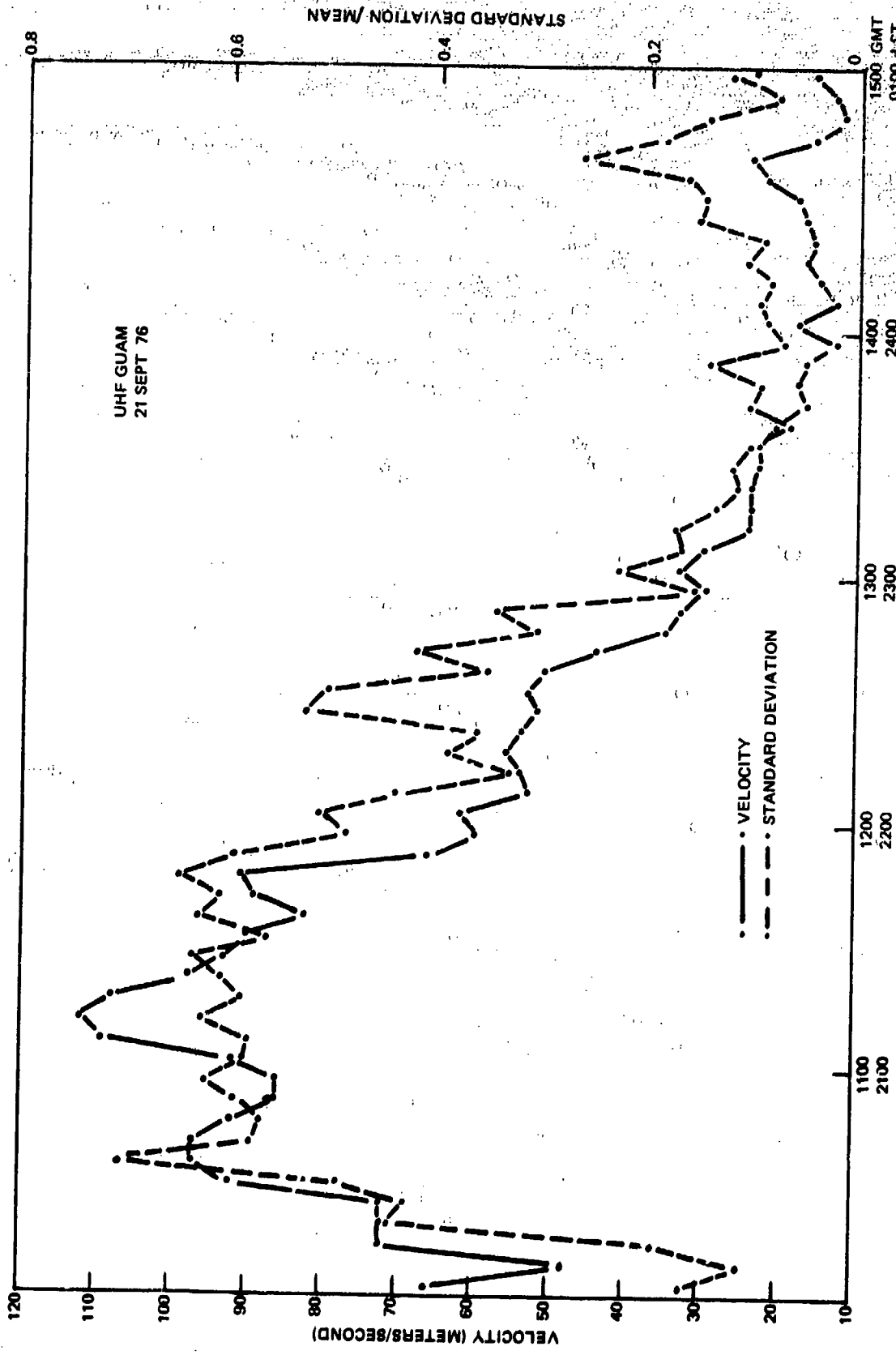


Figure 41. The east-west component of the apparent drift velocity, uncorrected for time decorrelation effects, is shown as a function of time and compared to the scintillation activity where the standard deviation divided by the mean is used as an indication of scintillation intensity.

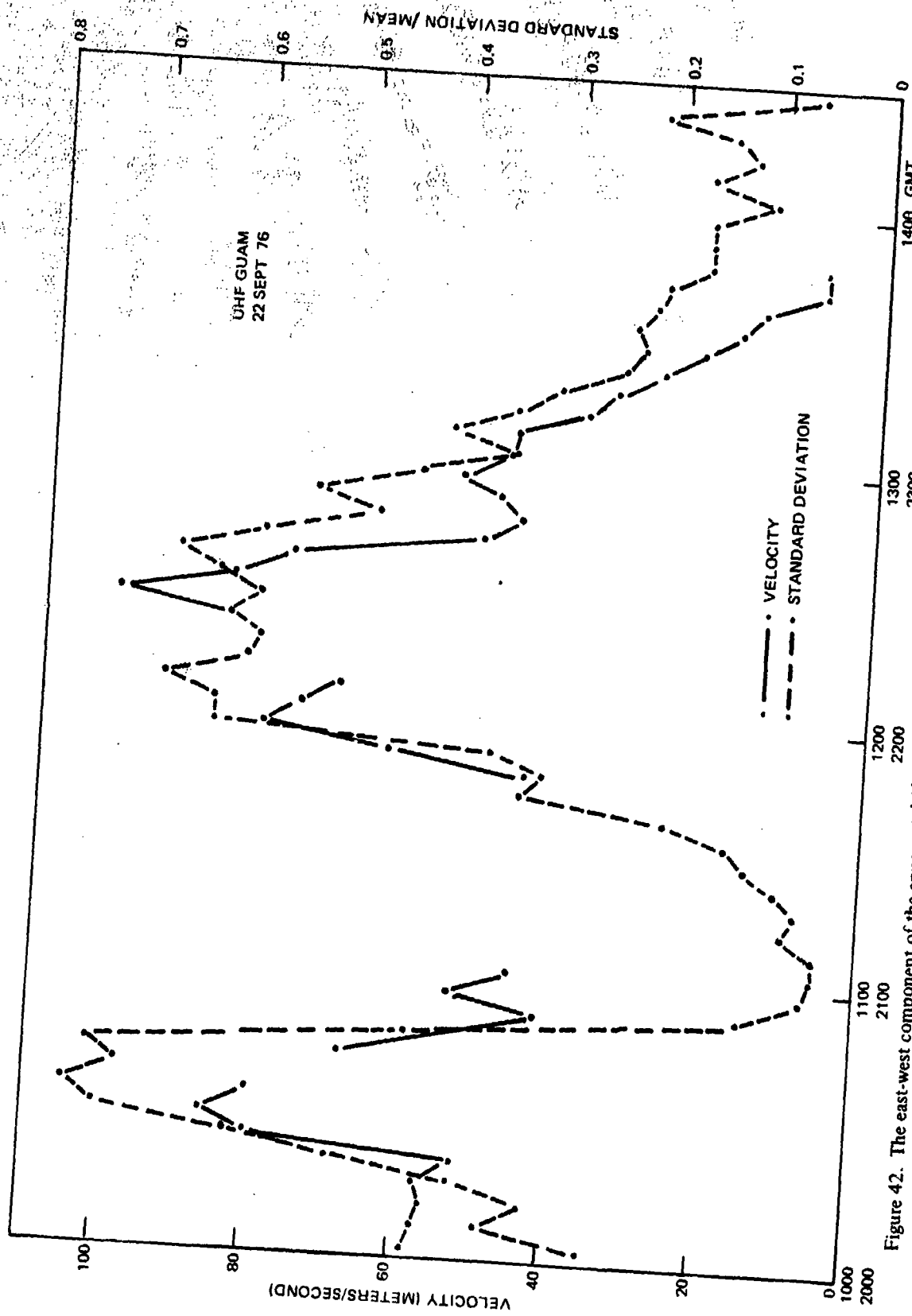


Figure 42. The east-west component of the apparent drift velocity, uncorrected for time decorrelation effects, is shown as a function of time and compared to the scintillation activity where the standard deviation divided by the mean is used as an indication of scintillation intensity.

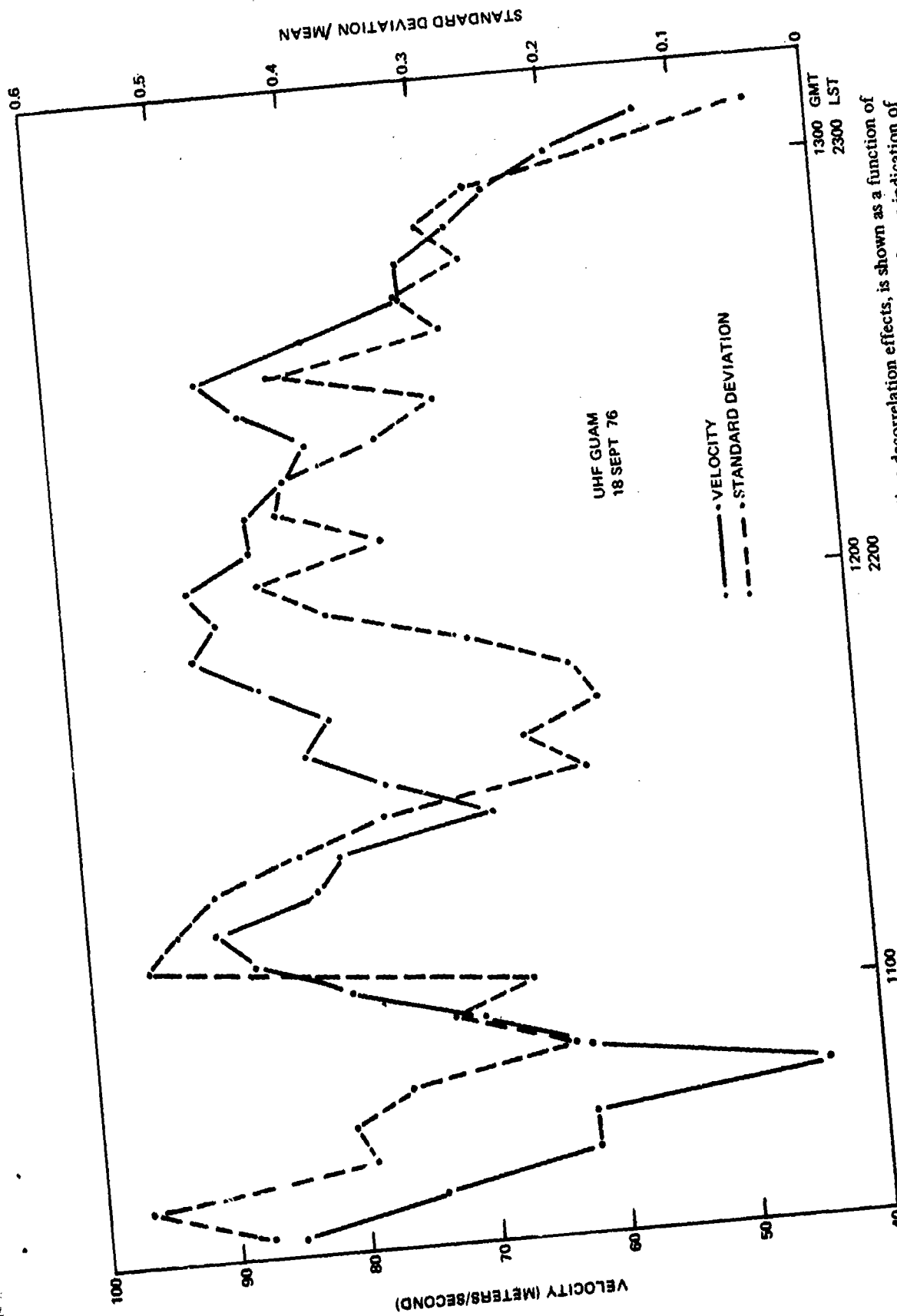


Figure 43. The east-west component of the apparent drift velocity, uncorrected for time decorrelation effects, is shown as a function of time and compared to the scintillation activity where the standard deviation divided by the mean is used as an indication of scintillation intensity.

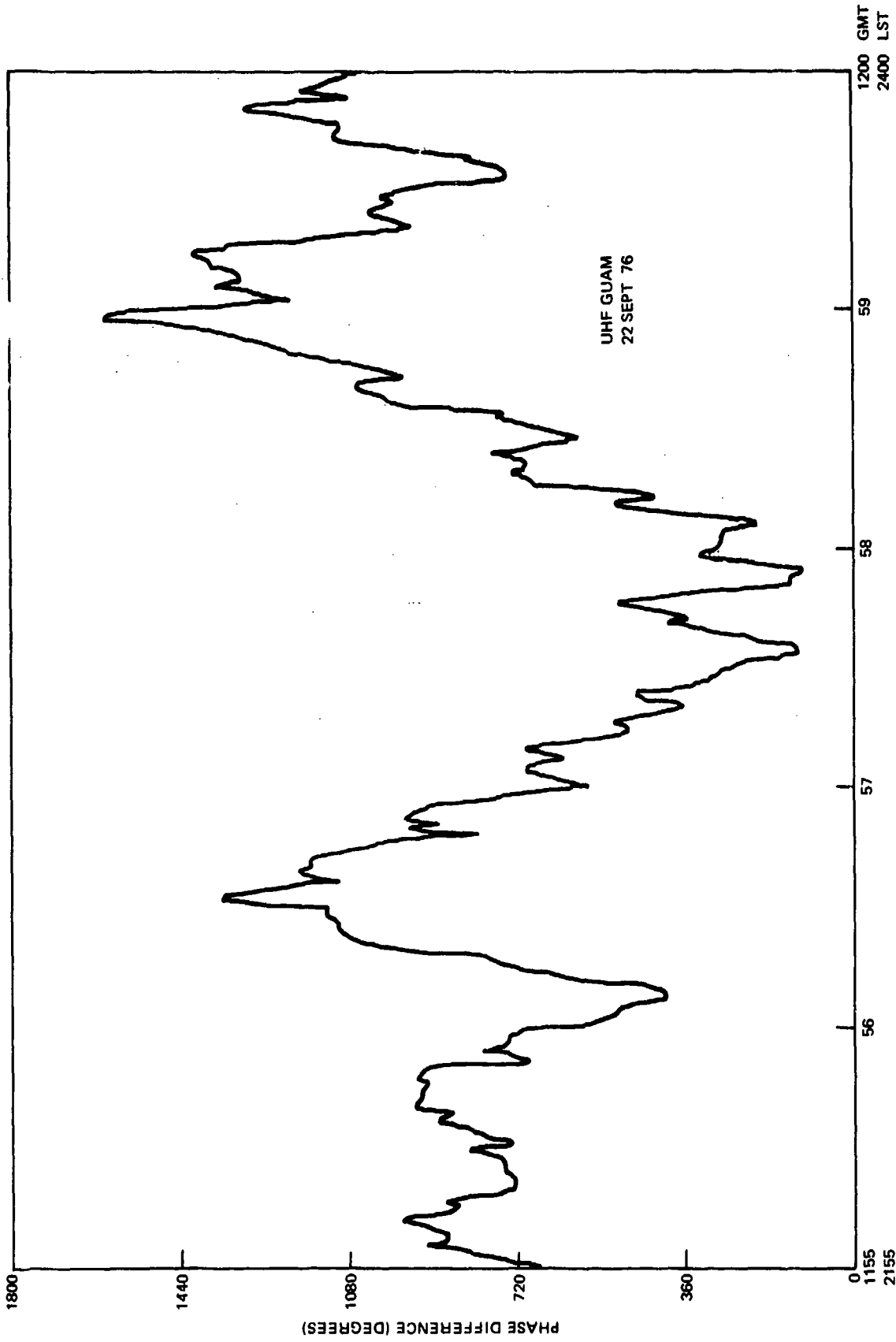


Figure 44. Temporal variation of UHF phase difference with the 1000 meter antenna spacing.

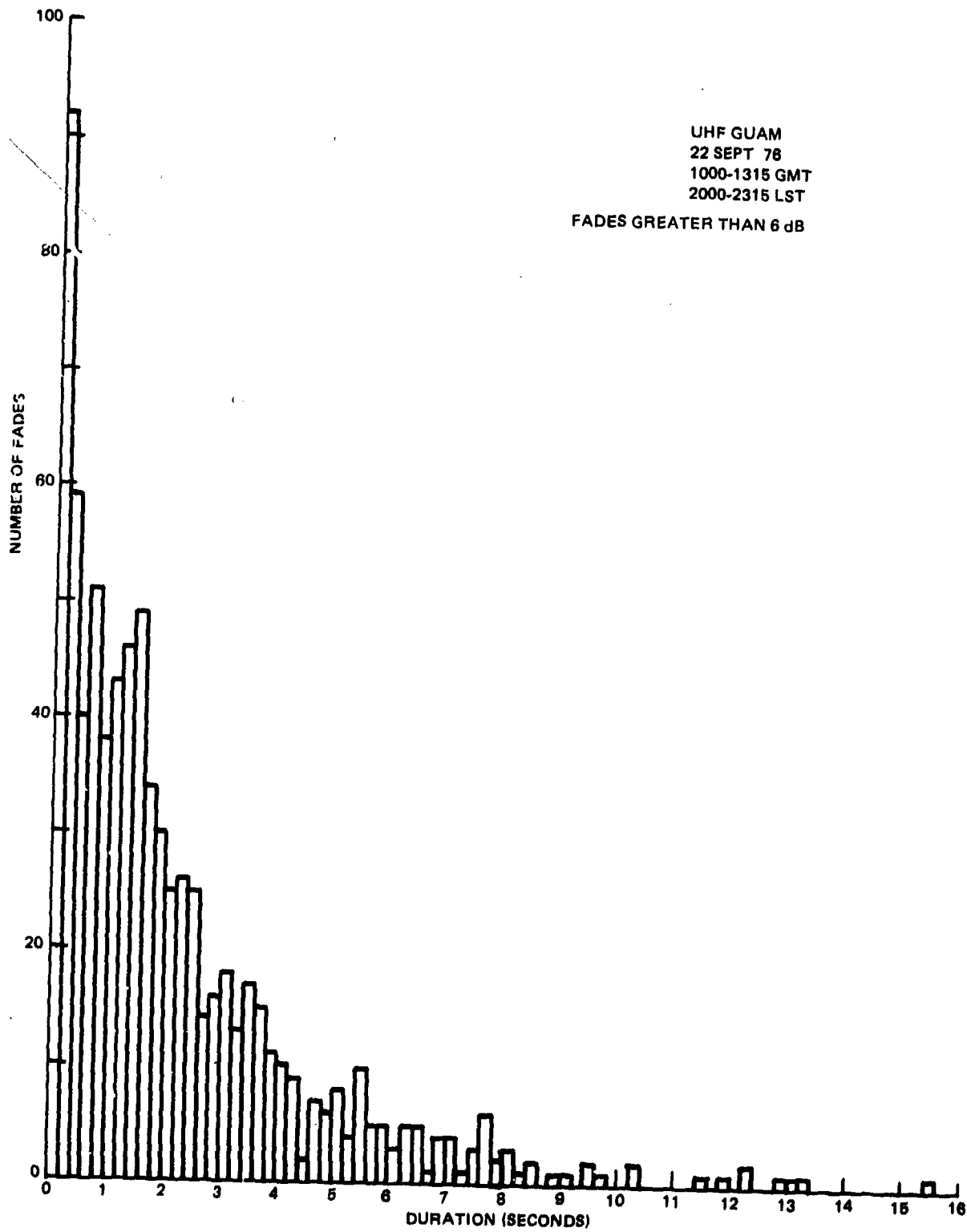


Figure 45. Fade duration distribution observed at Guam in 1976.

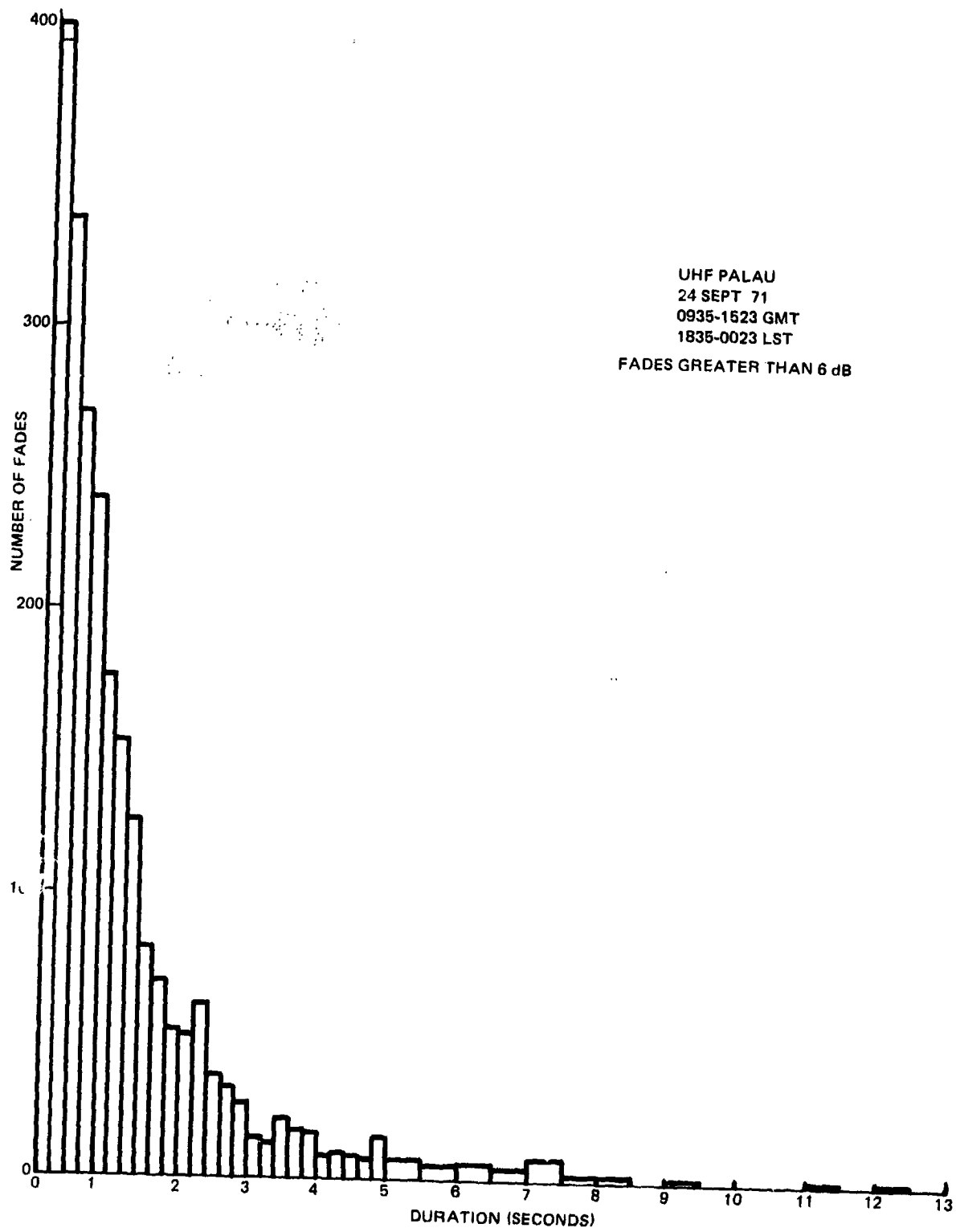


Figure 46. Fade duration distribution observed near Guam in 1971.

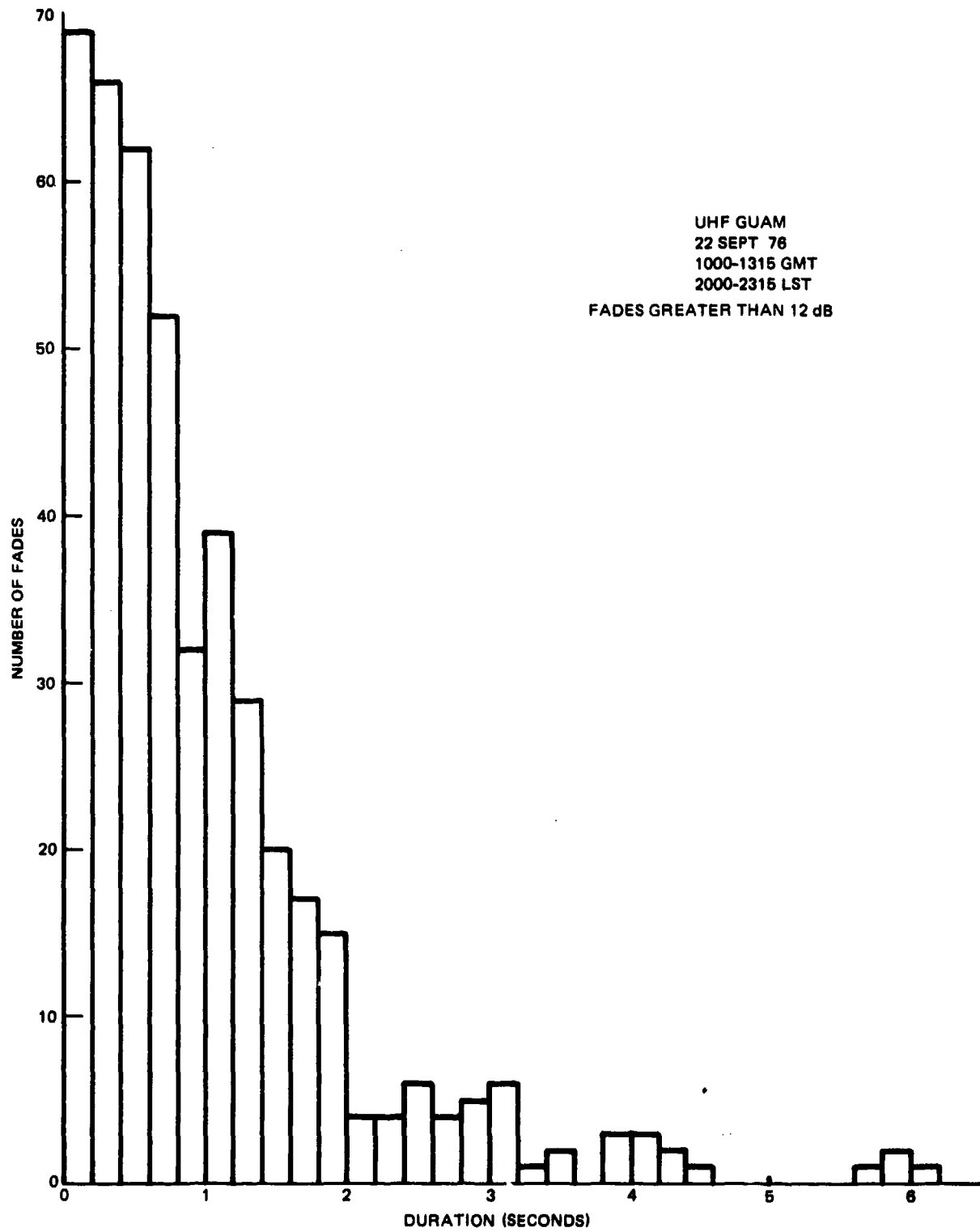


Figure 47. Fade duration distribution observed at Guam in 1976.

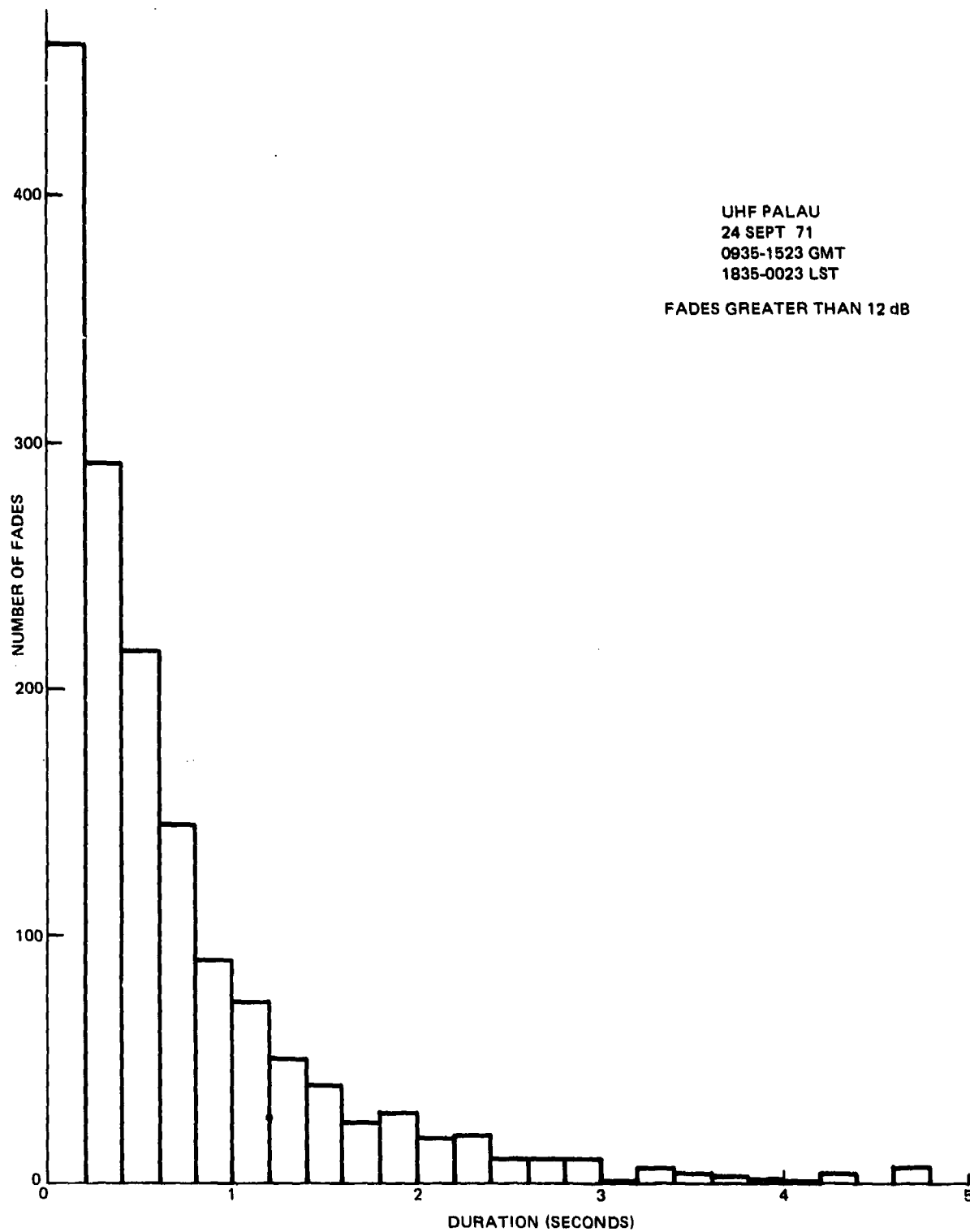


Figure 48. Fade duration distribution observed near Guam in 1971.

The reason this is of concern is that the look angle to the Indian Ocean GAPPILLER Satellite from Guam is only eleven degrees elevation and from Italy the look angle is 13 degrees. Also, a review of sporadic E observations indicates that Guam is in a region of the world high in sporadic E activity and Italy is not greatly less. Therefore, the two major NAVCAMS utilizing the Indian Ocean satellite may encounter prolonged degradation because of this. In view of the above a recommendation related to it will be included.

CONCLUSIONS

The primary conclusions of this investigation are as follows:

1. Space diversity can completely nullify the problem of high digital error rates caused by equatorial scintillation using baseline antenna separations around 700 meters and predetection diversity combining techniques for reception.
2. The AN/SSR-1 Fleet Broadcast receiver is ideally implemented for space diversity applications.
3. Three-level diversity is somewhat better than two-level and it permits use of three different baseline lengths which can compensate for long term (years) and short term changes in the fading statistics.
4. Scintillation activity is dependent on the level of solar disturbances as characterized by the sun-spot numbers and therefore is predicted to increase substantially as the solar cycle returns to increasing levels of activity from the 1976 minimum.
5. L-Band scintillation intensities are considerably less than at UHF and the necessary dimension for diversity is about one-half that at UHF. Though small, L-Band scintillation is large enough to adversely affect the small margins associated with GPS system.
6. Considerably higher L-Band scintillation fading than observed at Guam has been recorded in the DNA/SRI "wideband" satellite experiment in the South American equatorial region so the results reported for this investigation must be considered modest; although, as solar activity increases higher levels are expected to occur at Guam also.

RECOMMENDATIONS

There are several clear actions that could be taken to improve the performance of UHF SATCOM at equatorially located NAVCAMS:

1. The implementation of space diversity into the Fleet Broadcast service is a highly cost effective improvement that will provide error free down-links which, along with SHF up-links, will relieve the NAVCAMS of problems associated with scintillation fading. Since the AN/SSR-1 includes the necessary diversity combining capability, the only new hardware required is a remotely located antenna and preamplifier that are connected to the AN/SSR-1 by coaxial line.
2. The next phase that is considered low risk is the implementation of space diversity for the multiple channel Fleet SATCOM receiving system. To accomplish this the same

antennas used for Fleet Broadcast would be employed and diversity combiners for each of the channels would be added. A configuration the same as in the AN/SSR-1 is the likely approach.

3. Up-link diversity requires further investigation so it is recommended that implementation be withheld until that can be accomplished.

4. Detailed data relative to low elevation look angle fading is needed. It is recommended that recordings of signal strength suitable for analysis at NOSC be made at Italy on the Indian Ocean satellite and at Guam on both Indian Ocean and Pacific satellites. It would also be of value to evaluate the use of space diversity for low-angle fading which is statistically different from scintillation fading.

5. Continuous chart recordings of signal strength of the Fleet Broadcast channel would be beneficial to the NAVCAMS as an aid in differentiating between equipment problems and propagation effects.

6. With respect to the Global Positioning System it is recommended that observations of the effects of scintillation fading at the Guam monitor station be carefully analyzed to determine if limitations on range resolution result. An L-Band monitor on MARI-SAT would be useful as a sensitive 24-hour-a-day indicator of scintillation activity. Phase measurements should be included at the monitor station since this may have more effect on the GPS system than amplitude fading.

REFERENCES

1. MR Paulson, RUF Hopkins, Effects of Equatorial Scintillation Fading on SATCOM Signals, NELC/TR 1875, 8 May 1973.
2. PE Argo, JR Hill, Radio Propagation and Solar Activity, QST, February 1977, p 24-26 (also submitted to Nature).
3. TJ Conner, GPS NAV Link Margin, Aerospace Corporation, Interoffice Correspondence, 18 June 1975.
4. TW Salmi, Summary of Camp Parks TACSAT UHF Beacon Data, Aerospace Report TOR-0074 (4401)-1, prepared for SAMSO, 30 July 1973.

INITIAL DISTRIBUTION LIST

DoD		AIR FORCE GEOPHYSICAL LABORATORY DR JULES AARONS JOHN P MULLEN
NAVAL ELECTRONIC SYSTEMS COMMAND PME108 (R COFFMAN)	(8)	AIR FORCE WEAPONS LABORATORY CAPT LEON WITWER
DIRECTOR OF DEFENSE DEFENSE TELECOMMUNICATIONS AND COMMAND AND CONTROL SYSTEMS		AF SPACE & MISSILE SYSTEMS ORGANIZATION SK DYAX (EL SEGUNDO), MAJ LAWRENCE MALONEY
DEFENSE NUCLEAR AGENCY WARREN BERNING DOW EVELYN		OTHER GOVERNMENT ADDRESSES
DEFENSE ADVANCED RESEARCH PROJECTS AGENCY	(2)	NATIONAL AERONAUTICS & SPACE ADMINISTRATION GODDARD SPACE FLIGHT CENTER CODE 751 (TOM GOLDEN) DANDAN STATION (GUAM) DICK HYNSON
DEFENSE COMMUNICATIONS AGENCY (MSO) CAPT DW FISCHER DR FE BOND		DEPARTMENT OF COMMERCE OFFICE OF TELECOMMUNICATIONS INSTITUTE OF TELECOMMUNICATIONS SCIENCES RW HUBBARD MARTIN NUSENBERGS (SPECTRUM UTILIZATION)
DEFENSE COMMUNICATIONS AGENCY DEFENSE COMMUNICATIONS ENGINEERING CENTER TROY ELI INGTON		DEPARTMENT OF COMMERCE NATIONAL OCEANIC & ATMOSPHERIC ADMINISTRATION ROBERT COHEN CL RUFENACH LS FEDOR
DEFENSE DOCUMENTATION CENTER	(12)	DEPARTMENT OF COMMERCE NATIONAL BUREAU OF STANDARDS DR RH OTT, ITS
CHIEF OF NAVAL OPERATIONS NOP-941U (TSAPG) (CDR RM WELLS)		DEPARTMENT OF TRANSPORTATION TRANSPORTATION SYSTEMS CENTER PETER ENGLES LES KLEIN
COMMANDER, NAVAL TELECOMMUNICATIONS COMMAND N7 (CAPT RE ENRIGHT)	(4)	HIGH COMMISSIONER TRUST TERRITORY OF THE PACIFIC ISLANDS SAIPAN, MI COMMUNICATIONS CENTER (2)
COMMANDER OPERATIONAL TEST AND EVALUATION FORCE CODE 646 (LT STEINMAN)		FOREIGN ADDRESSEES
OFFICE OF NAVAL RESEARCH CODE 420 (DR TG BERLINCOURT)	(2)	DEPARTMENT OF COMMUNICATIONS COMMUNICATIONS RESEARCH CENTER PO BOX 490, STATION A OTTAWA, ONTARIO CANADA, K1N 8T5 LA MAYNARD
NAVAL RESEARCH LABORATORY CODE 4110 (DR JM GOODMAN)		WEAPONS RESEARCH ESTABLISHMENT BOX 1424 H GPO ADELAIDE, SO AUSTRALIA 5001 NF BARKHAM FB ANDREWS
NAVAL WEAPONS CENTER CODE 5012 (WL TEETER)		RADIO SCIENCE DIVISION NATIONAL PHYSICAL LABORATORY DELHI - 12 INDIA 110012 DK PASRICHA
NAVAL AIR DEVELOPMENT CENTER CODE 8131 (OLIVER DELL) AETC CODE 2033 (DICK HOGG)		
COMMUNICATIONS AREA MASTER STATION WESTERN PACIFIC	(2)	
NAVAL SHORE ELECTRONICS ENGINEERING ACTIVITY, GUAM CDR G BURMAN J SERVINO		
NAVAL SHORE ELECTRONICS ENGINEERING ACTIVITY, JAPAN		
INSTITUTE FOR DEFENSE ANALYSIS 400 ARMY-NAVY DRIVE ARLINGTON, VA 22202 DR JOSEPH M AEIN		
AIR FORCE AVIONICS LABORATORY AL JOHNSON WADE HUNT		

UNIVERSITY OF GHANA, LEGON
ACCRA, GHANA
WEST AFRICA
DEPT OF PHYSICS (REV JR KOSTER)

UNIVERSITIES & AFFILIATED ACTIVITIES

MASSACHUSETTS INSTITUTE OF TECHNOLOGY
LINCOLN LABORATORY
BOX 173
LEXINGTON, MA 02173
BE NICHOLS
JV EVANS
EA BUCHER

CAMP PARKS TEST STATION
PO BOX 550
PLEASANTON, CA 94566
JOHN MEYER

JOHNS HOPKINS UNIVERSITY
APPLIED PHYSICS LABORATORY
LAUREL, MD 20810
DR VINCENT PASACANE
MILLER WHISNANT (SPACE DEVELOPMENT DEPT)

UNIVERSITY OF ILLINOIS
ELECTRICAL ENGINEERING DEPT
URBANA, IL 61801
AL HEARN

PRIVATE COMPANIES & INDIVIDUALS

AEROSPACE CORP
PO BOX 92957
LOS ANGELES, CA 90045
VIRGIL WALL

AEROSPACE CORP
PO BOX 95085
LOS ANGELES, CA 90045
FL STRUBEL

AMERICAN INSTITUTE OF MERCHANT SHIPPING
(COMMUNICATIONS)
1625 K STREET, NW
SUITE 1000
WASHINGTON, DC 20006

COMMUNICATIONS SATELLITE CORP
COMSAT LABORATORIES
CLARKSBURG, MD 20734
JL LEVATICH
DR ROGER TAUR
DR BURT EDELSON

ELECTRONIC COMMUNICATIONS, INC
BOX 12248
1501 72ND STREET
NORTH ST PETERSBURG, FL 33733
KARL M ALLISON

ENVIRONMENTAL RESEARCH & TECHNOLOGY, INC
CONCORD, MA 01742
RK CRANE

MARTELLO COMMUNICATIONS, INC
277 78TH STREET
BROOKLYN, NY 11209
HF MULLEN

MITRE CORP
PO BOX 208
BEDFORD, MA 01730
MR DRESP

STANFORD RESEARCH INSTITUTE
MENLO PARK, CA 94025
DR EJ FREMOUW

TELEDYNE MICRONETICS
7155 MISSION GORGE ROAD
SAN DIEGO, CA 92120
DR STEVEN WEISBROD

PETER F SIELMAN
C/O AIL
CONAN ROAD
DEER PARK, NY 11729

DR JB SMYTH
3555 AEPO CC JRT
SAN DIEGO, CA 92123